

**The Geology and Rock Mass Quality of the
Cenozoic Kalahari Group,
Nchwaning Mine Northern Cape**

by

R.A. Puchner

Submitted in fulfillment of the academic requirements for the degree of
Master of Science
in the School of Geological and Computer Sciences, University of Natal, Durban.
December 2002

As the candidate's supervisor I have/have not approved this dissertation for submission.

Signed: _____ Name: _____ Date: _____

ABSTRACT

With the extension of the Nchwaning Mine shaft complex in the Northern Cape Province, various geological and geotechnical complications needed to be identified in order to ensure correct use of tunnelling methods and support techniques. An understanding of the geological history of the area and the resulting geotechnical nature was important in defining the rock mass quality ahead of shaft development. A total of 12 geotechnical boreholes were drilled, and an additional 18 old boreholes revisited to accurately determine the stratigraphy, geological structure and associated weathering effects. Various soils and rock testing helped quantify the materials encountered.

Sands of the Gordonia Formation form the surface cover of this area, and together with the weathered calcrete, calc-arenite, conglomerate and clay, they form part of the Cenozoic Kalahari Group. The 30m thick basal unit of red clay is common throughout this region. This silty clay material is problematic in that it is expansive and hygroscopic. The clay unit rests unconformably on folded, faulted and highly weathered shale of the Proterozoic Lucknow and Mapedi Formations of the Olifantshoek Supergroup. Unconformably below this sequence lies the manganiferous ore deposits of the Hotazel Member, which is contained within the Voëlwater Formation of the Griqualand West Supergroup.

For the development of the decline shaft through the Gordonia Formation a box cut was excavated to a depth of 25m. The anticipated poor geotechnical conditions for a further 125m below the Gordonia sands called for high quality permanent tunnel support in the upper weathered horizons. Barton's Q-analysis was adopted as a recognized tunnelling quality index to predict and quantify the rock mass characteristics ahead of the shaft. The highly variable and generally low Q-values from borehole core analysis indicated that precast tunnel lining be used for 800m (at 11.5°) through the entire weathered Cenozoic sequence and into the weathered shales immediately below the Red Clay.

PREFACE

The work described in this dissertation was carried out through the School of Geological and Computer Sciences, University of Natal, Durban from March 2001 to December 2002, under the supervision of Professor Mike Watkeys and co-supervision of Professor Colin Jermy and Professor Rodney Maud.

This dissertation represents original work by the author and has not otherwise been submitted in any form for any degree or diploma to any other tertiary institution. Where use has been made of the work of others it is duly acknowledged in the text.

Signed:  Name: Richard Puchner Date: 28/04/2003

CONTENTS

	Page
1 INTRODUCTION	1
1.1 Background	1
1.2 Objectives	4
1.3 Fieldwork	6
2 PHYSICAL DESCRIPTION AND REGIONAL GEOLOGY	10
2.1 Physical Description	10
2.2 Regional Geology	10
3 DETAILED SITE GEOLOGY	16
3.1 Kalahari Group	16
3.2 Red Clay Layer	28
3.3 Lucknow Shale	37
3.4 Ongeluk Andesite	38
3.5 Structural Geology	38
3.6 Geohydrology	39
3.7 Weathering	44
4 ROCK PROPERTIES AND EXCAVATION	46
4.1 Box Cut Excavation	46
4.2 Shaft Excavation – Rock Strength	50
4.3 Shaft Excavation – Rock Mass Assessment	57
4.4 Q-Value Results and Rock Mass Subdivision	61
4.5 Current Tunnelling Practice	66
5 CONCLUSIONS	70
ACKNOWLEDGEMENTS	72
REFERENCES	73

LIST OF FIGURES

		Page
Figure 1.1	Site locality of Nchwaning mine and the Kalahari Manganese Field.	2
Figure 1.2	Site photograph of Black rock and Nchwaning mines.	3
Figure 1.3	Aerial photograph of Nchwaning No.3 Decline Shaft box-cut.	7
Figure 1.4	Photograph of rotary core borehole drilling ahead of the No.3 Decline Shaft development.	7
Figure 2.1	Distribution of and thickness of the Kalahari Group of southern Africa.	11
Figure 2.2	Simplified stratigraphic column at Nchwaning Mine.	11
Figure 3.1	Geological cross section of the entire No.3 Decline Shaft Complex.	17
Figure 3.2	Geological cross section of the upper section of the No.3 Decline shaft.	18
Figure 3.3	Simplified representative borehole log of BH4 and BH7 drilled on the No.3 Decline Centreline, Nchwaning Mine.	19
Figure 3.4	Core photographs of BH4 showing the typical profile of the Kalahari Group and Red Clay.	20
Figure 3.5	Core photographs of BH7 showing the typical profile of the Lucknow Shale immediately below the Red Clay.	22
Figure 3.6	Photograph of the No.3 Decline Shaft box cut showing the Gordonia sand profile.	26
Figure 3.7	Photograph of the pebble lag at the base of the Gordonia Formation.	26
Figure 3.8	Photograph of the silcrete mottling within the calc-arenites of the Kalahari Group.	26
Figure 3.9	Sketch face map of Red Clay and overlying conglomerate contact.	30
Figure 3.10	Photograph of a block of Red Clay showing the white, polished joint and slickensided surfaces.	30
Figure 3.11	Potential expansiveness graph of average clay percentage vs. average plasticity index of all the tested clay samples.	35

LIST OF FIGURES (continued)

		Page
Figure 4.1	Graph of the average corrected N value of all DPSH tests with depth through the Gordonias sands.	49
Figure 4.2	The relationship between phi (friction angle) and depth through the Gordonias sands.	49
Figure 4.3	Comparison of inferred UCS from PLI testing with actual laboratory UCS results.	54
Figure 4.4	Calculated (inferred) UCS vs. depth from point load index testing carried out on Kalahari Group core samples from boreholes drilled along the No.3 Decline Shaft (BH2-BH5) and at the Vertical Person's Shaft (BH6).	55
Figure 4.5	Calculated (inferred) UCS vs. depth from point load index testing carried out within the Lucknow shale from boreholes drilled below the Red Clay layer (BH7 -BH9).	58
Figure 4.6	Graphs of Barton's Q-values vs. depth for each borehole drilled at the No.3 Decline Shaft (BH2-BH5) and at the Vertical Person's Shaft (BH6).	63
Figure 4.7	Graph of Barton's Q-values vs. depth within the Lucknow shale from boreholes drilled below the Red Clay layer (BH7 – BH9).	65
Figure 4.8	Photograph of the ITC machine and its conveyor belt 'tail'.	67
Figure 4.9	Photograph of the ITC machine as it begins the tunnelling into the weathered Kalahari Group calc-arenite.	67
Figure 4.10	Photograph of the sinking of the caisson of the Vertical Person's Shaft.	68

LIST OF TABLES

		Page
Table 1.1	Summary of all boreholes drilled.	8
Table 3.1	Summary of Gordonia sand grading and indicator and shear/phi test results.	24
Table 3.2	Averages of Gordonia sand grading and indicator and shear/phi test results.	24
Table 3.3	Summary of Red Clay XRD and XRF test results	31
Table 3.4	Summary of laboratory test results carried out on the Red Clay from grab and BH3 samples.	34
Table 3.5	Comparison of averages of laboratory test results carried out on the Red Clay from grab with BH3 samples.	36
Table 4.1	Summary of Penetrometer test results at the Box-cut.	47

LIST OF TABLES (in Appendix A)

Table A1	Face map summary during excavation of the No.3 Decline Shaft.	
Tables A2 a-p	Gordonia Formation Calculated Phi Values from tests DPSH1-DPSH16.	
Tables A3 a-h	PLI and calculated UCS for boreholes BH2-BH9.	
Tables A4 a-h	Calculation of Q value per core run of boreholes BH2-BH9.	

LIST OF APPENDICES

Appendix A	Data Tables
Appendix B	Borehole Logs
Appendix C	Laboratory Test Results

NOTE:

*All appendices are contained on the attached compact disc.
Only example sheets have been printed.*

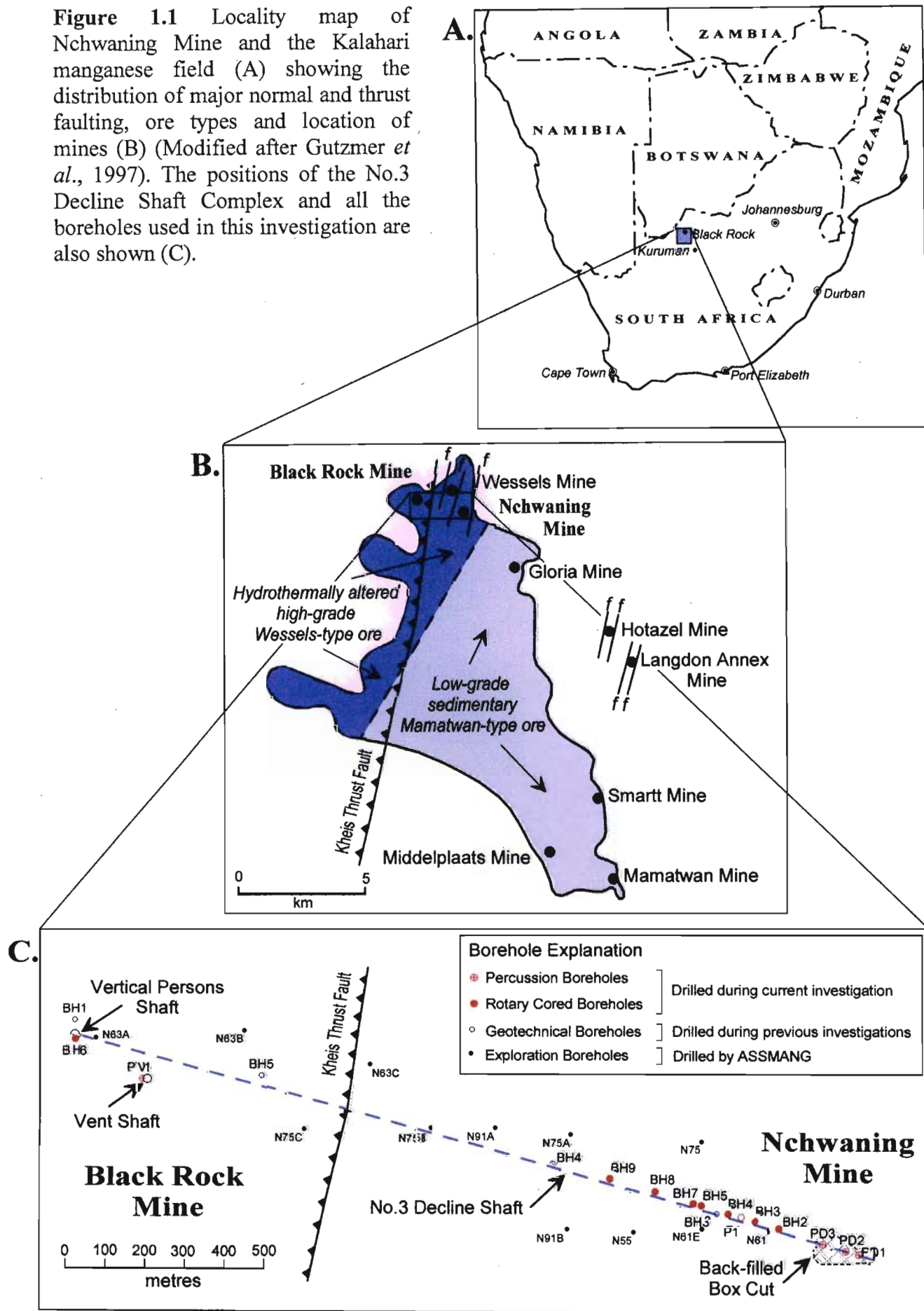
1 INTRODUCTION

1.1 Background

The small mining towns of Hotazel and Black Rock are approximately 70km north of Kuruman in the Northern Cape Province, South Africa (Figure 1.1). Their associated mines are well known for producing high-grade manganese ore from the Early Proterozoic Kalahari Manganese Field, which is amongst the largest land based sedimentary manganese deposits in the world (Kleyenstüber, 1984; Gutzmer *et al.*, 1997). The mine associated with Black Rock, Nchwaning Mine (Figure 1.1 and Figure 1.2), is currently extending its shaft complex by the addition of another decline shaft and associated vertical person's and ventilation shafts. The new 9m wide decline shaft (Nchwaning No.3 Decline Shaft) is inclined at 11.5° and will continue for 2.1km at the same gradient, where it will link up to the Vertical Person's and Ventilation shafts, some 400m below surface. Various geological and geotechnical complications had to be identified to ensure correct tunnelling methods and support techniques were employed, particularly within the weathered upper units. Prior to tunnelling through the varied geology, a box cut was excavated to facilitate entry of the decline shaft through the upper 20m of sand (see Figure 1.3).

The Kalahari region is characterized by low rainfall of less than 250mm per annum (Thomas and Shaw, 1990), high rates of evapotranspiration, and a general lack of surface water. Most of the Kalahari Manganese Field is buried beneath a cover of Cenozoic deposits comprising wind blown sands of the Gordonia Formation, as well as calcretes, calc-arenites, conglomerates and a thick unit of clay (SACS, 1980; Tankard *et al.*, 1982). All these units form the Kalahari Group. In the area of study, these sediments attain a thickness of up to 90m. The Kalahari Group has a relatively long history of study by previous authors (e.g. Du Toit, 1954; Thomas and Shaw, 1990; Haddon, 2000), but the remoteness of the terrain, poor exposure, and lack of suitable fossils for dating purposes, has resulted in an unclear understanding of their age and depositional history.

Figure 1.1 Locality map of Nchwaning Mine and the Kalahari manganese field (A) showing the distribution of major normal and thrust faulting, ore types and location of mines (B) (Modified after Gutzmer *et al.*, 1997). The positions of the No.3 Decline Shaft Complex and all the boreholes used in this investigation are also shown (C).



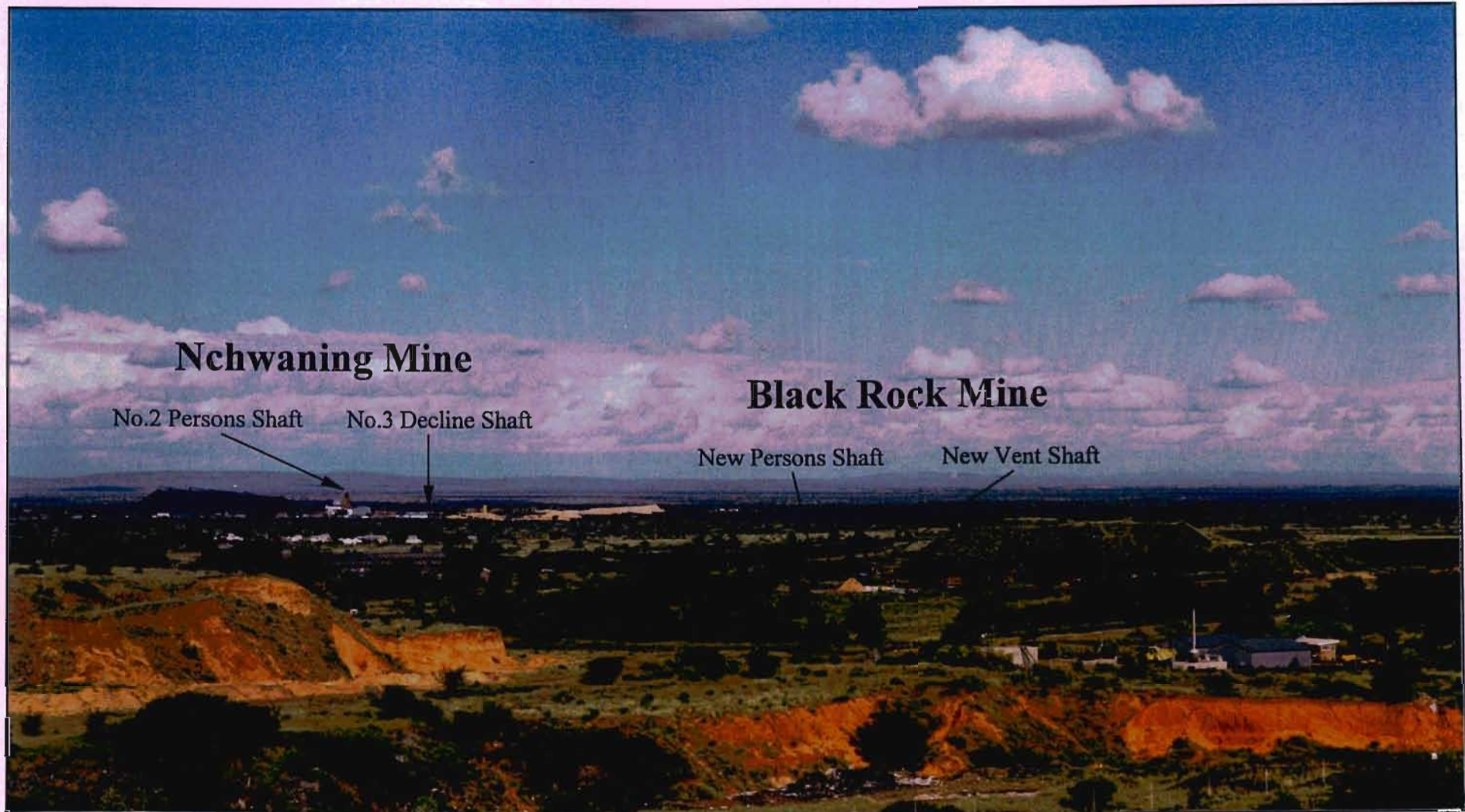


Figure 1.2 View south of the site showing the relative positions of the Black Rock and Nchwaning Mines. The approximate centreline of the No.3 Decline shaft is indicated by the dashed line. (Photograph: R. Puchner, March 2002)

The excavatability of the Cenozoic rock poses many problems mainly due to its weathered nature. However one unit of particular concern is a 30m thick unit of red clay. This clay is problematic in that it is expansive and incredibly hygroscopic. Not noted before from the previous geotechnical investigation of the No. 3 Decline Shaft (Warkwick and Spears, 1998) the Mesozoic shale of the Lucknow Formation below the clay unit has experienced intense faulting with associated folding. Ground water has been able to penetrate deep into the steeply dipping faults and facilitate weathering to over 100m below current ground level.

Geotechnical investigations carried out in this study along the centreline of the new decline shaft focused on determining the geotechnical nature of the upper calcified Kalahari Beds above the red clay layer, as well as the stratigraphy and geological structure of the rock mass immediately below the red clay layer. The red clay layer is well known in this area due to its very problematic nature. The red clay comprises a silty clay which is highly active and ranges in thickness from 25 to 35m. The upper unconformable scoured contact, below the Kalahari Group, is at approximately 64 to 68m below surface. The basal contact of the clay unit is 90 to 100m below surface and appears to rest unconformably on weathered shale bedrock.

Poor geotechnical conditions were anticipated and some concerns were raised as to the need for high quality permanent tunnel support in this zone. In order to establish a basis for understanding the rock mass characteristics of the weathered ground above and below the red clay layer, the Q-analysis procedure of Barton (1988) was adopted as a recognized tunnelling quality index. For this analysis, it was necessary to generate a number of rock mass parameters from the borehole core logging.

1.2 Objectives

When faced with rock, whether it be on surface for construction purposes or below surface for tunnelling, one must consider the characteristics of both the intact material as well as the discontinuities present within the rock mass. Input information needed for design purposes included geological characterization of

the rock mass in its natural state and was obtained from site investigations. According to Bieniawski (1984) geotechnical site investigations should provide an understanding of:

- a) Rock types to be encountered.
- b) Depth and character of overburden.
- c) Macroscopic scale discontinuities such as faults.
- d) Groundwater conditions.
- e) Special problems, such as weak ground or swelling rock.

All of these aspects are covered in this study. Pertinent parameters required for the understanding of the above points are obtained from the investigations in various ways. In this study these included data obtained from:

- a) Available geological maps, published literature and local knowledge.
- b) Geotechnical borehole drilling and core logging.
- c) Study of ground water conditions.
- d) Old exploration borehole log analysis.
- e) Rock sample testing.

From these data it was possible to prepare detailed geological sections showing all the lithological units present and more importantly the favourable and unfavourable zones in the rock mass. The close link between the rock mass classification and rock type, which includes its geological history in terms of tectonics and weathering, cannot be overlooked. To obtain a full understanding of the rock mass quality it is imperative to discover and disclose all the details pertaining to the pure geology of the site. It is the aim of this study to acquire a full understanding of the geology of the site before providing an assessment of the rock mass quality. This study will provide a closer look at the Cenozoic rock with a brief reference to the weathered shale immediately below in this manganese rich area around Black Rock in the Northern Cape.

As with the development of the Nchwaning No. 3 Shaft complex, other mines in the area may also extend their shaft complexes. A comprehensive understanding

of the geology to be intersected is critical to the design and excavation of the potential new shafts in the area. As part of the objectives in providing a link between geology and rock mass quality, it is hoped that this information may be of use for these new developments with similar geological complications.

1.3 Fieldwork

The field investigations involved the drilling of boreholes (percussion and rotary core) and the testing of soil consistency by means of Dynamic Probe Super-Heavy (DPSH) tests. The drilling of boreholes included three percussion holes for the box cut investigation (with 16 DPSH tests), eight rotary-cored boreholes to a maximum depth of 160m for the No.3 Decline Shaft investigation, one rotary-cored borehole to 105m depth at the Vertical Person's Shaft, and one percussion borehole to 150m depth at the Vent Shaft. A summary of the boreholes drilled is contained in Table 1.1. A plan of the site, Figure 1.1 shows the layout of the shaft complex and boreholes drilled in this investigation, and Figure 1.4 shows the drilling of a borehole from this investigation ahead of the No.3 Decline Shaft.

All the core drilled during this investigation has been geotechnically logged by the author. Point load index (PLI) testing was also conducted in the field on the borehole core and laboratory Unconfined Compressive Strength (UCS) testing was carried out on selected core samples. The drilling from surface through the sandy Gordonia Formation, the weathered Kalahari Beds, and the heaving red clay layer involved two methods of borehole drilling:

- a) The drilling through the sandy Gordonia Formation was done by means of washboring (poor material recovery) with immediate installation of temporary steel casing. Once through the sands diamond rotary core drilling was done with a NDW4 core barrel. This barrel is a split double-tube, which minimizes drilling vibrations and provides maximum core recovery. Poor core recovery was indicative of poor rock mass quality. The NX sized core is 54mm in diameter. Temporary casing was still needed within these units, especially when drilling through the conglomerate beds.



Figure 1.3 Aerial photograph showing a southward view of the Nchwaning No.3 Decline Shaft box-cut. (Photograph: C. McKnight, November 1999)



Figure 1.4 View southeast of rotary core borehole drilling ahead of the No.3 Decline Shaft development (Note the box-cut position near the orange spoil heap). (Photograph: R. Puchner, March 2000)

TABLE 1.1 Summary of Boreholes Drilled

Borehole Number	Percussion Drilled to (m)	Wash Bored to (m)	Rotary Cored to (m)	Comments
PD1	31.1	-	-	Percussion drilled though Gordonia Sands and stopped in calcrete.
PD2	30.1	-	-	Percussion drilled though Gordonia Sands and stopped in calcrete.
PD3	35.1	-	-	Percussion drilled though Gordonia Sands and stopped in calcrete.
BH2	-	19.5	68.3	Hole stopped due to collapse in red clay layer.
BH3	-	21.6	82.4	Hole stopped due to collapse in red clay layer. Piezometer installed.
BH4	-	52.5	115.3	Original hole collapsed at 66.6m. Re-drilled by percussion to 97.0m.
BH5	-	20.5	76	Hole stopped due to collapse in red clay layer. Piezometer installed.
BH6	-	14.5	105.5	Drilled at Vertical Person's Shaft. No red clay layer present.
BH7	100	-	150.6	Percussion drilled though red clay, and continued with rotary coring.
BH8	100	-	152.7	Percussion drilled though red clay, and continued with rotary coring.
BH9	130	-	157.8	Percussion drilled though red clay, and continued with rotary coring.
PV1	150.0	-	-	Percussion drilled only at Vent Shaft. Aquifer testing carried out.

b) Where the boreholes were required to penetrate the 30m thick clay layer into the underlying shale it was necessary to first drill a permanently cased pilot percussion hole (21.6cm diameter) to a depth just below the clay layer (approximately 90m below surface). Previous attempts of drilling through the clay with conventional diamond rotary core drilling, which involved drilling fluids, caused the hole to collapse and the drilling rods to become stuck within the hole. Once the percussion hole had been drilled and cased (done within 24hrs or the hole would also fail) the rotary core drilling (by means of a NDW4 core barrel) could continue. Rotary core drilling within the shale immediately below the clay also proved to be a great challenge. The highly weathered and broken shale caused drilling to proceed very slowly, and core recovery was very poor.

During the advance of the No.3 Decline Shaft numerous visits to the face of the tunnel were recorded by the author (Table A1 in Appendix A). The face maps of the geology encountered accurately corresponded to the core from the boreholes drilled ahead. A few samples of the red clay layer (and Gordonia Formation sands) were selected and tested in a commercial laboratory.

Piezometers were installed in select boreholes drilled along the No.3 Decline Shaft, and at the Vertical Person's Shaft. The water levels were monitored and recorded. A single hydrological percussion borehole was drilled at the Vent Shaft. Pump out and recovery tests were conducted to quantify the aquifer present within the conglomerate unit of the Kalahari Beds at the position of the Vent Shaft.

2 PHYSICAL DESCRIPTION AND REGIONAL GEOLOGY

2.1 Physical Description

The Black Rock area is situated on an inland plateau at an elevation of approximately 1000m amsl. The relief is generally low with a broad flat infilled valley of the low mountain ranges to the far east and west. The area of the Kalahari in which the manganese field is situated is referred to as the Gordonia region. It is relatively flat and sand covered, with arid type vegetation comprising scattered grasses and small thorned acacia trees and shrubs. Owing to the regions semi-arid nature no permanent surface water is found. The regional drainage pattern is northwards and the few river courses are ephemeral and flow extremely infrequently (Verhagen, 1985). The average annual rainfall is in the range of 150 to 250mm, of which some 60 per cent occurs in the months of January to April (Thomas and Shaw, 1990). Monthly evaporation rates can exceed the precipitation by a factor of six or more (Meyer *et al.*, 1985).

2.2 Regional Geology

The entire Early Proterozoic (2300 to 2100Ma) Kalahari manganese field (Gutzmer *et al.*, 1997) in the Kuruman area is covered by calcretized sediments of the Cenozoic Kalahari Group (Key *et al.*, 1998; Gutzmer *et al.*, 1997; Thomas & Shaw, 1990; Jennings, 1986; Nel *et al.*, 1986). Figure 2.1 shows the distribution and thickness of the Kalahari Group across southern Africa. The basin into which the Kalahari Group sediments were deposited is elongated in a north northeast to south southwest direction.

The Kalahari Group comprises up to 20m of windblown, unlithified sand of the Gordonia Formation (Pleistocene to Holocene), which unconformably overlies calcified sand, and gravel. The upper section of the Kalahari Group has undergone pedogenesis to form a thick capping of calcrete. The Kalahari Group is up to 65m in thickness and unconformably overlies a 30m thick red clay layer. The red clay layer in turn unconformably blankets the Olifantshoek Supergroup. Figure 2.2 provides a simplified stratigraphic column of the geology present at

WEST

EAST

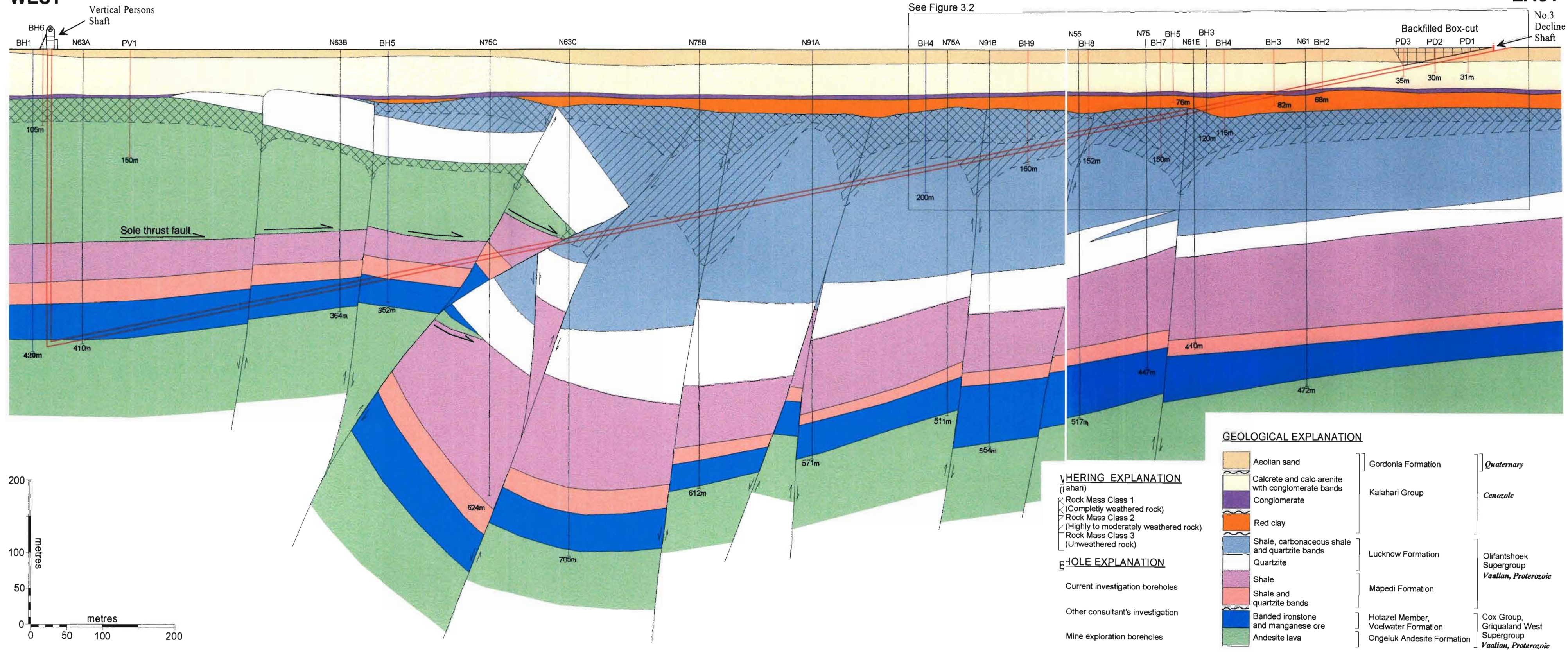


Figure 3.1 Geological cross section of the Nchwaning No.3 Decline Shaft Complex showing geological interpretation and weathering fronts.

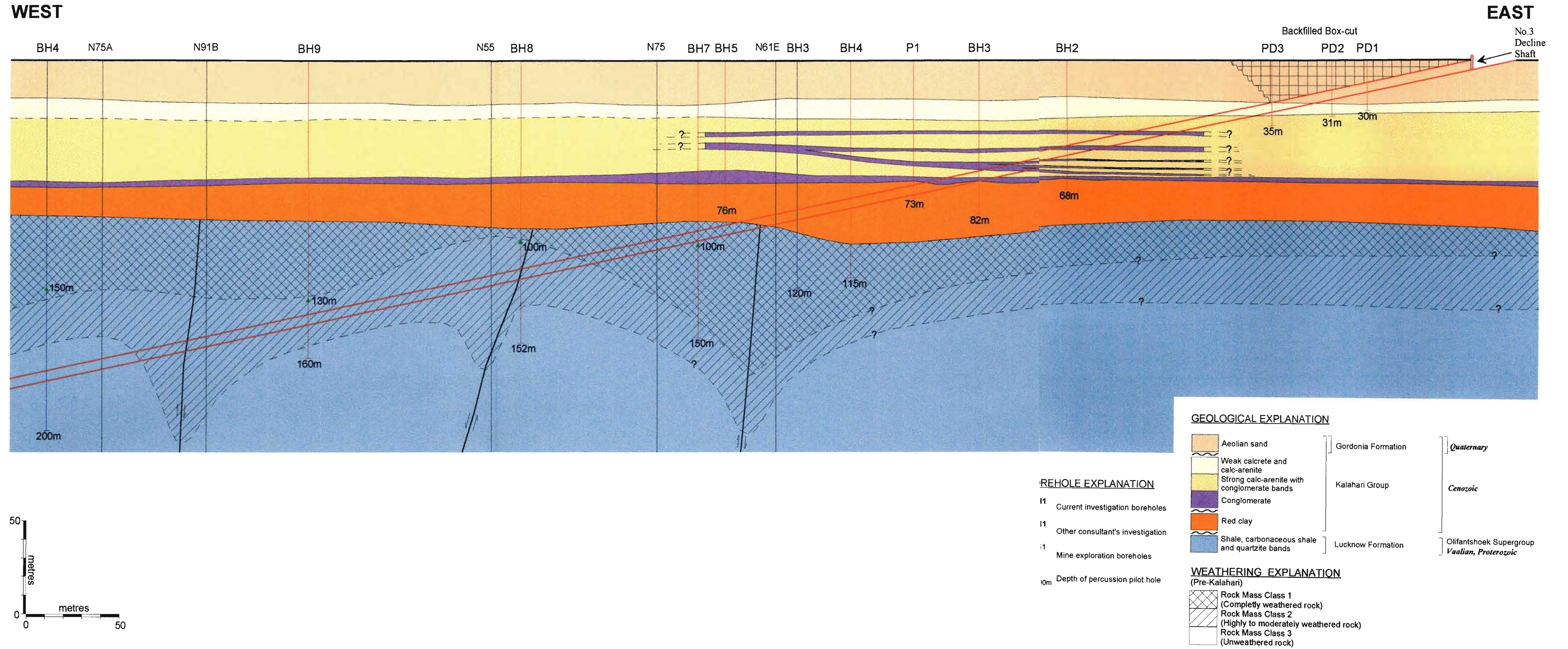


Figure 3.2 Geological cross section of the upper section of the Nchwane No.3 Decline Shaft through the weathered Cenozoic geology.

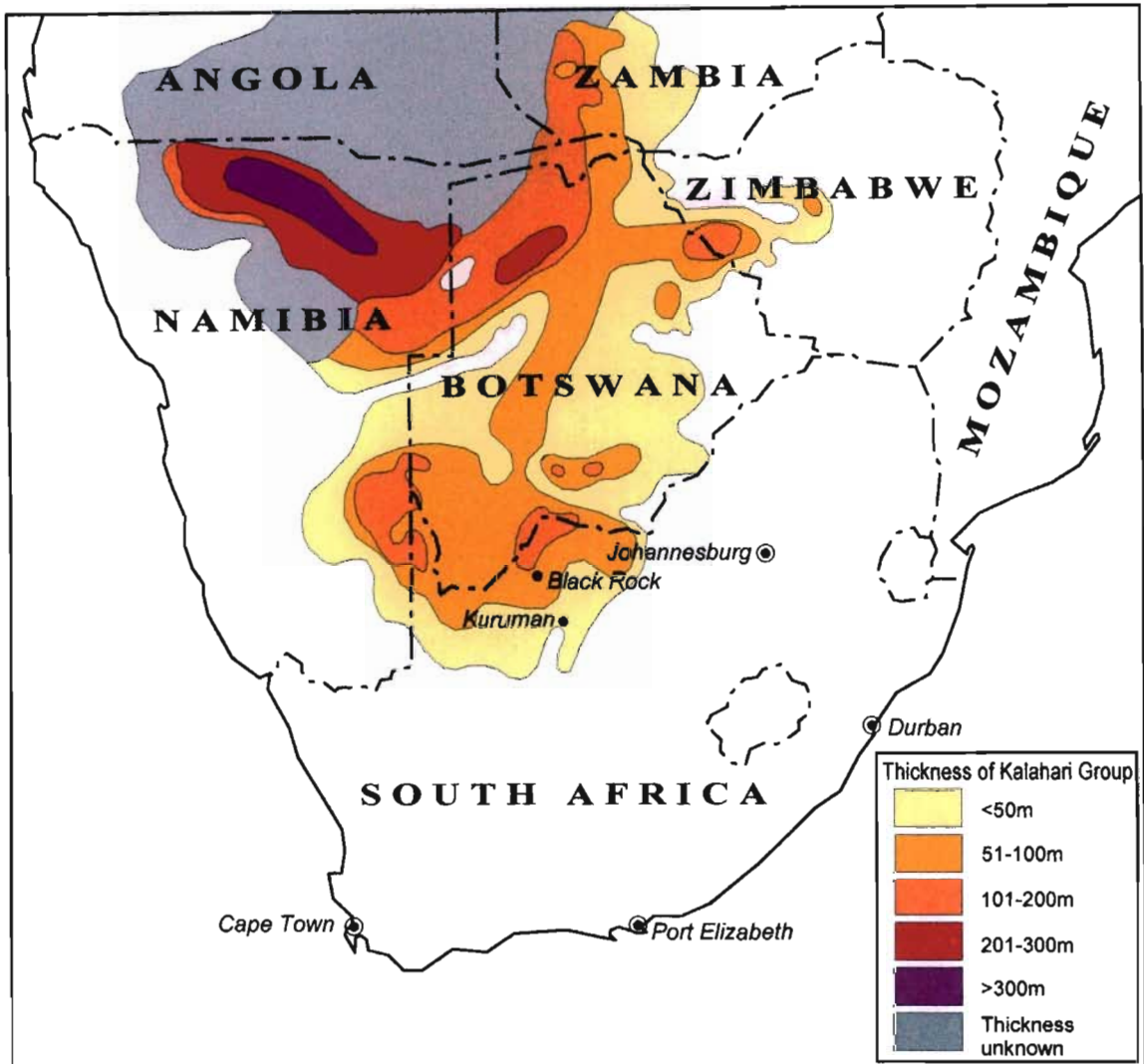


Figure 2.1 Distribution and thickness of the Kalahari Group of southern Africa (After Thomas and Shaw 1990, and Thomas and Shaw 1991).

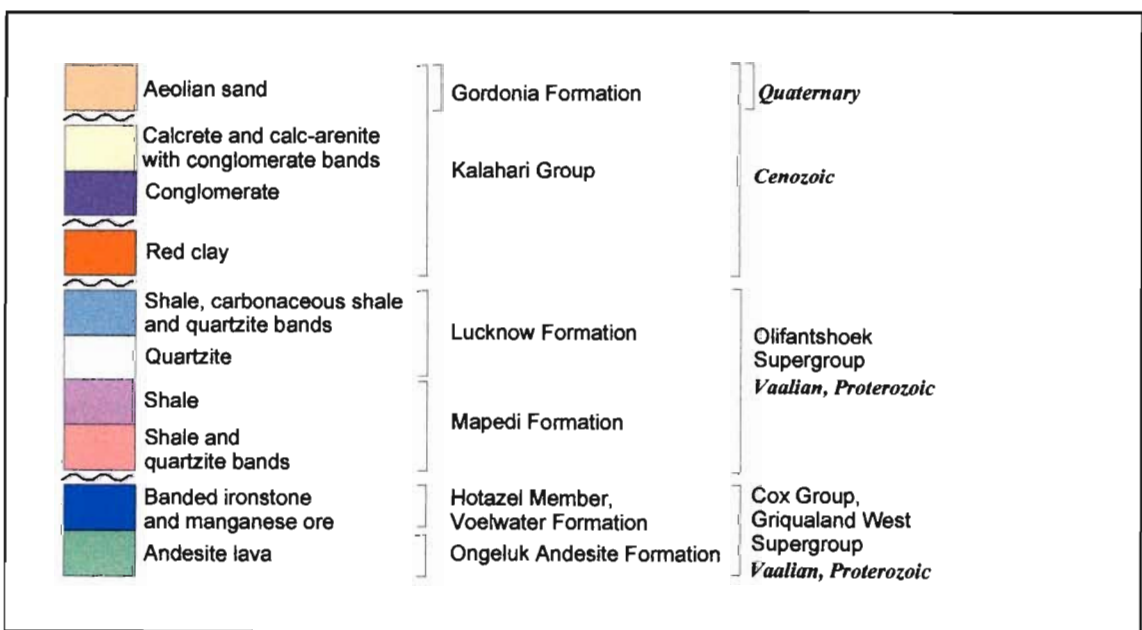


Figure 2.2 Simplified stratigraphic column of the geology encountered at Nchwaning Mine (After SACS 1980; Visser, 1984 and Grobbelaar et al., 1995).

Nchwaning Mine. The presented stratigraphic column has been adapted from SACS (1980), Visser (1984) and Grobbelaar *et al.* (1995) as well as from the findings of borehole drilling and tunnel excavation by the author.

The Olifantshoek Supergroup comprises shales and quartzites of the Lucknow Formation and are underlain by shales with quartzite bands of the Mapedi Formation. Unconformably below this sequence lies the volcanogenic-sedimentary jasperlites and manganese ore deposits of the Hotazel Member, which is contained in the Voëlwater Formation. Both the Voëlwater Formation and the underlying Ongeluk Andesite Formation form part of the Cox Subgroup, which in turn form part of the Griqualand West Supergroup. The Ongeluk lavas, which form the basal lithology of the area investigated, formed as a thick shallow-marine volcanic sequence of pillow lavas, massive flows and hyaloclastite (Cornell *et al.*, 1996). The volcanics attain a thickness of approximately 900m (Jennings, 1986). Both the Griqualand West Supergroup, and the Lucknow and Mapedi Formations of the Olifantshoek Supergroup, are Vaalian in age (Visser, 1984).

The entire sequence of pre-Cenozoic rock has been influenced by the Proterozoic Kheis and Namaqua orogenies (Grobbelaar *et al.*, 1995). Thrust faulting in the area provides evidence of compressional tectonics associated with the Kheis orogeny. The major thrust fault of Black Rock (described as a sole thrust) has been named as the Kheis Thrust by Beukes and Smit (1987). The Kheis Thrust spans more than 270km extending north of the Black Rock area and continuing south to the Rooinekke Mine (Grobbelaar *et al.*, 1995). At Black Rock the lithologies of the Voëlwater and Ongeluk Andesite Formation have been thrust onto the younger Mapedi Formation of the Olifantshoek Supergroup. The post-Kheis tectonothermal event occurred as the Namaqua (Kibaran) orogeny. Some of the pre-existing faults in the Black Rock and Rooinekke area were reactivated as gentle dextral shears and new faults and lineaments on a N-S trend developed (Grobbelaar *et al.*, 1995). Further evidence of this faulting is provided by work done on metamorphic and hydrothermal minerals in the area by Kleynstüber (1984) and Gutzmer *et al.* (1997). They state that the faulting supplied the hydrothermal fluids that upgraded the manganese ore, known as the Wessels type

ore of the Kalahari Manganese Field (Figure 1.1). After compressional stresses relaxed, a tensional stress field developed where the above mentioned structures reverted to normal faults, forming horsts and grabens. It is well documented that a prominent N-S trending graben structure exists between Black Rock and Nchwaning mines.

The presence of the Karoo Supergroup in the Gordonia area is well documented by various authors. From boreholes drilled in the Tshabong area of southern Botswana (to the northwest of the manganese field) Key *et al.* (1998) found two southwest-trending valleys infilled with lower Karoo Supergroup strata. These formations were identified as a thick basal glacial sequence of Dwyka Group tillites, followed by sandstones of the Eccca Group and overlying argillites of the Beaufort Group. Jennings (1986) indicates 50 to 180m of Dwyka tillite overlying the Voëlwater Formation at the Middelplaats Mine, some 20km south of Black Rock. Numerous exploration boreholes drilled in the Black Rock area identified Dwyka Group tillite occurring below the red clay layer. The presence of these tillites resting unconformably on Precambrian basement rocks provides evidence that the southern part of the Kalahari basin has been in existence from the Palaeozoic (Thomas and Shaw, 1991). Although there may well be Dwyka Group tillite and shale infilling palaeo-glacial valleys below the Kalahari Group in this area, this glacial lithology was not found in any of the boreholes drilled for the investigation of the No.3 Decline Shaft centreline, nor was it seen during the excavation of the tunnel.

For a long time the term Kalahari Formation has been used to describe the oldest post-Karoo deposits of the Kalahari. Where studies are done on Precambrian rocks of central southern Africa, the Kalahari beds form a “frustrating” mantle of continental debris (Key and Rundle, 1981). Although SACS (1980) states that the Kalahari deposits extend in age down to at least Paleocene to Oligocene, other authors suggest an earlier start to the formation of the Kalahari basin. Du Toit (1954) states that the development of the Kalahari basin started in the Cretaceous, Partridge and Maud (1987) say toward the end of the Cretaceous. However it seems most likely to have its earliest origins during the late Jurassic, related to the breakup of Gondwana (Haddon, 2000).

It is well known that climate during much of the Cretaceous was warm and humid (Tyson and Partridge, 2000), which not only allowed deep weathering mantles to develop (Partridge and Maud, 2000), but also facilitated rapid erosion and the formation of the African Erosion Surface (King, 1962). The epeirogenesis and widespread erosion of the weathered mantle characterized the Cenozoic history of southern Africa (Tankard *et al.*, 1982). Haddon (2000) states that much of the sediment accumulation occurred in arid or semi-arid climates between the Middle Miocene and the Upper Pliocene or Early Pleistocene, finally attaining an average thickness of 100-200m. Most authors concur that the main development of the Kalahari basin was during the Cenozoic.

SACS (1980) has created the Kalahari Group to include continental sedimentary strata of Quaternary alluvium and aeolian sand (i.e. Gordonina Formation), terrace gravels, surface limestone and silcrete. Although the Gordonina sands, the gravels, limestones and silcretes have been combined into one group (the Kalahari Group), a hiatus of unknown time is presumed between the Gordonina Formation and the rest of the Kalahari Group below. Due to the great expanse of the Kalahari Group, great variations occur in different units and their thicknesses. Thomas and Shaw's (1990) analysis of 320 borehole records of the Kalahari region have revealed a wide range of stratigraphic associations between the various lithological units of the Kalahari Group. They state that a typical stratigraphic description of the sediments on a regional scale is not possible, but a unit which is commonly present throughout the Kalahari area is the basal gravels and conglomerates. At Nchwaning Mine these overly a thick unit of red clay. The contact with the underlying red clay layer has been scoured and is irregular in topography. Conglomerate filled channels are preserved within the red clay. Rip up clasts of red clay are also preserved within the conglomerate.

Even though these red clays have been described by many authors (e.g. Du Toit 1954, Smit in SACS 1980 and Jennings 1986), sometimes as marls, it does not appear to have its own stratigraphic name. Locally it is simply referred to by the mines and the exploration drilling contractors as the "Rooi Klei" or Red Clay. The name Red Clay will be retained here. The Red Clay layer has been described

as filling in hollows of the pre-Kalahari surface (Thomas and Shaw, 1991) and this behaviour is noted from boreholes drilled in this investigation and from exposures seen during the development of the No.3 Decline Shaft.

Du Toit (1954) reported up to 60m of pink and red calcareous clays along the upper Molopo River in the northern part of the Northern Cape Province, occurring beneath limestone and chalcedonic quartzite (presumably the Kalahari Group). Smit (1974, in SACS 1980) defines a calcareous gravelly clay obtaining a maximum of 100 metres. At the Middelplaats Mine, Jennings (1986) indicates 25m of red clay. The Red Clay layer is also known to be present in the Sishen area, but only obtains a thickness of approximately 10m. Although Thomas and Shaw (1991) mention that the clay is impersistent in its distribution throughout the entire Kalahari basin, they agree that the Red Clay is indeed a laterally extensive massive unit within the southern tip of the basin.

The aeolian sand of the Gordonia Formation, which forms the cover sands of the area have been included in the Kalahari Group. Although the Kalahari sand commonly has the attributes of an aeolian deposit, it is not always possible to distinguish the wind and water lain units on sedimentological grounds alone (Thomas and Shaw, 1990). A gradational increase in reddening of the upper few metres of sand is clearly present in the Black Rock area. This is affected by many variables, including subsurface lithologies, climate, mineral availability and mobilization (Thomas and Shaw, 1991). A number of authors have attempted to provide an age for the Kalahari sand, however Thomas and Shaw (1991) say “we are no clearer today in determining the age of the Kalahari sand than were earlier workers”. The ages postulated range from Miocene to as late as Acheulean (Early Stone Age), but are probably Quaternary in age. Work done by Heine (1990) on the dunes of the western Kalahari also indicate a Quaternary age.

3 DETAILED SITE GEOLOGY

The surface borehole drilling investigations involved determining the ground conditions ahead of the No.3 Decline Shaft (specifically of the Kalahari Group, the Red Clay layer and the shales immediately below the clay) and have been correlated with the *in situ* geology as the tunnel advanced. Only the geological units encountered from these investigations carried out by the author are described in detail in the sections that follow. A geological cross section presented in Figure 3.1 provides a detailed illustration of the following geological units to be discussed and the entire No.3 Decline Shaft Complex. The geological section presented in Figure 3.2 shows a more detailed look at the Cenozoic geology of the upper section of the Decline Shaft. A merged and simplified borehole log of BH4 and BH7 (Figure 3.3) shows the Cenozoic geology, as well as the Lucknow shale immediately below the clay at the Nchwaning Mine. The core photographs of the presented borehole log illustrate the logged profile of the Kalahari Group and Red Clay (BH4, Figure 3.4) and the Lucknow Shale immediately below the Red Clay (BH7, Figure 3.5). The geology will be described from surface as encountered from borehole drilling.

3.1 Kalahari Group

With the exception of a small hill of black manganiferous rock to the west of Black Rock, the entire area surrounding the town and Nchwaning Mine is blanketed by orange sands of the Gordonia Formation. The Gordonia Formation comprises a layer of unconsolidated sands approximately 20m thick at the No.3 Decline Shaft. At the Vertical Person's and Vent Shaft it is only 6m thick (closer proximity to the Black Rock hill). The silty medium and fine sands are generally orange to pale brown in colour and slightly cemented. A gradational change of colour and grading occurs with depth within the sandy unit.

Evidence exists for both fluvial (Moore and Dingle, 1998) and aeolian depositional environments (Bond and Fernandes, 1974) for the Kalahari sands of the Gordonia Formation. Although the 20m of sands may have been deposited through alluvial processes, the Gordonia Formation sands were probably

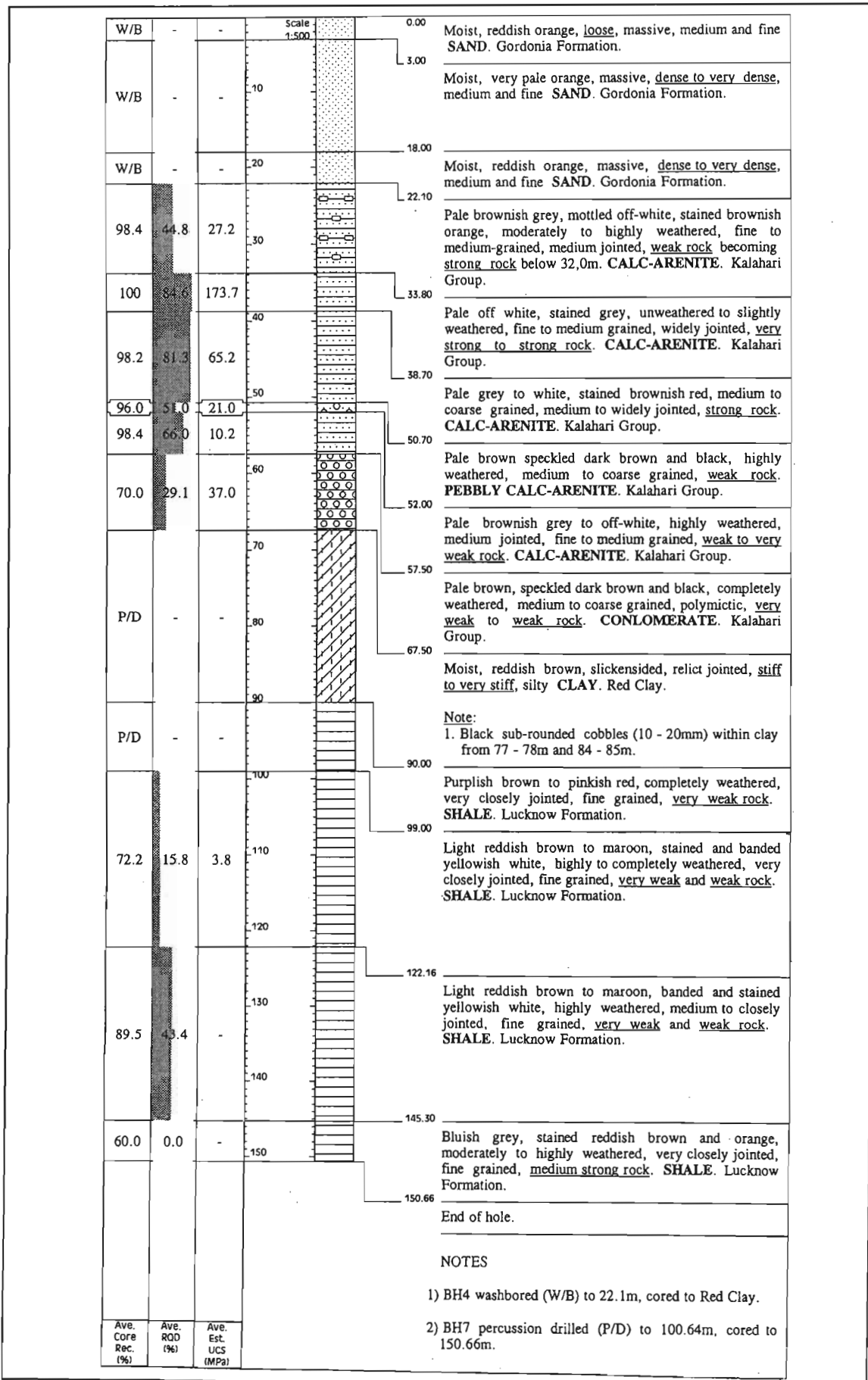


Figure 3.3 Simplified representative borehole log of BH4 and BH7 drilled on the No.3 Decline Centreline, Nchwaning Mine.



Figure 3.4 Core photographs of BH4 showing the typical profile of the Kalahari Group and Red Clay. (Photographs: R. Puchner, May 2000)

Borehole BH4

42.54m



Figure 3.4 (Continued) Core photographs of BH4 showing the typical profile of the Kalahari Group and Red Clay. (Photographs: R. Puchner, May 2000)



Figure 3.5 Core photographs of BH7 showing the typical profile of the Lucknow Shale immediately below the Red Clay. (Photographs: R. Puchner, July 2000)

reworked and deposited as aeolian dunes. Fossilized linear dunes in the area (Haddon, 2000; Helgren and Brookes, 1983; Heine, 1990) and the lack of fluvial gravel beds or channels within the unit further confirm this.

In the area of the No.3 Decline Shaft the upper 4.5 to 6.0m of the Gordonia Formation consists of moist, reddish orange, medium and fine grained sand. This material is cohesionless with a low clay content (2 to 8%). The aeolian sand becomes paler in colour with depth, changing to orange yellow below the oxidized layer (Figure 3.6). Natural moisture content varies with depth from 6% within the upper 12m to 3% below. In the basal drier zone, the material is usually more orange in colour. The sand deposit appears weakly stratified with lenses of very fine sand interlayered with slightly coarser material.

The abovementioned soils testing, and all other physical soils testing referred to from hereon, were carried out by Soiltech Laboratories in Johannesburg according to standard test methods (Standard methods of testing road construction materials TMH1, 1986). The relevant pages of the publication have been included in Appendix C.

Numerous samples of the Gordonia Formation sands were obtained at incremental depths from percussion drilling of the box-cut investigation. These samples were tested (at Soiltech Laboratories, Johannesburg) and the results of which have been summarised in Table 3.1. All original test results are contained within Appendix C.

Table 3.2 shows the averages of the laboratory test results above, which have been grouped into three arbitrary depth zones. It can be seen from the table that as the clay content increases with depth, the plasticity index increases slightly with depth. The natural moisture content is highest within the middle zone of the sandy unit and lowest in the lower 12 to 20m of the profile. This correlates to the highest silt content in the middle zone and the probable lack of hygroscopic movement of water beyond this zone to the lower zone.

TABLE 3.1 Summary of Gordonia Sand Grading and Indicator and Shear/Phi Test Results

Sample No.	PD 2/1	PD 2/2	PD 2/3	PD 2/4	PD 2/5	PD 2/6	PD 2/7	PD 2/8	PD 2/9	PD 2/10
Sample depth (m)	1.7	3.7	5.7	7.7	9.7	11.7	13.7	15.7	17.7	19.7
Liquid Limit	24.0	18.0	29.0	25.0	23.0	27.0	33.0	29.0	22.0	22.0
Plasticity Index	0.9	1.2	0.9	5.1	0.9	1.0	5.3	5.2	1.0	1.4
Nat. Moist. Cont.	4.4	5.7	5.8	5.7	5.5	5.7	3.2	3.4	3.1	3.3
% Gravel	0.0	0.0	0.0	0.0	0.0	0.1	0.0	0.1	0.1	0.1
% Sand	91.7	91.8	87.2	81.8	47.3	89.5	84.7	86.9	83.4	81.4
% Silt	6.1	6.0	7.7	12.4	46.9	4.6	8.4	8.0	8.2	10.9
% Clay	2.2	2.2	5.1	5.8	5.8	5.8	6.9	5.1	8.3	7.6
Unified Class	SP/SM	SP/SM	SM	SC/SM	ML	SM	SM	SM	SM	SM
Cohesion (kN/m ²)	12			17			16			
Friction angle N	30.7°			30.4°			31.4°			

TABLE 3.2 Averages of Gordonia Sand Grading and Indicator and Shear/Phi Test Results

Depth (m)	0 - 6	6 -12	12 - 20
Liquid Limit	23.7	25.0	24.3
Plasticity Index	1.0	2.3	2.5
Nat. Moisture Content	5.3	5.6	3.3
% Gravel	0.0	0.0	0.1
% Sand	90.2	72.9	83.9
% Silt	6.6	21.3	9.0
% Clay	3.2	5.8	7.0
Unified Class	SP/SM	SC/SM	SM
Cohesion (kN/m ²)	12	17	16
Friction angle N	30.7°	30.4°	31.4°

At the base of the aeolian sand there is a prominent medium to coarse grained gravel lag (approximately 50 to 100mm thick) of subrounded and rounded gravels which forms an unconformity with the underlying older calcretes (Figure 3.7). This layer is uncalcified and the base is gently undulating and varies from 21.0m to 22.5m depth. Passarge (1904, in Thomas and Shaw, 1991) also noted that the base of the Kalahari sands contained fluvial gravels in places.

The older calcified medium and fine grained sand deposits and conglomerate beds of the Kalahari Group lie below the Gordonia Formation. This material is residual calc-arenite that has been re-cemented as a pedogenic layer (calcrete). At the No.3 Decline Shaft the total thickness may vary from 24 to 28m, whereas at the Vertical Person's and Vent Shaft the Kalahari Group is 60 to 68m thick.

In the area of the No.3 Decline Shaft the calcified medium and fine grained sand deposits are fining upward arenaceous sediments. The upper 11 to 13m of this calcrete layer has deteriorated due to weathering into a friable weak to medium strong rock. Note that for description purposes the following strength categories of the International Society of Rock Mechanics (ISRM, 1981) were adopted:

<i>Description</i>	<i>UCS (MPa)</i>
Very weak rock	<5
Weak rock	5 - 25
Medium strong rock	25 - 50
Strong rock	50 - 100
Very strong rock	100 - 250
Extremely strong rock	>250

This calcrete layer is pale brownish grey in colour and stained pale orange brown, highly weathered, fine to medium grained, medium to very closely fractured rock. Irregular pockets of completely weathered calc-arenite do occur and the unit may range from strong to very weak in strength. Secondary calcretization is evident. There are patches of brown silicification (Figure 3.8), scattered fine rounded gravels and rip-up clasts scattered throughout this unit. Occasional slickenside surfaces are present. Joint surfaces may be stained brown,

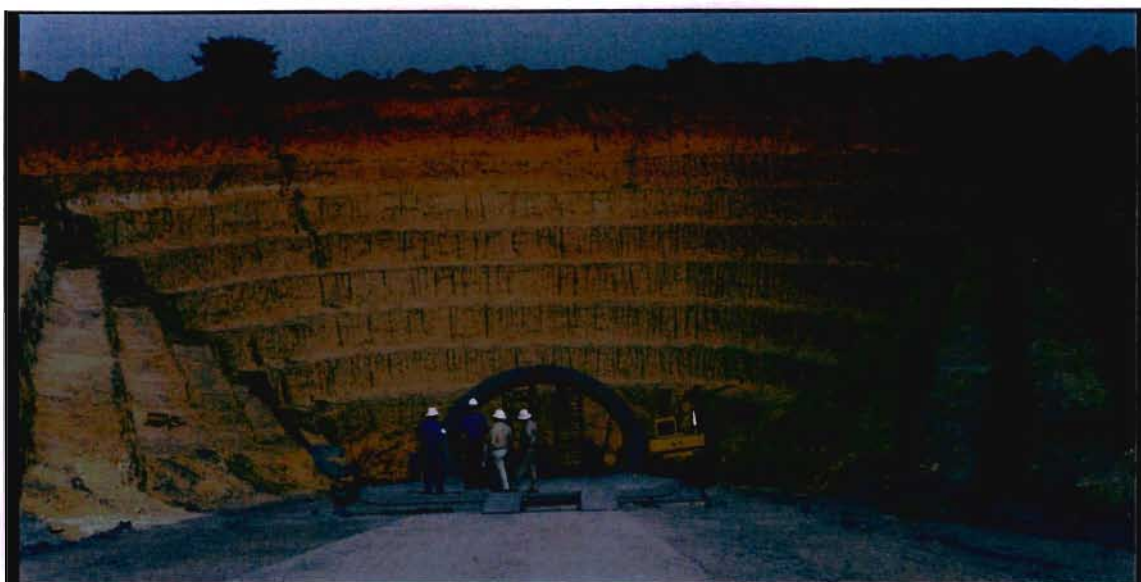


Figure 3.6 View westward of the No.3 Decline Shaft box cut showing the Gordonia sand profile. (Photograph: C. McKnight, November 1999)



Figure 3.7 The pebble lag at the base of the Gordonia Formation exposed in the No.3 Decline Shaft box cut. (Photograph: R. Puchner, March 2000)



Figure 3.8 Brown silcrete mottling within the calc-arenites of the Kalahari Group exposed in the No.3 Decline Shaft box cut. (Photograph: R. Puchner, April 2000)

and may have preserved within them fine rootlets. Small dissolution structures are occasionally present.

With depth, the calcrete layer becomes increasingly whiter in colour and stronger (very strong rock), with distinct zones of brown silicification mottles. The strong calc-arenite layer is 5 to 8m thick, massive and generally occurs from 31.5 to 39.5m vertical depth. It is off-white stained pink to pale red in colour and is more widely jointed. It may contain thin gritty or small pebble conglomerate bands. From approximately 39.5m depth, the calc-arenite becomes slightly weaker in strength, with a coarser grain size and variable colour from white to pale greenish brown. Slickenside surfaces are common and pebbly horizons appear. The core ranges in strength from weak to strong rock. Fine dissolution structures may be present.

The basal 6.5m to 17m of the Kalahari Group consists of highly weathered, medium to coarse grained fluvial gravel and cobble beds. These conglomerate layers are generally off-white to light brown in colour, becoming reddish brown as weathering increases. Predominantly a friable weak rock, this unit may tend to residual conglomerate. Completely to highly weathered weaker zones of rock often overlie more competent or impervious, less weathered zones.

The gravel channel lenses are polymictic and both clast and matrix supported beds occur. The matrix is generally medium to coarse-grained sand, varying in proportion relative to the conglomerate clasts. Clasts are sub-rounded and sizes vary from gravels to cobbles and boulders up to 250mm in diameter and include banded ironstone, shale and quartzite. Gravel channels and sandy bars appear to be laterally discontinuous. Evidence of such channels stems from borehole correlations (Figure 3.2) and from underground mapping within the No.3 Decline Shaft during advance (Figure 3.9). Interbedded sandy units occur and are cross-bedded and very friable. The degree of calcification is quite low and typically no matrix was recovered during rotary borehole drilling. Fracturing is not clearly defined as cobbles and boulders form the contact of rock breakages.

At the Vertical Person's Shaft the main calc-arenite occurs from 16.0m to 55.8m. The fine to medium grained calc-arenite is off-white to pale brownish green and highly weathered to moderately weathered. This layer ranges in strength from weak to very strong rock. Slickensided surfaces are also present as are minor fine dissolution cavities. Pale brown patches of silcrete commonly occur. From 55.8m to 68.0m (12.2m in thickness), there is a fining upward layer of fluvial gravels and cobbles of the deeply weathered basal conglomerate. The conglomerate band is polymictic and mostly clast supported. Rotary core drilling recovery was generally very poor due to the highly leached nature of the carbonate cement. The *in situ* strength of the unit is defined as a weak rock.

The Kalahari Group sediments are probably an aggrading fluvial fan (proximal and distal) deposit that formed as a result of epeirogenic uplift along the Griqualand-Transvaal axis to the south of Kuruman during the Late Cretaceous period (Partridge and Maude, 1987). The conglomerate layer is considered to be the basal unit of the aggrading Kalahari Group.

Where the No.3 Decline Shaft intersected the contact between the conglomerate and the clay layer, the depth from surface was approximately 3.0m deeper than anticipated from borehole correlations. Undulating erosion of the clay layer by local scour within a large alluvial system occurred into which channel fill was deposited. Face exposure on 6th August 2000 clearly showed the erosive nature of the contact (Figure 3.9).

3.2 Red Clay Layer

The intersection of No.3 Decline Shaft and the unconformable contact of the Kalahari Group conglomerate with the Red Clay layer clearly illustrates the channelised nature of the above conglomerates. A localized one metre deep scoured channel on the contact with the Red Clay layer is clearly recorded in Figure 3.9. The channels create an undulating contact which varies from approximately 64.5m to 69.0m below surface.

The 30m thick moist red to reddish brown clay layer is homogeneous and consists of very stiff heavily slickensided silty clay, with carbonate alteration along individual very smooth surfaces (Figure 3.10). The slickensided surfaces are continuous (over metres in length in places) and well polished. There appeared to be no pattern to their orientation. When the clay comes into contact with water, it becomes soft and highly unstable. Chemical analysis shows that this material contains palygorskite (laboratory testing discussed below).

It is believed by the author that the clay layer is completely weathered (by deep chemical weathering) lacustrine sediments which were deposited on the gently undulating African Surface (King, 1962) during the formation of the Kalahari basin. Thoughts for the source of the lacustrine deposits include air borne volcanic ash or outfall from a meteoric impact (pers. comm. McKnight 2001).

Explosive volcanic eruptions of the kimberlite province in the Cretaceous period could have provided the very fine grained material which was trapped in the watery repository. The clayey lacustrine sediments could also have been derived from a nearby meteoritic impact. The Late Jurassic Morokweng impact structure dated at 144 ± 1 Ma (Hart *et al.*, 2002) lies 100km to the north east of the town of Black Rock. It is almost entirely covered by the sediments of the Kalahari Group, reaching up to 110m in thickness (Andreoli *et al.*, 1999). Evidence of air-born tuffaceous material or fallout debris from the meteorite impact in the form of microscopic angular quartz shards was not found. The thin section analysis of the Red Clay carried out by Dr. Marco Andreoli of the Atomic Energy Corporation in Pretoria could only confirm the very fine and highly homogeneous nature of the clay.

X-ray diffraction (XRD) and X-ray fluorescence (XRF) testing was done on a random grab sample of the clay by a qualified laboratory technician at the University of the Witwatersrand (results are contained in Appendix C and summarised in Table 3.3 below).

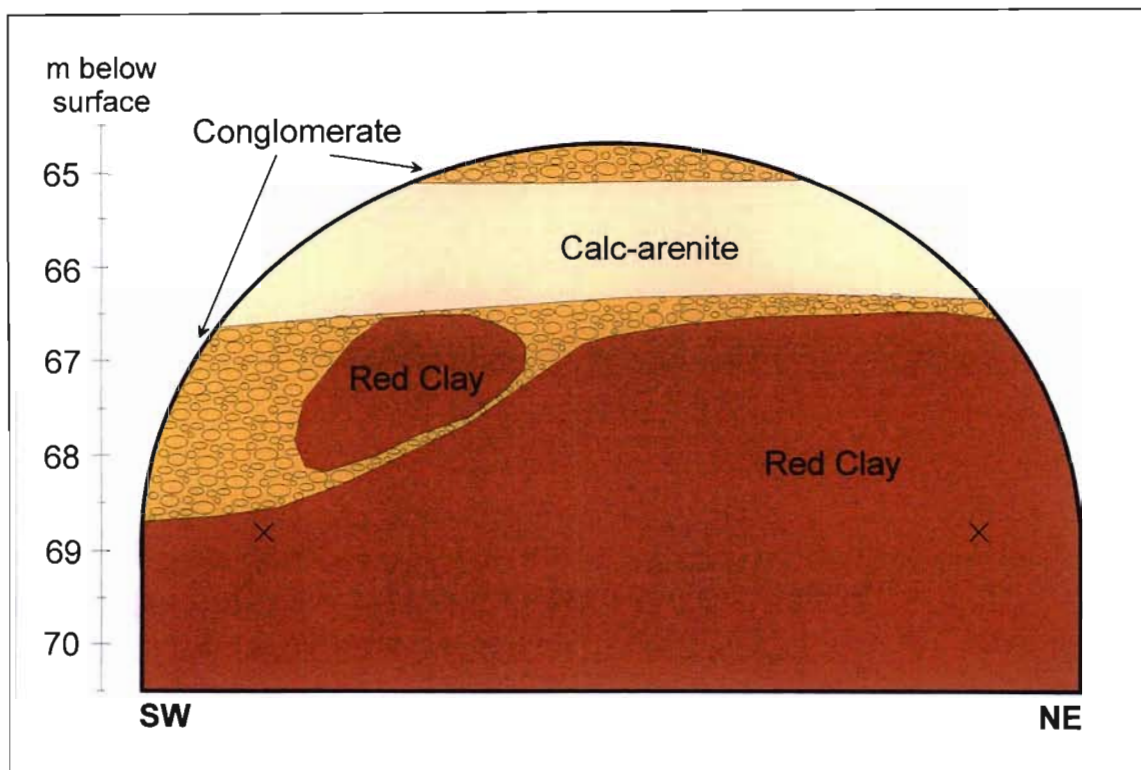


Figure 3.9 A sketch map of the exposed face of No.3 Decline Shaft at the contact of the Kalahari Group and the Red Clay.



Figure 3.10 A block of Red Clay obtained from the tunnel face shown in Figure 3.9. Note the polished white joint and slickensided surfaces. (Photograph: R. Puchner, December 2001)

TABLE 3.3 Summary of Red Clay XRD and XRF test results

Description	Results
<u>XRD</u>	
Quartz	46-1045
Dolomite	36-0426
Palygorskite	31-0783
Hematite	24-0072
Saponite (Fe)	12-0160
Magnetite	03-0863
<u>XRF</u>	
	<u>%</u>
SiO ₂	32.89
TiO ₂	0.50
Al ₂ O ₃	6.80
Fe ₂ O ₃	3.79
MnO	0.34
MgO	12.49
CaO	12.82
Na ₂ O	0.00
K ₂ O	0.15
P ₂ O ₅	0.06
LOI	30.43
TOTAL	100.26

The methodology of the testing was as follows. A Phillips PW1830 with a copper target tube was used for the XRD analysis. No treatments were used, only the sample powder was tested. The results were run through the Phillips PC-APD mineral identification software, and the best matches were chosen. For the XRF analysis of the major elements, a Phillips PW1400 with a rhodium tube was used on the fused sample. The Norrish and Hutton (1969) method was used for both the major and trace element testing. However for the trace element analysis the Phillips PW2404 (also with a rhodium tube) was used. The crushed and milled fine powder sample was mixed with a 2% mowiol (a polyvinyl glue) and pressed into a pellet within an aluminium cup with a pressure of 10 tonnes per square

inch. Matrix correlation was done by using the De Jongh model with Super Q software, which automatically calculates the concentrations.

The results of the XRD testing revealed that the main mineral composition of the sample was quartz, palygorskite and dolomite. The redness of the Red Clay suggests the presence of iron-rich minerals. When looked for, the presence of hematite and magnetite is possible, however their main peaks coincide with that of the dolomite peaks, and is thus not conclusive. Another possible mineral containing iron is saponite. This mineral was also not conclusive in the analysis.

The XRF results indicated the presence of high SiO_2 with CaO , MgO and lesser amounts of Al_2O_3 , Fe_2O_3 . Since no Na_2O was found, the suspected presence of montmorillonite was abandoned. The presence of palygorskite is confirmed by the relatively high content MgO .

In light of the high dolomite content of the clay sample it would appear that a sedimentary lacustrine deposit, rather than volcanic or meteoritic impact fallout, is the most likely origin of the Red Clay. Chamley (1989) says “a general correspondence exists between the mineral composition of most fresh water lakes and the average clay mineralogy of the rocks and soils in the surrounding drainage basins”. The dolomite content could have been transported by rivers flowing into the lake from chemically weathered dolomitic areas (Ghaap Plateau formed by the Campbell Group, Griqualand West Supergroup) to the northeast, east, southeast and south of Black Rock.

Although palygorskite is a relatively rare mineral, it may occur locally in abundance in certain lacustrine and peri-marine basins (Chamley, 1989). Several of the most extensive deposits of lacustrine Mg-smectites are characterized by thick beds of these clays, often in close association with deposits of the fibrous clay minerals palygorskite and sepiolite (Veld, 1995). The shallow water lacustrine occurrences required for the clay's formation are only found in arid to semi-arid climate settings adjacent to areas of intensive chemical weathering and subjected to strong evaporation and frequent mixing with supplies of fresh water (Veld, 1995).

Although palygorskite is not strictly a sheet silicate it has chemically absorbed water, similar to that of smectites, within its needle like structure (Veld, 1995). It is thus able to swell, and heave. The swelling Red Clay Layer is highly unstable, with very short stand-up times as observed in the decline tunnel and it exhibits a potential free swell strain of up to 15% (Warkwick and Speers, 1998). These high swelling pressures are possible once the clay material is exposed to additional water. When exposed to air for extended periods of time the clay desiccates and the stability begins to deteriorate as small slabs fall off the decline face. This was evident when the material was exposed within the No.3 Decline Shaft tunnel. Numerous failures in the tunnel roof and from the decline face in the form of large slumps occurred during excavation.

A clay layer in the vicinity of the Vertical Person's and Vent Shafts has been previously misinterpreted as being the equivalent of the Red Clay layer. From these investigations it has been identified as completely weathered andesite. Where the clay material at the Decline Shaft is a red sedimentary deposit, the clay at the Vertical Person's and Vent Shafts is in fact pale orange, completely weathered andesite. The gradational weathering effects of which were clearly visible in a borehole (BH6) drilled at the Vertical Person's Shaft.

A number of samples of the Red Clay layer were taken from BH3 as core samples and from the tunnel face as grab samples during the advance of the No.3 Decline Shaft. The laboratory results of both sampling methods has been summarised in Table 3.4 (The original laboratory results from Soiltech in Johannesburg are contained within Appendix C). The results of laboratory testing show that the clay layer is actually a clayey silt (MH) and is potentially highly active and nearly fully saturated. Prior to any testing done on the clay, it was suspected that the potential expansiveness of the clay was high. When plotting the average of the clay percentage versus the plasticity index of all the tested clay samples, it plotted within the high to very high zones of the Potential Expansiveness graph of van der Merwe (1964) (Figure 3.11). The clay shows some grading with depth, where the silt and clay percentage increases and the sand percentage decreases. The *in situ* moisture content shows no apparent trend with depth, and averages 23.6%.

TABLE 3.4 Summary of Laboratory Tests Carried out on Red Clay Grab Samples from the No.3 Decline Shaft and From Borehole Core Samples

Description	Grab Sample Results							Borehole Core Results		
	8/8/	6/8/	8/8/	9/8/	12/8/	18/8/	21/9/	20/4/	20/4/	20/4/
Date Sampled (/2000)	8/8/	6/8/	8/8/	9/8/	12/8/	18/8/	21/9/	20/4/	20/4/	20/4/
Sample No.	A2	MC1	MC2	MC3	MC4	MC5	MC6	BH3/1	BH3/4	BH3/5
Depth below surface (m)	68.76	68.00	68.76	68.94	69.78	71.78	78.50	65.37	75.57	76.76
Liquid Limit (%)	n/t	65.1	66.6	70.4	67.4	74.3	88.4	84.8	71.7	93.4
Plastic Limit (%)	n/t	43.6	39.2	44.7	43.8	45.8	46.2	51.8	40.7	39.7
Plasticity Index (%)	n/t	21.5	27.4	25.8	23.6	28.5	42.2	33.0	31.0	53.7
Moisture Content (%)	23.8	23.8	26.3	20.8	22.1	24.3	23.9	27.8	26.3	28.2
Liquidity Index (%)	n/t	-0.92	-0.47	-0.93	-0.92	-0.75	-0.53	-0.73	-0.46	-0.21
Linear Shrinkage (%)	n/t	10.7	13.3	14	13.3	16.7	16.7	14.0	14.0	19.3
Gravel (%)	n/t	0.1	0.0	0.0	0.0	0.0	0.2	0.0	0.0	0.0
Sand (%)	n/t	15.1	8.6	6.4	5.3	12.4	0.1	9.1	11.4	8.9
Silt (%)	n/t	60.2	48.2	54	67.8	56.3	72.2	53.1	47.2	42.5
Clay (%)	n/t	24.7	43.2	39.6	26.9	31.2	27.5	37.7	41.4	48.6
Potential Heave	n/t	Med.	high	high	Med. to high	high	n/t	Very high	high	very high
Classification	n/t	MH	MH	MH	MH	MH	MH	MH	MH	MH
Dry Density (kg/m ³)	1650.0	1168.1	1609.4	1704.5	1635.3	1493.3	1591.0	1554	1554	1511
Initial Void Ratio (e)	0.649	1.386	0.713	0.548	0.563	0.771	0.723	n/t	n/t	n/t
Specific Gravity (G _s)	2.72	2.787	2.756	2.638	2.556	2.644	2.742	n/t	n/t	n/t
Deg. of Sat. (S _r) %	100	48	102	100	100	83	90.6	n/t	n/t	n/t
Est. Overburden (kPa)	1550	1550	1550	1550	1550	1550	1550	1550	1550	1550
Pre-Consolidation (kPa)	1700	1700	1700	1700	1700	1700	1700	1700	1700	1700
Approx. OCR	1.1	1.1	1.1	1.1	1.1	1.1	n/t	n/t	n/t	n/t
Free Swell Strain (%)	12.7	n/t	n/t	n/t	n/t	n/t	n/t	n/t	n/t	n/t
Swelling Pressure (kPa)	1200	n/t	n/t	n/t	n/t	n/t	n/t	n/t	n/t	n/t
Stiffness (wet) (kPa)	7.3	n/t	n/t	n/t	n/t	n/t	n/t	n/t	n/t	n/t
Cohesion (kPa)	n/t	n/t	n/t	n/t	n/t	n/t	n/t	74	74	78
Friction Angle (phi)	n/t	n/t	n/t	n/t	n/t	n/t	n/t	26.6	22.3	21.2

n/t = Not tested

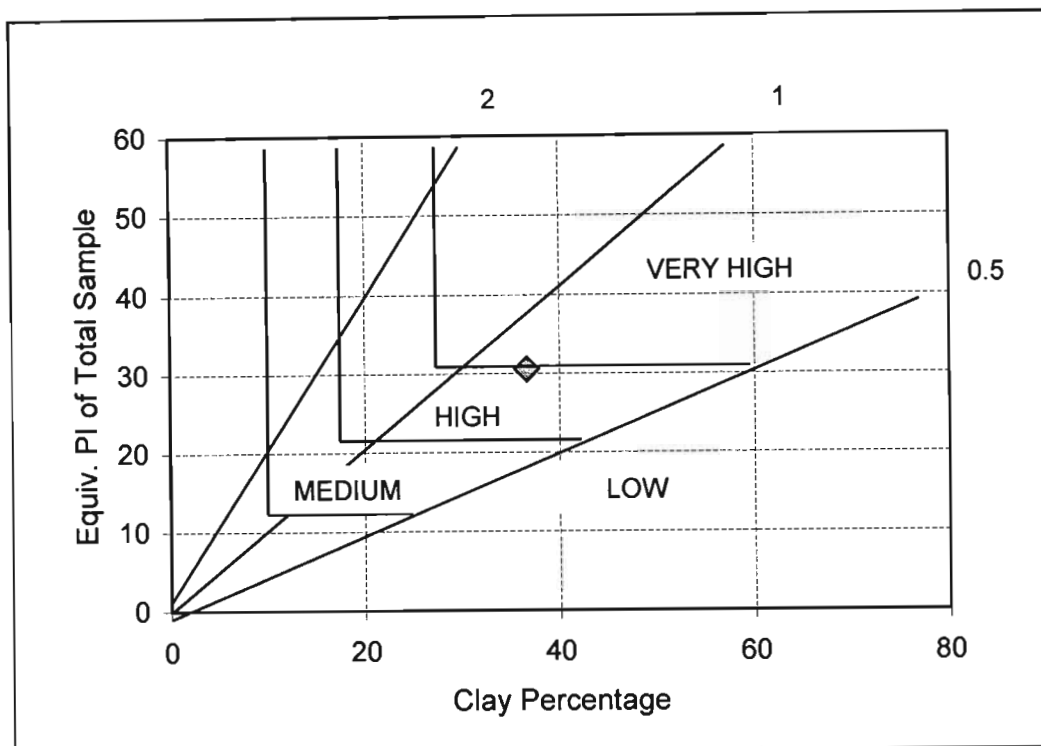


Figure 3.11 Potential expansiveness graph of average clay percentage vs. average plasticity index of the tested Red Clay samples (after van der Merwe, 1964)

The liquid limit of the grab samples increases with depth, ranging from 65.1 to 88.4%. The plasticity index and linear shrinkage also increases with depth ranging from 21.5 to 28.5% and 10.7 to 16.7% respectively. All samples tested provided an average dry density of 1545kg/m^3 and a specific gravity of 2.7.

During borehole drilling the clay reacted quickly with the drilling fluid (water and 'Ezee-mix') and broke down rapidly to a highly plastic silty clay. This reaction with water was also noticed during the excavation of the No.3 Decline Shaft. The core samples obtained from BH3 (prior to the decline shaft's excavation) were thus not of *in situ* moisture content. Although larger intact core samples less influenced by the drilling fluid were selected, the moisture content was still affected. This is apparent in Table 3.5, which compares the average laboratory results of the core samples with the average laboratory results of the grab samples. It can be seen that the moisture content is slightly higher in the core samples.

TABLE 3.5 Comparison of Average Red Clay Grab and Average Red Clay Borehole Core Laboratory Test Results

Description	Results (Average)	
	Grab	Core
Sample Type	Grab	Core
Depth below surface (m)	70.65	72.57
Liquid Limit (%)	68.8	83.3
Plastic Limit (%)	43.4	44.1
Plasticity Index (%)	25.4	39.2
Moisture Content (%)	23.6	27.4
Liquidity Index (%)	-0.80	-0.47
Linear Shrinkage (%)	13.6	15.8
Gravel (%)	0.02	0.00
Sand (%)	9.6	9.8
Silt (%)	57.3	47.6
Clay (%)	33.1	42.6
Potential Heave	high	very high
Classification	MH	MH
Dry Density (kg/m ³)	1550.2	1539.7

Other comparisons between the two sample types include variations in the liquid limit and plasticity index, which are also higher in the core samples. This relates to the higher silt content and the lower clay content of the grab samples. These variations, linked to the grading properties of the material, are not clearly explained between core and grab samples. It could be that the differences in grading of the clay do not only occur vertically in stratigraphy, but horizontally too. The results of the clay from the face of the No.3 Decline Shaft were generally fully saturated. Despite this high degree of saturation, the clay still has the ability to swell enormously if saturated.

The reason for this huge hygroscopy of the clay is that the measured saturation ratio only accounts for the free water in the sample. As the clay is known to contain palygorskite (magnesium-rich 2:1 clay), the 2:1 layer lattice is able to adsorb water both within and around the individual clay minerals. As additional

water is absorbed into the clay minerals, swelling occurs. Upon full saturation, the swelling pressure that can be exerted will be in the order of 1200kPa. The calculated swell percentage is 3 to 4%. The amount of heave will be proportional to the thickness of clay wet up below the floor panels. Thus it was deemed imperative that water be kept away from the red clay exposed within the No.3 Decline Shaft. This was however not always possible.

The calculated free swell strains of the clay range from 3 to 15% (Warkwick and Speers, 1998) and the Atterberg limits clearly reflect this property. The clay material is over-consolidated ($LI < 0$) with a high to very high linear shrinkage. Due to poor quality samples being recovered from the borehole core, no further free swell tests were carried out. The shear strength parameters are for remoulded saturated samples and show an unusually high friction angle. For design purposes, it was recommended that safe values of $C = 75\text{kPa}$ and $\phi = 0$ degrees be utilized.

3.3 Lucknow Shale

Underlying the Red Clay is a layer of completely weathered, residual shale of the Lucknow Formation. This material is white to pale brown in colour, closely to moderately fractured with fine secondary dissolution cavities. It is believed that the previously weathered shale was further weathered during the same chemical weathering period that affected the overlying clay sediments. The calcification occurring in places within the shale could have originated from the dolomite rich Red Clay above.

From percussion drilling fine gravel-sized fragments of yellow brown residual/very weak rock shale are the only indication of the material immediately below the Red Clay layer. In some exploration boreholes drilled (and logged) by the mine this material had been erroneously referred to as calcrete of the Kalahari Group, and could be misinterpreted as Dwyka tillite from percussion chip logging. From the bedding orientations of the Lucknow shales logged from borehole core, and confirmation from what was seen upon excavation of the No.3 Decline Shaft, the shale contains medium scale asymmetric folds. Localized

chevron type folding may be more apparent adjacent to the main dislocations. The shale layers within the sequence acted as a high strain zone during major tectonic events.

The limit of the weathering and appearance of unweathered shale is highly variable, but is not expected to be shallower than 120m below ground level. The variable depth of weathering appears to be controlled primarily by the major faulting identified from borehole correlations (Figure 3.1).

3.4 Ongeluk Andesite

The Cenozoic stratigraphy at the Vertical Person's Shaft is similar to that which occurs at the No.3 Decline Shaft, but differs in that there is no Red Clay layer. Andesites of the Ongeluk Group occur immediately below the Kalahari Group here.

The borehole drilled adjacent to the Vertical Person's Shaft intersected pale orange to dark orange brown, completely weathered andesite from 68m to 91.5m. This material has been deeply weathered below the African Erosion Surface to form slightly to moderately plastic, clayey and fine sandy silt, with relict fine calcite veining and fractures. This material ranges from very stiff residual soil to weak rock. Below 91.5m, the less weathered andesite becomes green in colour and tends to medium strong rock.

3.5 Structural Geology

As discussed previously and confirmed by boreholes drilled in the Black Rock area, the bedrock layers below the Kalahari Group sediments are intensely thrust and faulted (Figure 3.1). It is not the intention of this investigation to describe the engineering geological nature of the pre-Cenozoic bedrock layers or the tectonics involved in their deformation. However the following important points can be noted.

From the analysis of old mine exploration boreholes and current geotechnical boreholes, a single plane interpretation of the local structural geology (along the No.3 Decline Shaft centreline) has been produced (Figure 3.1). The major structural feature identified in this area, the near horizontal sole thrust fault or Kheis Thrust, is indeed present to the west (confirmed by the mine). During this event the basal Ongeluk andesites were thrust over the mangiferous Hotazel Member and Mapedi Formation. Evidence for this thrust feature was seen during the sinking of the Vertical Person's Shaft. Brecciated andesite occurred at the contact with the shale of the Mapedi Formation. This porous brecciated contact zone also serves as an effective conduit for ground water, which provided difficulties during the sinking of the shaft below this point.

Eastwards at the toe of this feature are a series of fault-bound wedges, creating a large graben-type feature. The steep faults continue to the east creating large stepped blocks, giving the impression of strata dipping to the west. These near vertical structures would have played a large role in controlling the infiltration and migration of ground water, and as a result weathering patterns will display some degree of correlation to the spatial distribution of these major fractures. The basal weathering front is quite variable over short distances as weathering has shown to penetrate deeper along these zones of major fracturing.

A cavity was intersected in BH8 and could probably be a result of large tension gashes that are present close to fault zones. It is also possible that such cavities have developed as a result of wash-out of residual soil during the intense weathering event.

3.6 Geohydrology

Groundwater also plays an important role in rock mass stability. Water on joints decreases the rock mass strength considerably, and thus plays an important role when excavating through it. The Kalahari region has low rainfall and high rates of evapotranspiration, with a general lack of surface water. According to Verhagen (1985) the ground water of the Gordonia region occurs mainly in the pre-Kalahari rocks. In places where the Kalahari Group is thicker, the rest levels

may be shallower (typically along the banks of the Kuruman River to the north), and the groundwater may occur within the Kalahari sediments. Borehole yields in the area are generally poor (a few m³ per hour), but are higher and of better water quality along the Kuruman River bed (Verhagen, 1985). Rest levels range from a few tens of metres to over 100m below surface.

It was found by Verhagen (1985) that for the Gordonia region direct rain recharge does occur to groundwater (usually very slow) away from the river beds and bedrock outcrops. It was also found that at least part of the salination of the ground waters occurs during such recharge. This salinity, he states, may be derived from incompletely leached evaporite horizons in closed surface basins such as pans and from salt loads which have built up in the unsaturated zones during periods of low rainfall. To establish if the groundwater was possibly present in the Kalahari Group piezometers were installed in some of the boreholes drilled along the No.3 Decline Shaft.

3.6.1 Piezometric Observations

Prior to the geotechnical drilling along the No.3 Decline Shaft centreline, it was anticipated that there would be a potentially strong perched water table above the Red Clay. However during the drilling of percussion boreholes drilled along the centreline, there was no evidence of water. An experienced exploration drilling company of the area (Booyesen Bore) indicated that, the majority of the percussion boreholes drilled above the clay layer on this mine property were dry. Most water boreholes in this area are drilled to below the Red Clay and drilled well within the underlying shale.

The absence of the predicted water above the Red Clay layer may be due to the fact that the clay layer has a very high water absorption capacity. Rain water that infiltrates through the Kalahari Group is rapidly soaked up by the clay layer. The clay is known to have a saturation ratio of greater than 98%. Only in exceptionally wet periods may the clay become totally saturated and allow a perched water table to form above.

Some water may be held in localized conglomerate lenses (calcified at their base) just above the clay layer, thereby forming a perched water table. Another important factor of the climate of the area is that water evaporates at a greater rate than the recharging rain fall (Meyer *et al.*, 1985), and thus rain water is not able to efficiently infiltrate and recharge the Kalahari Group.

Standard piezometers were installed in two boreholes (BH3 and BH5) near the new decline box-cut. After the installation of the piezometers the water levels dropped significantly (dispersion of drilling water) and reached apparent rest levels. The levels were not the same between the two boreholes, but were still dropping very slowly. It is thus believed that these levels have resulted from a decreased permeability with depth within in the boreholes and that the residual water had not fully drained away. No conclusive water table was found above the clay layer from the piezometers.

During the excavation of the decline shaft some water ingress was noted. Initially believed to have been the drilling water of the geotechnical holes, the persistent ingress suggested that there may indeed be small localized aquifers above the clay layer, possibly within deeply scoured Kalahari Group basal conglomerate channels. From observations made during the advance of the No.3 Decline Shaft, the following has been noted:

From about 299 m along the decline (59.6m below surface), the first signs of groundwater were seen. At the time ingress of water consisted of a trickle from a coverhole drilled ahead of the decline face. At 303m (60.4m below surface), the lower 1.5 m of the face was wet in patches. No signs of strong infiltration were seen on the face. Overall, the water seepage was minimal, not adding much to the already present water from charge hole drilling, which was ponding at the base of the tunnel. Once the water was encountered in the tunnel, the water level in piezometer BH3 begun to drop steadily. The seepage from chainage 303m continued

and attempts to seal the area off failed. This water initially caused some problems on the footwall below the concrete floor panels but steps were taken by the mining contractor to properly drain this excess water into a sump and pump it out. Three months later the inflow rate dropped. The piezometer in BH3 also showed that the water level dropped significantly since the passing of the tunnel excavation.

Once within the Red Clay layer water seepage had almost ceased on the face, with minor drips originating from the crown area of the decline shaft. The Lucknow shales were wet, but only showing signs of slight water ingress at fault zones. Overall the rock mass stability did not appear to be adversely affected by the slight ingress of water.

At the position of the Vertical Person's Shaft more water was anticipated. A piezometer installed in the adjacent borehole (BH6) revealed a constant water level at 37m below surface. This initial level was suspected to correspond to either drilling water that remained in the borehole since flushing and had not drained away fully, or a perched water table could have been present within the Kalahari Group calc-arenite. Without any further investigatory work requested, the potential aquifer parameters could not be established. Only once the Vertical Person's shaft progressed beyond 37m did it become apparent that large volumes of water were present within the Kalahari Group basal conglomerates. Later, when the new Vent Shaft nearby was due for construction, a pumpout test was carried out.

3.6.2 Pumpout Testing

A single rotary percussion drilled borehole (PV1) was completed down to a depth of 150m for the purposes of aquifer determination at the position of the new Vent Shaft. The hole was permanently cased with slotted steel casing. Chip samples were acquired and logged for each metre drilled. The geological profile for the borehole is presented in Appendix B. The chips obtained from this borehole showed a good correlation to the

stratigraphy obtained from the rotary cored hole (BH6) drilled at the Vertical Person's Shaft some 200m to the north west of the Ventilation Shaft. Upon the completion of the drilling, a well of PVC slotted screen casing with surrounding gravel pack was installed. The initial water strike occurred at 60m and the standing water level was recorded at 45m four days later.

A step test, constant discharge test, and constant discharge recovery test were conducted to establish the aquifer parameters and to calculate the potential quantity of groundwater inflow. Step testing, which provides the drawdown response in the borehole for different pumping rates, allows for the identification of the correct pumping rate to be used for the constant discharge test. It also provides an indication of the maximum safe borehole yield. The constant discharge test indicates the long-term drawdown response of the borehole and allows for the determination of the extent of the aquifer. This was conducted at a discharge rate of 0.83 litres/second for 6 hours with the pump at a depth of 66m. The constant discharge recovery test provides an indication of how quickly the groundwater level recovers after prolonged pumping.

The aquifer was identified as the basal conglomerate bed of the Kalahari Group, between 60 and 68m depth. The average hydraulic conductivity for the aquifer, was calculated as 0.42m/day. The coefficient of permeability (k) is therefore 4.8×10^{-6} m/sec. By application of Darcy's Law, the estimated groundwater inflow into the shaft would be 32m³ per day or 0.37 litres/second, assuming a shaft diameter of 3m (and thus exposed aquifer area of approximately 75 m²). The potential for high groundwater inflow into the Ventilation Shaft is expected to be low.

As mentioned above, during the percussion hole drilling, the first (and only) water strike occurred at 60m below surface. This confirms the suspicion that the Kalahari Group basal conglomerate forms an aquifer, with it being restricted to this unit. The fact that four days later, the standing water level was recorded to be at 45m indicates that there is a

piezometric head of approximately 15m at the position of Vent Shaft. As the water within the aquifer is under a head of approximately 15m, the expected water pressure within is around 150kPa. The pressure gradient developed upon excavation is likely to cause a collapse of the aquifer material as ingress of water into the excavation takes place.

It is thought that this head of water within the aquifer is possibly from recharge of water to the basal conglomerate at the prominent outcrop surface feature of the Black Rock hill. The basal conglomerate (although not proven) would terminate against this prominent surface feature. Rainwater, which runs off from the hill, would infiltrate into the conglomerate thereby directly recharging the aquifer.

3.6 Weathering

From the logging of the rotary cored boreholes drilled during this investigation, the total depth of weathering was found to range from 130 to 150m below surface. This range in weathering within the older shale bedrock was dependant on the degree of fracturing. Given that the base of the Red Clay is at 90m below current ground level, the original weathering front within the shales (below the African Erosion Surface) was approximately 50m. Such deep chemical weathering would have occurred during the humid Late Cretaceous and prior to the epeirogenic uplift along the Transvaal-Griqualand axis.

The lacustrine sediments of the Red Clay then accumulated on the ancient African Erosion Surface. This unit, which may not have fully lithified, was then subsequently weathered with further deterioration of the underlying shales having occurred. The Kalahari sediments then buried the ancient weathered regolith that formed on the Late Cretaceous land surface. Carbonate cement of the Kalahari beds was possibly still derived from chemical weathering of dolomite from the Campbell Group to the south and south-east and transported northwards as dissolved salts by rivers and streams. Locally the calcium may have been derived from the weathering of the Ongeluk lavas. It is evident that isolated pockets of weak rock have been calcified below the clay layer since the

deposition of the Kalahari sediments. Such zones of pedogenesis are probably related to the permeable near-vertical fault zones present in the area (Figure 3.1).

The unweathered stratigraphy of the Lucknow Formation consists of layered massive grey shale with intermittent bands of banded carbonaceous shale and weakly silicified greenish-grey shale. Upon weathering the original colour becomes dusky red to maroon, grading with depth into yellow and pale brown rock. The rock strength appears to increase in quality with depth as weathering effects decrease. Weathering patterns are complex and vary considerably over a short distance.

The completely weathered Ongeluk Andesite at the Vertical Person's Shaft has been deeply weathered below the African Erosion Surface. Weathering effects slowly decrease with depth, creating a range in consistency from very stiff residual soil to weak rock, and finally to unweathered, medium strong, rock below 91.5m.

From the mine borehole logs it was noted that remnants of tillite and shale belonging to the Karoo Supergroup may be present just below the clay layer. The Karoo sedimentary rocks would have been preserved as erosional remnants in keels of glacial valleys below the early Tertiary African Erosion Surface. The anticipated palaeo-Karoo valley was however not present on the decline centreline. It is likely that some misidentification occurred due to the inherent difficulty in accurately logging chip and dust samples.

4 ROCK PROPERTIES AND EXCAVATION

4.1 Box Cut Excavation

The excavation of the No. 3 Decline Shaft box-cut, was entirely within the sandy Gordonia Formation. The soft tunnelling section was to begin at a maximum depth of 18.5m below surface. Figure 3.6 shows the original box cut excavation. The geotechnical investigation for the box cut included rotary percussion holes and Dynamic Probe Super Heavy (DPSH) penetration tests. A total of three rotary percussion boreholes (PD1, PD2 and PD3) were drilled along the centreline of the decline to a maximum depth of 35m. Percussion chips/sand were sampled and logged and the penetration rate was recorded. In addition, sixteen DPSH penetration tests were carried out on either side of the decline centreline (results shown in Table A2 a-p, Appendix A). Table 4.1 below provides a summary of the DPSH results. Laboratory testing was carried out at Soiltech in Johannesburg to determine grading, Atterberg limits, cohesion, friction angle and natural moisture content of the profile (discussed in Chapter 3.1)

From the investigation it was found that the Gordonia Formation could be subdivided into two distinct zones of weakly coarsening upward sand. Clay content trends were shown to increase gradually with depth. This could be due to the fines either infiltrating down with rainwater, or having been blown away during earlier deposition. The upper unit is reddened (or oxidised) to about 6.0m depth and is generally medium dense to 6.0m to 10.0m. At the base of this unit is a silty fine sand horizon. This zone was found to be moist.

The lower zone is pale orange yellow in colour becoming orange near the base with a basal lag. The consistency is dense to very dense with a potentially collapsible grain structure. Towards the basal contact the sand becomes drier with a higher clay content (5% to 6%). At the base the material may well be slightly looser and more friable.

TABLE 4.1 Summary of Penetrometer (DPSH) Test Results Through the Gordonia Sands at the No.3 Decline Shaft Box-cut

DPSH Test No.	Total depth (m)	Depth of Refusal (m)	Depth to Dense Sand (m) (N>30 blows/300mm)	Depth to Very Dense Sand (m) (N>50 blows/300mm)
1	10.5	-	7.2	-
2	10.2	-	7.5	10.2
3	10.2	-	6.3	10.2
4	10.2	-	6.3	9.9
5	13.2	13.2	6.0	12.6
6	8.4	8.4	6.0	8.4
7	15.0	-	6.9	12.3
8	13.8	13.5	6.3	12.6
9	10.2	10.2	8.4	9.3
10	6.9	6.9	5.7	6.0
11	14.1	14.1	7.5	10.2
12	11.1	11.1	6.3	10.5
13	17.1	17.1	6.3	16.2
14	12.0	-	6.6	10.2
15	11.1	-	6.9	9.3
16	13.5	-	5.1	9.0

The average corrected N values of each DPSH test have been plotted against depth below surface (Figure 4.1). As one would expect with increasing depth, and therefore increasing overburden pressure, the sands generally become more dense with depth. There are however two notable decreases in the profile from 1.0 to 2.7m and from 13.8 to 16.0m. The upper decrease is an apparent decrease. The upper metre or two of the sands is slightly cemented by salts. A cyclic process of surface water runoff carrying dissolved salts into the sand and evaporative forces drawing the salts back to the surface creates a concentration near the surface. So initially the density of the upper crustal metre of sand shows a higher density, then returns to the normal increasing trend.

The lower decrease from 13.8 to 16.0m appears to correlate with a dramatic relative decrease in moisture content from 5.7 to 3.2% (see Table 3.1). Although the curve of the graph increases again beyond 16m, and the moisture content remains low, the clay content of the sands increases. These changes in moisture content and grading properties will all affect the penetration of the DPSH cone through the material, providing the curve seen in Figure 4.1.

Determination of phi (ϕ') from DPSH testing (Tables A2 a-p, Appendix A) showed that to approximately 8.0m depth, the value increases steadily from 30° to 35° (Figure 4.2). Below 8.0m a wide scatter of results ranged from 33° to 45°. Results of the remoulded shear box tests produced lower values of 30° to 31° due to permanent destruction of the interlocking nature of the sand particles during drilling. The original design slope angle, as specified on the construction drawing of the box cut, was 37.5°. However the test results (Table 3.1) indicated that the batter should be revised.

Two changes were recommended according to two main zones. From 0 to 8m below surface the revised batter was 30° (estimated factor of safety 1.0 to 1.1), and from 8.0 to 18.5m given as 35° (estimated factor of safety 1.0 to 1.5). For the subgrade of the proposed decline, it was recommended that the upper 8.0m be recompacted prior to placement of a matrix fill below the precast floor slabs. Matrix fill was used over the entire length of the box cut and within the calcrete and calcified sand. At the maximum depth of the box cut excavation, the head wall face was locally steepened to present a workable face for soft tunnelling to commence. The risk of such a steepened slope within the Gordonias sands collapsing was feared and reported. Shortly afterwards the face collapsed. The box cut design was re-evaluated and enlarged to facilitate deeper access to the calcrete below before any tunnelling was to commence directly into the calcrete.

No water was encountered during excavation, but adequate drainage measures were taken around the excavation to prevent ingress of storm water. Saturation of the soil profile could have led to collapse settlement of the precast floor slabs.

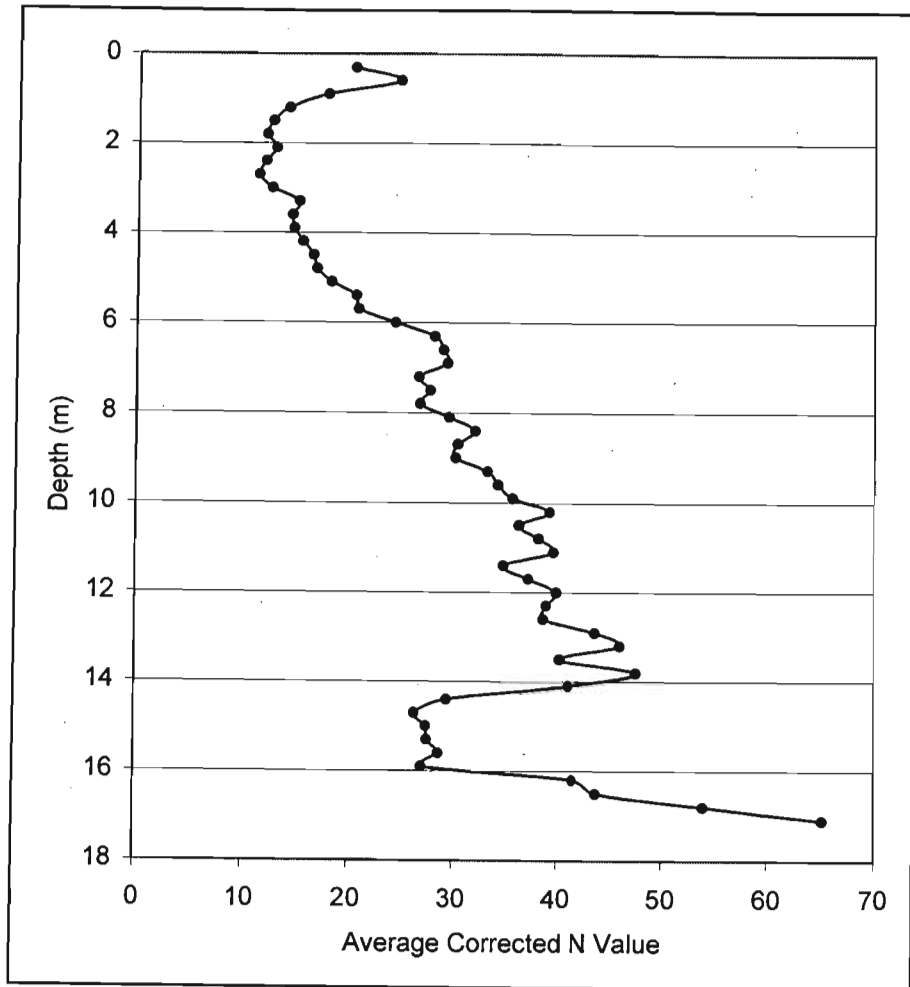


Figure 4.1 Graph of the average corrected N value of all DPSH tests carried out through the Gordonia Formation sands with depth.

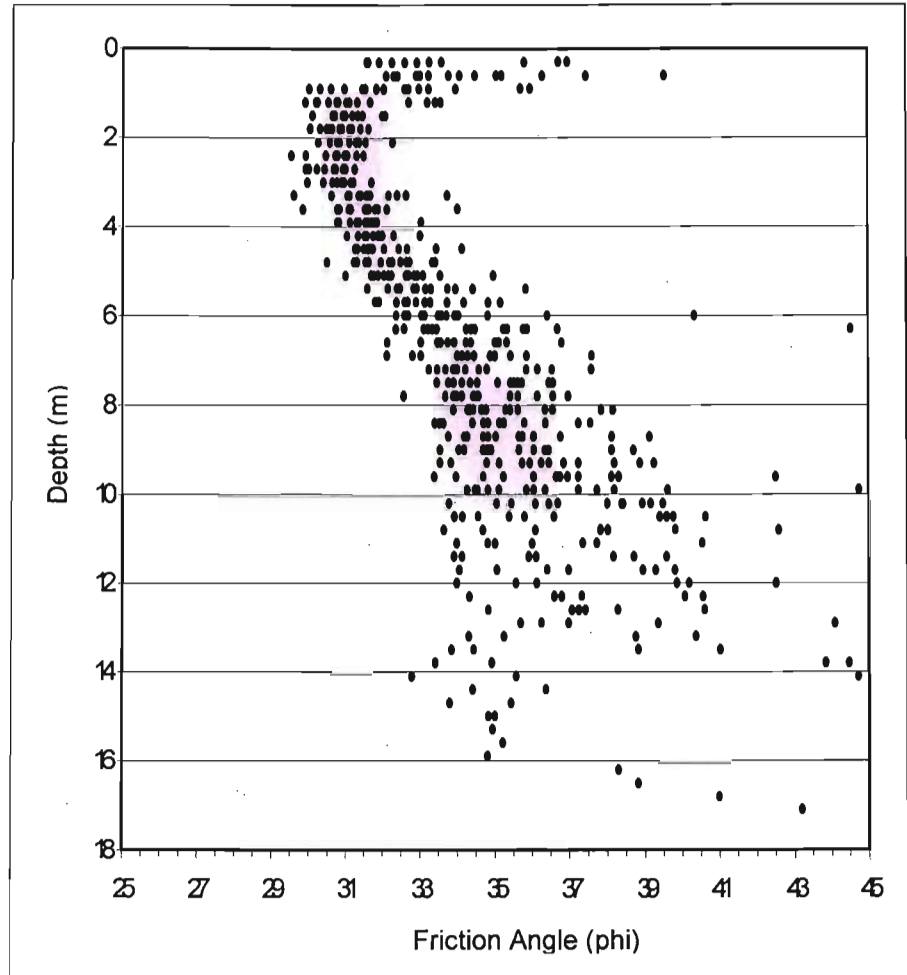


Figure 4.2 The relationship between phi (friction angle) and depth below surface throughout the profile of the Gordonia Formation.

4.2 Shaft Excavation – Rock Strength

Previously there was very little knowledge of the engineering geological nature of the partly lithified calcretes, sandstones and conglomerates that comprise the Kalahari Group. From geotechnical borehole drilling ahead of the new decline shaft it was evident that tunnelling conditions would be poor within the upper weathered zone. As such the need for high quality permanent tunnel support was required. In order to establish a basis for understanding the rock mass characteristics of the weathered ground ahead of the No.3 Decline Shaft a number of parameters were recorded from the logging of the borehole core and used to quantify the rock mass characteristics.

One such parameter is the rock strength, which is important when considering excavations within a rock mass. The qualitative descriptions given while logging borehole core provide a relative scale of changes in rock strength with depth. More accurate descriptions of the rock strength are done by quantitative methods such as point load index testing, which can be done in the field, and UCS testing done in the laboratory. The following sections describe these testing methods as carried out in this study.

4.2.1 Unconfined Compressive Strength (UCS) Testing

For UCS testing carried out on cylindrical rock core samples, the sample preferably has a height:diameter ratio of 2:1. A total of 32 unconfined compressive strength (UCS) tests were carried out on core samples obtained from the borehole drilling ahead of the No.3 Decline Shaft. These samples were tested in a commercial laboratory. Due to cost constraints only samples from BH2 and BH3 were tested. Although the few samples tested does not provide a detailed rock strength profile of the lithology intersected by the boreholes, the UCS testing is primarily used to confirm the point load index test results and the conversion thereof to inferred or calculated UCS values (described in 4.2.2).

Due to the broken nature of the core from shale below the Red Clay layer, no reasonable lengths of core samples could be selected and it was only possible to carry out field point load index testing on a few sections. Also worth noting is that strata orientation has a notable influence on the measured UCS (Hawkins, 1998). All the UCS results (actual UCS) and PLI test results are shown in Tables A3 a-h, Appendix A.

4.2.2 Point Load Index (PLI) Testing

The PLI testing equipment was developed when strength became a normal part of rock core descriptions. Although quite rudimentary, this testing method provides a rough guide to the intact compressive strength of the material. Due to its ease of use and low cost, it has increasingly become the only test undertaken to provide rock strength. Although the PLI test results are not easily correlatable with laboratory UCS values, it is important to consider both forms of testing when evaluating the rock strength profiles of the core drilled.

A number of PLI tests were carried out on core samples obtained from the highly variable degrees of calcified Kalahari Group sediments, and a few on the Lucknow shale immediately below the Red Clay layer. The testing procedure entails a core sample placed between two spherically truncated conical platens. The one hydraulically driven platen steadily compresses the core sample against the other fixed platen until the sample fails (all the PLI and UCS tests in this study were carried out as diametral tests). For both tests (PLI and UCS) sample failures which occurred along discontinuities were rejected, as this does not provide an accurate indication of the intact rock strength. The gauge reading (in Newtons) is recorded, but needs to be converted to a value comparable to the UCS values measured in MPa. The inferred UCS results from the PLI testing is then calculated as I_s values (MPa) using the formulae (ISRM, 1981):

$$I_s = P/D^2 \quad \text{where } P = \text{corrected test load (Newtons)}$$

$$D = \text{core diameter (mm)}$$

The I_s value (in MPa) is then corrected to the equivalent value for 50mm core by the following factor:

$$F = (D_{\text{act}}/50)^{0.45} \quad \text{where } D_{\text{act}} = \text{actual core diameter}$$

$$\text{Then } I_{s(50)} = I_s \times F \text{ (MPa)}$$

This factor (F) is usually derived from the inverse of the gradient of the trend line plotted on a graph of PLI results ($I_{s(50)}$) versus actual UCS from laboratory testing carried out on the same rock material. A linear trend should become evident from the plotted graph.

Due to the highly variable degree of calcification with depth, and the compounded effect of differential weathering between calcified lenses and silcrete mottles, it was often not possible to select a sample for UCS testing immediately adjacent to a PLI test. Hence the data plotted on the graph of Figure 4.3 shows a large degree of scatter.

The trend line which was plotted on the graph has a gradient of 0.0782 and when inversed gives a factor of 12.8. This factor, which includes the full range of varying rock strength grades present in the Kalahari Group rocks, provides a somewhat conservative factor when applied to the stronger zones. For this study the updated recommended conversion factors of Hawkins (1998) was considered. For dry sedimentary rocks, the conversion factors to UCS are as follows:

<u>$I_{s(50)}$ - MPa</u>	<u>Conversion factor to UCS</u>
<2	15
2-5	20
>5	25

Most workers would only apply a standard conversion factor of 24 for all strength categories, however all factors were applied accordingly in this study. All the PLI test results and calculated UCS values are shown in Tables A3 a-h, Appendix A. For description purposes the strength categories of the International Society of Rock Mechanics (ISRM, 1981) were adopted (page 25).

Although the inferred UCS values of the PLI testing may not be accurate in this study due to the high variability in rock strength, the usefulness (and cost effectiveness) of PLI testing down a borehole profile becomes evident when looking at a graph showing the change in inferred UCS values with depth (Figure 4.3). Due to the increased number of tests that are carried out per borehole, the graph shows a higher resolution of the rapidly changing rock strengths with depth. For comparative purposes the few laboratory UCS results were then plotted against depth and compared to the now converted PLI results, or inferred UCS results, for boreholes BH2 and BH3 (Figure 4.3). The few UCS tests carried out do not clearly show this variation with depth. When comparing two graphs of laboratory UCS results with that of the inferred UCS results from the field PLI tests, it becomes evident that they do not correlate directly with any accuracy in this study. Once again this is attributed to the highly variable change in rock strength with depth and the inability of sourcing two samples of similar rock strength.

The graphs in Figure 4.4 show the change in rock strength with depth from all the PLI tests carried out on the Kalahari Group core samples obtained from the boreholes drilled along the Decline Shaft (BH2 – BH5), including at the Vertical Person's Shaft (BH6). Again, the higher resolution of the PLI testing highlights the lateral zones of stronger and weaker rock. The well-cemented calc-arenites intersected above the Red Clay layer at the No.3 Decline Shaft show a distinct strong to very strong rock zone from 30 to 40m vertical depth.

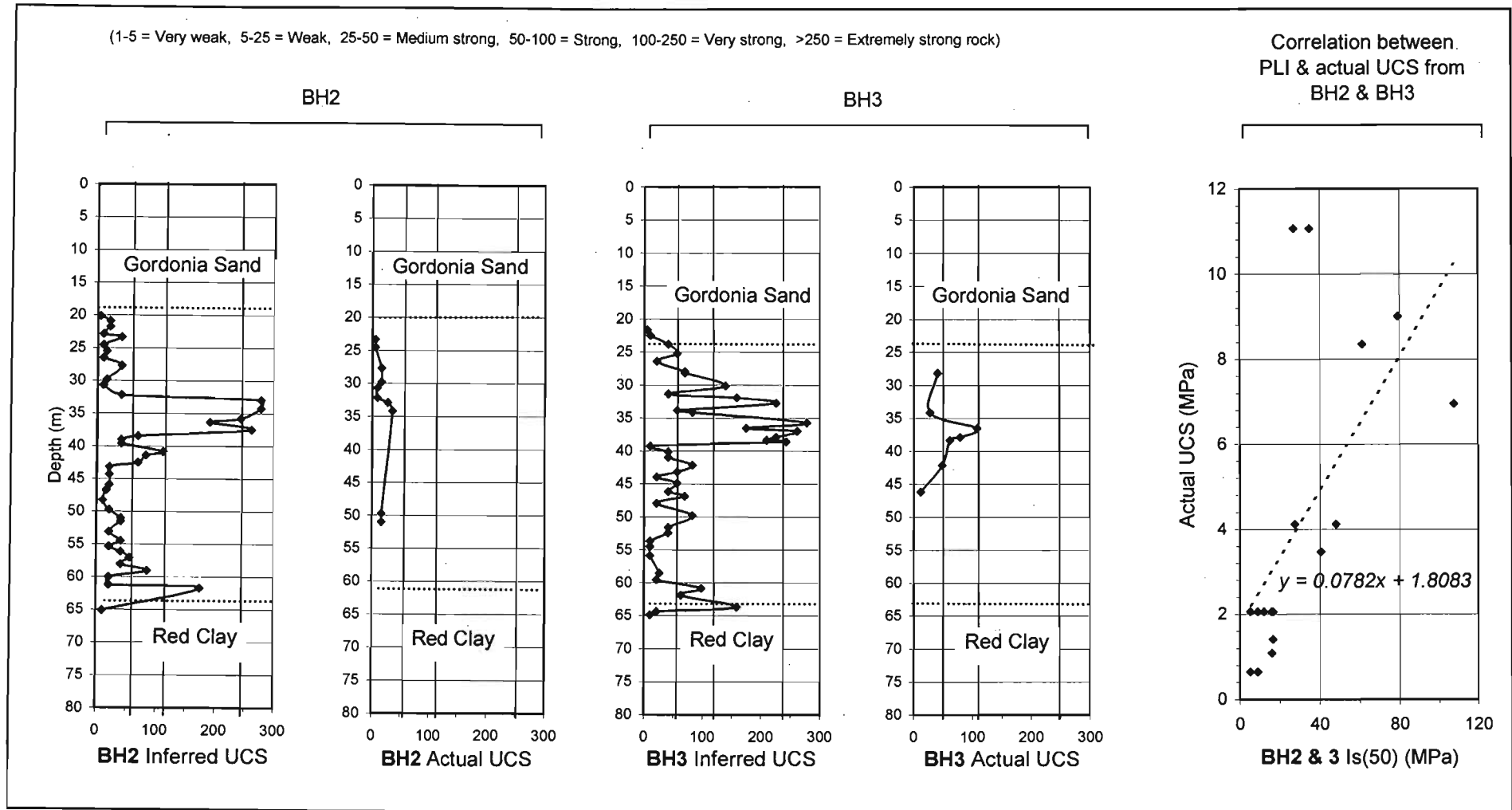


Figure 4.3 Comparison of inferred UCS from PLI testing with actual laboratory UCS results carried out on the calc-arenites of the Kalahari Group (indicated between the dotted lines).

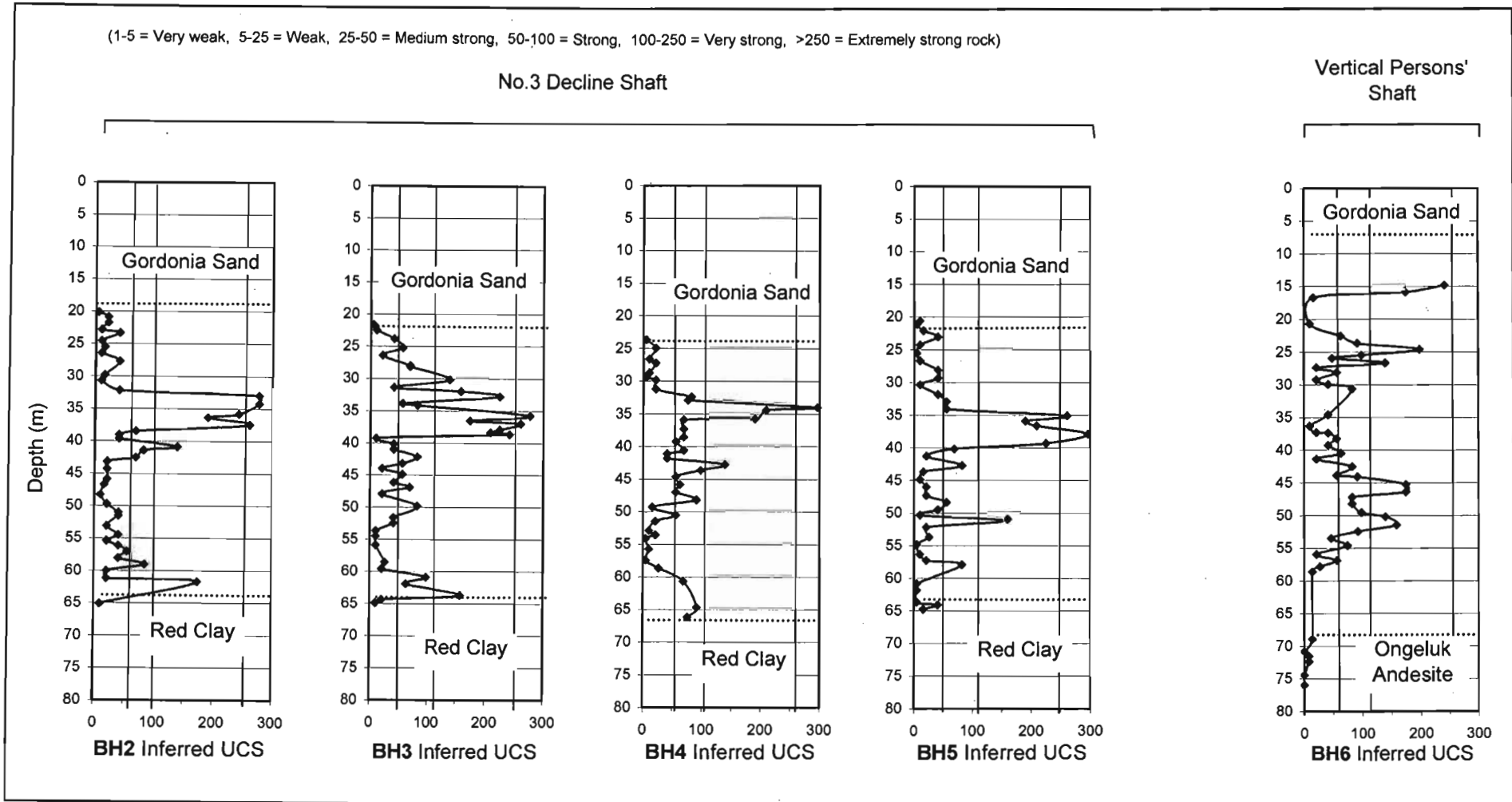


Figure 4.4 Graphs of inferred UCS vs. depth within the Kalahari Group calc-arenites (indicated between the dotted lines). Tests done from core of boreholes drilled at the No.3 Decline Shaft (BH2-BH5) and at the Vertical Person's Shaft (BH6).

Within this zone, pale brown silicification has been identified in core logging. This material, which has UCS values well in excess of 200MPa required blasting in addition to mechanical excavation.

Below 40m depth, the calculated strength of the calcified sediments decreases to strong to medium strong rock quality. The reason for this variation in strength is attributed to the variable degree of calcium carbonate cementation that has occurred during the lithification and subsequent pedogenesis of the Kalahari sediments. The effect of later weathering has served to reduce the quality of cementation.

The calcified sandstones were weathered to depths of approximately 28 to 30m. They thus form a weaker more friable zone. The basal gravel beds also appear to have been weathered by the perched water table that periodically overlies the Red Clay layer. These gravel beds are most certainly friable with potentially loosened areas where the cement has been completely weathered out.

The percussion borehole drilled near the Vertical Person's Shaft (BH1 SRK) was being used as a guideline to indicate the stratigraphy ahead of the shaft. However, the limited knowledge obtained from percussion chips did not indicate a very strong rock zone at 15m. During the sinking of the Vertical Person's Shaft precast caisson, the excavations at the toe of the concrete sheath went smoothly through the sands of the Gordonia Formation and the upper completely weathered Kalahari Group. However blasting of the silicified zone at 15m below surface caused delays in the shaft sinking schedule, and it was then decided to drill a rotary cored borehole immediately adjacent to the vertical shaft (BH6).

The core obtained from the borehole also indicates a distinct strength pattern in the calc-arenites of the Kalahari Group (Figure 4.4). Bands of stronger rock occur where silicification and increased calcification have

occurred. Where the strength decreases, the calcium cement has been removed by weathering effects, and a similar decrease in strength occurs within the conglomerate. The caisson of the vertical shaft was sunk to a final depth of 25m, where it was anchored into the very strong rock zone identified by the core drilling as seen in Figure 4.4.

With the extremely poor core recovery (if any at all) of the Red Clay, no PLI testing was carried out, or was possible due to the crumbling nature of the core samples. The fact that the few core samples obtained could be easily peeled by a pocket knife indicated its extremely weak to very weak strength. This was confirmed by underground exposure with the No.3 Decline Shaft, where the Red Clay was very easily excavated with the ITC machine (see Figures 4.8 and 4.9 on page 67).

Below the Red Clay layer the three boreholes which were able to core the underlying highly weathered and closely jointed shale Lucknow Shale (BH7 to BH9) provided poor core recovery. The few PLI tests on core samples from the shale below the clay layer were certainly reduced due to the laminated nature of the rock. Sliding occurred on the inclined bedding surfaces. It can be seen from the graph in Figure 4.5 that the shale strength increases slightly with depth, indicating a reduction in the weathering effects with depth. Overall the rock mass can be described as very weak rock to 115m and weak rock below. Medium strong rock is encountered below 135m depth.

4.3 Shaft Excavation – Rock Mass Assessment

Additional parameters were required from the logging of the borehole core to further quantify the rock mass quality ahead of the No.3 Decline shaft, and of the Vertical Person's Shaft. These parameters are required for the tunnelling index of Barton (1988), known as the Rock Tunnelling Quality Index, or Q-analysis. This index was proposed by Barton, Lein and Lunde in 1974 (Barton, 1988) for the determination of rock mass characteristics and tunnel support requirements (Hoek *et al.*, 1998).

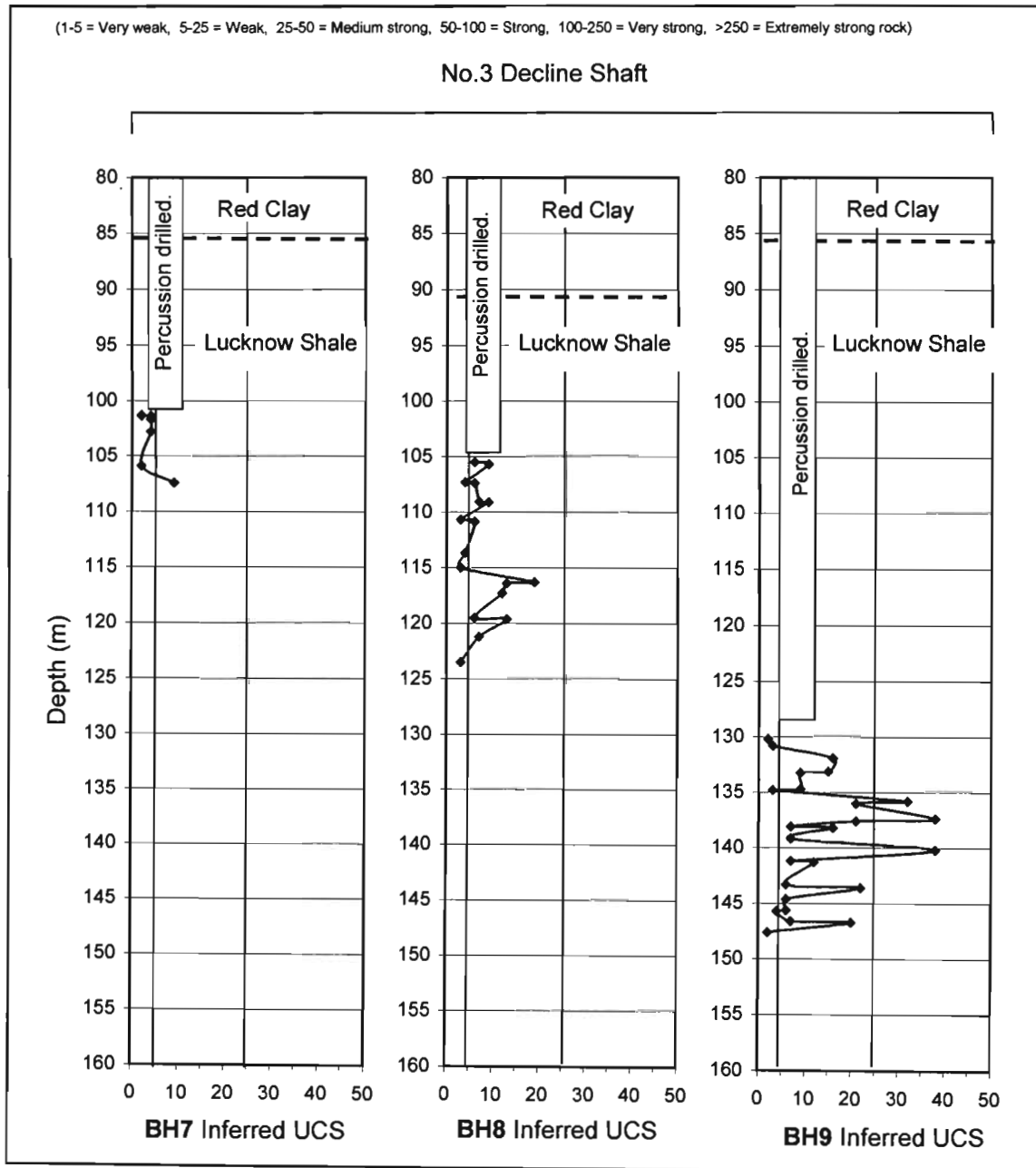


Figure 4.5 Calculated (inferred) UCS vs. depth from point load index testing carried out within the Lucknow shale from boreholes drilled below the Red Clay layer (BH7 -BH9). (Note that a different strength scale has been used due to the very low UCS values.)

It provides valuable insight to the expected tunnelling conditions ahead. This index allows support design to be concluded well ahead of the excavations. The numerical value of the Q-index varies on a logarithmic scale from 0.001 to a maximum of 1 000.

For the tunnelling of the weathered rock at Nchwaning, where the rock quality was shown to be poor (a Q-value of less than 2), the tunnel with a 9m span

needed to be permanently and actively supported (Pers. Comm. Mr Kotze, 2000). The best option of permanent support was considered by design engineers to be precast concrete lining of floor slabs and ribs.

The basic parameters measured from logging of core in order to calculate Q are as follows:

RQD	=	rock quality designation
J_n	=	joint set number
J_r	=	joint roughness number
J_a	=	joint alteration number
J_w	=	joint water reduction factor
SRF	=	stress reduction factor

The tunnelling quality index (Q) is then calculated as follows:

$$Q = (RQD/J_n) \times (J_r/J_a) \times (J_w/SRF)$$

The three quotients of the equation above provide measures of block size (RQD/J_n), inter block shear strength (J_r/J_a), and active stress (J_w/SRF) (Hoek *et al.*, 1998). The following section outlines the methodology in obtaining all the data required for Barton's Q Index.

4.3.1 Rock Quality Designation

This primary parameter was determined by the summation of all intact core lengths >100mm over a drill run length (typically 1.5m) and expressed as a percentage of the drill run length. This value expresses the blockiness of the rock mass as a percentage. If this value is zero, then the Q value will be zero. It should be noted that the action of drilling can serve to reduce the apparent RQD of the core.

4.3.2 Joints

The main factors in determining the rock mass quality according to the Q-method concerns the identification of the number of joint sets, as well as their overall roughness and filling.

i) Joint Set Number

Within the Kalahari Group sediments the core was generally broken due to the weathered nature of the rock. Core breaks were generally near horizontal, with few angled joints (some with slickensided surfaces). Although the core was not orientated during drilling, joint sets were evident from similar dip angles within the vertically drilled core. At least three joint sets were assumed and bedding.

For the weathered shale, because the core was generally very broken, it was difficult to accurately determine the number of joint sets in the rock mass. From the core drilled through the shale at least three fracture sets were identified and bedding. Underground mapping in the No.3 Decline Shaft confirmed the number of fracture sets as estimated from the core logging.

ii) Joint Set Roughness

The Kalahari Group showed general rough and non-oriented joint sets. Fractures within the shale were smooth and planar with some thin clay filling in places. Underground mapping confirmed the joint roughness condition.

iii) Joint Set Filling

Most fractures in the Kalahari Group were clean, having no clay filling. For the shale below the clay layer however, most fractures appeared to have either a thin silty or clay coating. It is also possible that there has

been some loss of material during core recovery on the wide clay filled fractures noted during tunnelling.

4.3.3 Ground Water

Negligible ground water inflow occurred during the decline excavation within the Kalahari Group. Slight inflow did occur toward the base of the Kalahari Group, within the conglomerates. This could have been from water trapped in a very small localized perched aquifer above the Red Clay. Some ground water inflow occurred from within the shale rock mass and generally occurred in areas of fracture and fault zones. The estimated amount of water was approximated at less than 5 litres per minute. For this analysis, J_w was thus assumed to be 1.0 (dry to negligible inflow) for the Kalahari Group as well as the weathered shale.

4.3.4 Stress Reduction Factor

In determining the Q-value for the Kalahari Group, the SRF was assumed to be 1.3 (low to medium stress, near surface). Within the shale below the clay layer the SRF was taken to be 2.5 where the rock mass consists of weak zones (probably single fractures/faults which contain clay or chemically disintegrated rock) causing loosening during excavation.

4.4 Q-Value Results and Rock Mass Subdivision

All the above data have been applied to Barton's equation and Q-values have been obtained for each of the boreholes drilled during the current investigation. The data tables are presented in Tables A4 a-h, Appendix A. The graphs in Figure 4.6 show the changing results of the Q-values as a function of depth within each borehole drilled within the Kalahari Group at the No.3 Decline Shaft and at the Vertical Person's Shaft. From the graphs, it can be seen that the Q-

values are quite variable with depth through the Kalahari Group sediments, and laterally along the Decline Shaft.

Referring to Figure 4.6, it can be seen that immediately below the contact between the Gordonina Formation sands and the Kalahari Group Calc-arenites, the rock mass quality according to the Q-values is shown to be of poor tunnelling quality (Q-values < 4). This corresponds to the highly weathered upper zone of the Kalahari Group just below the Gordonina Formation. At the Vertical Person's Shaft this zone of weathering is deeper. Along the Decline Shaft there is a general trend of increased Q-values between 35 and 50m, indicating fair tunnelling quality (Q-values between 4 and 10), in some instances reaching good quality (Q-values > 10). This corresponds to the generally less weathered, more calcretised calc-arenite with increased rock strength. Decreases in the Q-value profiles often correspond to pebbly layers and conglomerate units, which have a highly weathered matrix and low cohesive strength. The poor rock quality of the basal conglomerate is clearly identified by the Q-values. Water is contained within this unit and would reduce the Q-values, however the poorly consolidated nature of the unit is largely responsible for the deterioration of rock mass quality at depth.

The Ongeluk Andesite immediately below the basal conglomerate is completely weathered and, as the Q-values confirm, of poor tunnelling quality. Problems were experienced during the sinking of the vertical shaft, namely due to the crumbling nature of the conglomerate. The rest of the excavation within the weathered andesite was exacerbated by continuous inflow of water from the basal conglomerate.

With no (or very little) core recovery within the Red Clay, the Q-values could be assumed to be zero or extremely low. Although water was used during the borehole drilling of the Red Clay, thereby dramatically reducing its natural physical properties, observations within the No.3 Decline Shaft confirmed the poor nature of the material. Jointing was clearly visible (medium to widely jointed), however the joints were planar and very smooth (soapy to the touch). Many joints were severely slickensided.

been some loss of material during core recovery on the wide clay filled fractures noted during tunnelling.

4.3.3 Ground Water

Negligible ground water inflow occurred during the decline excavation within the Kalahari Group. Slight inflow did occur toward the base of the Kalahari Group, within the conglomerates. This could have been from water trapped in a very small localized perched aquifer above the Red Clay. Some ground water inflow occurred from within the shale rock mass and generally occurred in areas of fracture and fault zones. The estimated amount of water was approximated at less than 5 litres per minute. For this analysis, J_w was thus assumed to be 1.0 (dry to negligible inflow) for the Kalahari Group as well as the weathered shale.

4.3.4 Stress Reduction Factor

In determining the Q-value for the Kalahari Group, the SRF was assumed to be 1.3 (low to medium stress, near surface). Within the shale below the clay layer the SRF was taken to be 2.5 where the rock mass consists of weak zones (probably single fractures/faults which contain clay or chemically disintegrated rock) causing loosening during excavation.

4.4 Q-Value Results and Rock Mass Subdivision

All the above data have been applied to Barton's equation and Q-values have been obtained for each of the boreholes drilled during the current investigation. The data tables are presented in Tables A4 a-h, Appendix A. The graphs in Figure 4.6 show the changing results of the Q-values as a function of depth within each borehole drilled within the Kalahari Group at the No.3 Decline Shaft and at the Vertical Person's Shaft. From the graphs, it can be seen that the Q-

In view of the joint condition alone, the Q-values would be very low. Adding to the extremely poor tunnelling quality of the Red Clay are its hygroscopic and swelling properties, aggravated by tunnelling procedures. The three boreholes which penetrated the Red Clay layer (BH7 to BH9) provided poor core recovery of the Lucknow Shale. Highly weathered and closely jointed, the shale immediately below the Red Clay exhibits very poor Q-values (Figure 4.7). A simple material zonation pattern has been defined for the Lucknow Shale and is shown below (also refer to Figure 3.2):

- *Rock Mass Class 1*: totally discoloured, completely weathered and highly broken shale (RQD ~0) with possible wide clay filled fracture planes. Possible water in fracture zones and very poor stability.
- *Rock Mass Class 2*: partially discoloured, highly to moderately weathered, highly broken to broken shale (RQD <30) with stained smooth fractures and thin clay filling in places.
- *Rock Mass Class 3*: generally slightly weathered to unweathered rock, more intact (RQD >30) with some discoloured fractures. In general weak to medium strong rock material.

Figures 3.1 and 3.2 shows the weathered rock mass classes that have been identified below the Red Clay layer. All three classes of rock consist of folded and faulted shale. The boundaries between each class are diffuse and gradational. Deeper weathering pockets were also expected along fault/fracture planes. Such a zone was observed during an inspection of the No.3 Decline Shaft past the reinforced concrete rib support. Decreased joint spacing and slight water ingress marked the predicted fault zone near the exploration borehole N91B (Figure 3.1). Beyond which tunnelling conditions improved (temporarily).

Numerous similar poor rock mass zones were encountered during the rest of the Decline Shaft excavations, marking the highly fractured fault zones. In order to

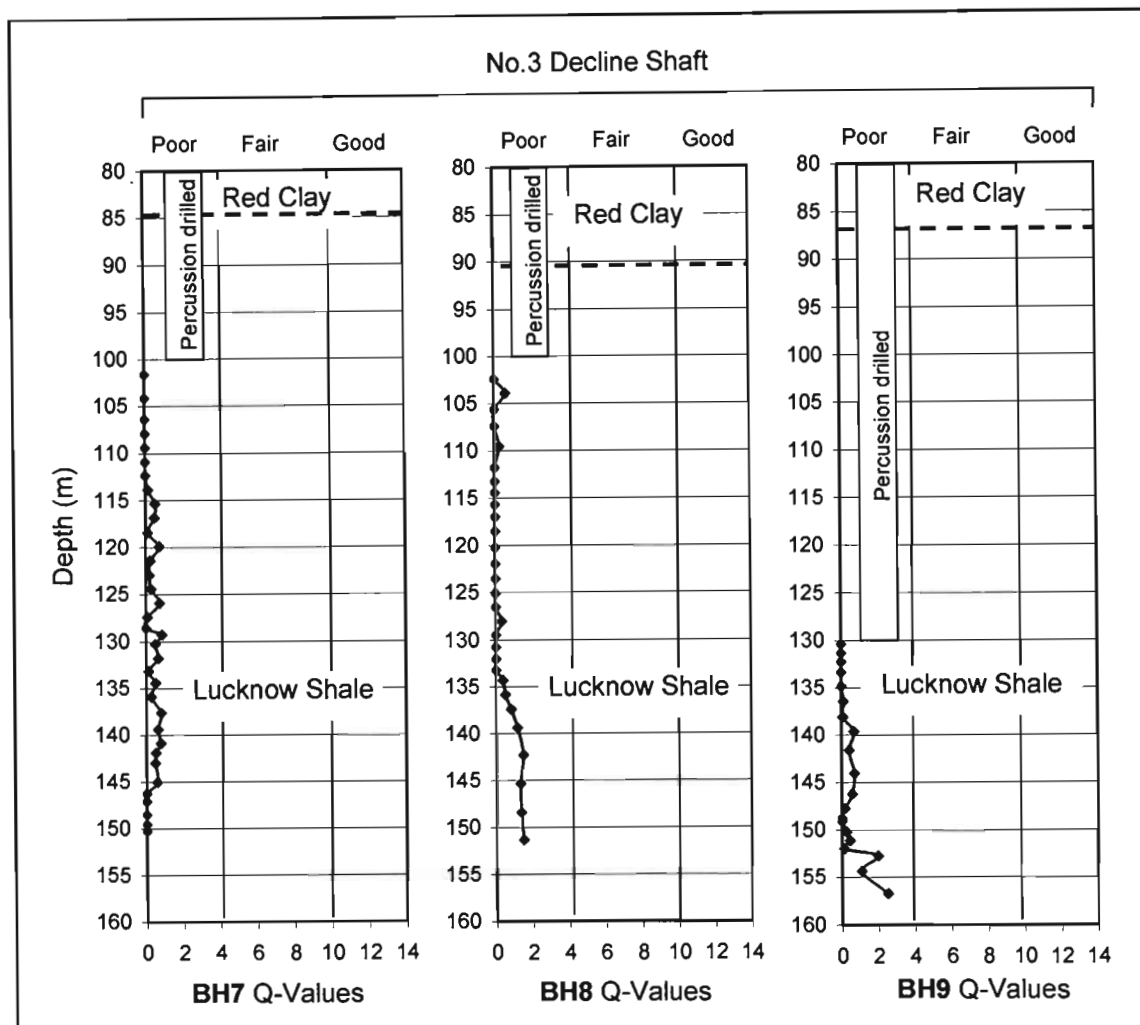


Figure 4.7 Graph of Barton's Q-values vs. depth within the Lucknow shale from boreholes drilled below the Red Clay layer (BH7 – BH9).

confirm the need for permanent/temporary tunnel support, the equivalent dimension (D_e) of the Decline Shaft was estimated. Given that the span is approximately 9m and the excavation support ratio (ESR) is 1.6, the D_e value for the Decline is 5.6. According to Hoek and Brown (1980), the minimum value for an unsupported tunnel with a D_e of 5.6 is $Q > 10$ (good to very good rock). The calculated Q-values showed that the overall rock quality is fair, with significant poor areas that would definitely require permanent support. In this regard, the option of permanent concrete ribs was used to provide long-term support for the tunnel in the poor to fair zones.

4.5 Current Tunnelling Practice

The first section of the tunnel was excavated by an imported ITC soft ground tunnelling machine (Figure 4.8 and 4.9, which show the ITC machine as it started to excavate in the Kalahari Group calc-arenite). This portion of the tunnel was lined with continuous, segmented 3-piece, pre-cast reinforced concrete ribs and floor slabs to a chainage length of approximately 800m (equating to a vertical depth of 160m). This provided permanent support of the weaker and calcified sediments of the Kalahari Group, including the Red Clay and broken Lucknow shale. Beyond the 800m chainage length only shotcrete and patterned rock bolting was used for roof and sidewall stabilization.

The ITC machine is limited in excavation strength to the very weak rocks of the Kalahari Group (20 to 30MPa). For excavation of stronger rock, comprising calcretised weak to very strong calc-arenite and calcrete of the Kalahari Group, low intensity blasting was required. Below the hard calc-arenite layers, the lower weak rock conglomerate bands were friable, with boulder sized clasts falling from the tunnel roof. The precast ribs had to be placed into position quickly to minimise this.

During the excavation of the older No.2 Decline Shaft, a 3 month delay occurred while excavating through the Red Clay layer. Collapse of the face and roof occurred with very poor traffickability problems arising from wet clay. For the 11.5 degree No.3 Decline Shaft, the total length of tunnelling within clay was approximately 150m. The method successfully used in penetrating the very unstable Red Clay layer within the Kalahari Group sediments consisted of, incremental face excavation (top heading) by no more than a metre at a time and the careful and prompt placement of the segmented concrete floor slabs and ribs. Immediately after advancing the decline face by 1m, the waste was removed and the entire exposed area ahead of the precast ribs coated with shotcrete. This attempted to reduce desiccation as well as wetting of the clay. Despite these precautionary measures, large blocks would still slip out from the face and fall from the decline roof.



Figure 4.8 View westwards down the No.3 Decline Shaft with the ITC machine and its conveyor belt 'tail'. (Photograph: R. Puchner, April 2000)



Figure 4.9 The ITC machine as it begins the tunnelling into the weathered Kalahari Group calc-arenite. (Photograph: R. Puchner, April 2000)

For the 6m diameter Vertical Person's Shaft a cylindrical caisson (Figure 4.10) was lowered in stages to a founding depth of 25m below ground level on medium strong to strong rock calc-arenite. The depth of the caisson founding level was based on information obtained from borehole BH6. Analysis of the core and PLI results shows that the lining had been lowered to a suitable depth within material of adequate founding strength.



Figure 4.10 View westwards showing the sinking of the caisson of the Vertical Person's Shaft.

Both above and below, the calcrete weakens and becomes more friable. During installation, the concrete lining went out of plumb, but was corrected by

hydraulic jacking. Additional stabilization of the caisson included two rows of ground anchors which were placed within the very strong silcrete layer at 15.0m and 15.5m respectively (see inferred UCS graph of the Vertical Person's Shaft, Figure 4.3). The method of support beyond the caisson during shaft sinking to 400m included shotcrete with cable anchors on a 1.5m grid spacing.

6 CONCLUSIONS

With the extension of the Nchwaning Mine shaft complex, various geological and geotechnical complications had to be identified to ensure that correct tunnelling methods and support techniques were used. An understanding of the geological history of the area and the resulting geotechnical nature was important in defining rock mass quality to be expected ahead of shaft development.

The Cenozoic cover of the area largely comprises the Kalahari Group aeolian deposits, calcretised sandstones, conglomerates and the Red Clay layer. The 20m of aeolian sands are of the Gordonia Formation and are Pleistocene-Holocene in age. The unit is unconsolidated and changes in colour, moisture and consistency with depth. A prominent gravel lag defines the base of this unit. For the development of the No.3 Decline shaft a box cut was excavated to a depth of 25m. From the results of various soil testing, batter slopes of 30 to 35° were advised. The boxcut was then backfilled over a series of precast segments, which would continue for a total length of 800m at the decline dip of 11.5°.

Below the Gordonia Formation is a package of calcareous arenites and conglomerates, which are on average 25m thick at the No.3 Decline shaft and 55m at the new vertical shafts. This package varies from weak and medium strong weathered zones, to very strong rock calcareous and siliceous zones. Much of the rock mass is highly weathered and medium to very closely fractured. The conglomerate bands are usually weak in strength, tending to residual material. The above mentioned units are thought to have been deposited as an aggrading fluvial fan which formed as a result of epirogenic uplift along the Griqualand-Transvaal axis to the south of Kuruman.

Barton's Q-analysis provided valuable insight to the expected tunnelling conditions ahead. The highly variable and generally low Q-values from borehole core analysis highlighted the necessity to continue using the precast tunnel lining. The precast segments were installed through the entire weathered Cenozoic sequence and into the weathered shales immediately below the Red Clay.

The Red Clay unit below the basal conglomerate is homogeneous, very stiff and heavily slickensided. Its hygroscopic nature and free swell strains of up to 15% cause it to be highly unstable while tunnelling through it. This unit is believed to be completely weathered lacustrine sediments. XRD and XRF analyses show high amounts of dolomite, with quartz and palygorskite. This confirms that the clays and carbonates probably originated from chemically weathered dolomites in the region.

The underlying Lucknow shale of the Olifantshoek Supergroup has been folded and faulted, the effects of which are evident in its highly broken nature and low Q-values. The shales were deeply weathered during the Late Cretaceous to depths equivalent of 50m below the then ground level. This weathering front has been preserved and is now 130 to 150m below surface. Deeper weathering pockets correlate with fault zones. A material zonation pattern of three rock mass classes for the shale was defined ranging from completely weathered shale to unweathered shale. Q-values were consistently poor.

The andesites of the Ongeluk Group form the bedrock of the mine some 470 to 700m below surface. Due to thrust faulting and the creation of the Kheis Thrust Fault during the Proterozoic Kheis orogeny, Ongeluk lavas were found to be much shallower at the position of new vertical shafts (68m below surface). The effects of weathering have also had an adverse effect on its rock mass quality. Only below 91.5m does it become less weathered tending to medium strong rock.

Ground water was not found to be problematic during the excavation of the No.3 Decline shaft through the Cenozoic sequence, or shale immediately below. At the Vertical Person's shaft ingress of water from the basal conglomerate above the clayey residual Ongeluk andesite slowed shaft sinking activities. Pump-out testing at the position of the Vertical Vent shaft indicated a relatively low 32m² per day could be anticipated from the conglomeratic horizon. A pressure gradient of 150kPa would be likely cause collapse of the aquifer material while sinking the shaft.

From this study it is clear that the importance of a comprehensive understanding of the geology prior to the sinking of shafts (vertical and decline) is crucial for the effective determination of the rock mass quality. The quantification of the rock mass is important in effective design for tunnelling methods and support techniques, which can be made well in advance of shaft development. Rotary core drilling provides the means for this valuable insight into the lithology and rock mass quality to be expected. Additional rock testing forms part of quantifying the rock mass, understanding its mechanics and providing a base to make recommendations upon.

ACKNOWLEDGEMENTS

The author wishes to thank Prof. M. Watkeys, Prof. C. Jermy and Prof. R. Maud for their valuable reviews and suggestions, and Mr C. McKnight for facilitating the field work. The staff of Black Rock Mine are also thanked for their assistance during the geotechnical borehole drilling investigations, particularly Mr A. Pretorius for valuable discussions of the mine geology, and permitting the use of the mine exploration borehole logs. The author is also grateful for Dr. Marco Andreoli's contribution.

REFERENCES

- Andreoli, M. A. G., Ashwal, L. D., Hart, R. J., and Huizenga, J. M., 1999. A Ni- and PGE-enriched norite impact melt complex in the Late Jurassic Morokweng impact structure, South Africa. In: Dressler, B. O., and Sharpton, V. L., eds. *Large Meteorite Impacts and Planetary Evolution II*: Boulder, Colorado, Geological Society of America Special Paper 339.
- Barton, N., 1988. Rock mass classification and tunnel reinforcement selection using the Q-System. In: Kirkaldie, L., ed. *Rock Classification Systems For Engineering Purposes*. American Society for Testing and Materials. 59-88.
- Bieniawski, Z. T., 1984. *Rock Mechanics Design in Mining and Tunnelling*. A. A. Balkema. 272pp.
- Bieniawski, Z. T., 1989. *Engineering Rock Mass Classifications*. Wiley, New York. 251pp.
- Beukes, N. J., Smit, C. A., 1987. New Evidence for Thrust Faulting in Griqualand West, South Africa: Implications for Stratigraphy and the Age of the Red Beds. *Trans. Geol. Soc. S. Afr.* **90**, 387-394.
- Bond, G. and Fernandes, T. R. C., 1974. Scanning electron microscopy applied to quartz grains from Kalahari type sands. *Trans. Geol. Soc. S. Afr.* **77**, 191-199.
- Cornell, D. H., Schütte, S. S. and Eglington, B. L., 1996. The Ongeluk basaltic andesite formation in Griqualand West, South Africa: Submarine Alteration in a 2222 Ma Proterozoic sea. *Precambrian Research*. **79**, 101-123.
- Du Toit, A. L., 1954. *The Geology of South Africa*. 3rd ed. Oliver and Boyd, Edinburgh, 611p.
- Haddon, I. G., 2000. Kalahari Group sediments. In: Partridge, T. C. and Maud, R. R., 2000. *The Cenozoic of Southern Africa*. Oxford University Press. 173-181.
- Hart, R. J., Cloete, M., McDonald, I., Carlson, R. W., and Andreoli, M. A. G., 2002. Siderophile-rich inclusions from the Morokweng impact melt sheet, South Africa: possible fragments of a chondritic meteorite. *Earth and Planetary Science Letters*, Elsevier. **198**, 49-62.
- Hawkins, A. B. 1998. Aspects of rock strength. *Bull. Eng. Geol. Env.*, **57**, 17-30.
- Helgren, D. M. and Brooks, A. S., 1983. Geoarchaeology at GI, a Middle Stone Age and Later Stone Age site in the northwest Kalahari. *J. Archaeol. Sci.* **10**, 181-197.
- Heine, K., 1990. Some Observations concerning the age of the dunes in the western Kalahari and palaeoclimate implications. *Palaeoecol. Afr.* **21**, 161.
- Hoek, E. and Brown, E. T., 1980. Underground excavations in rock. *Inst. Min. Metall.* London. 527pp.

- Hoek, E, Kaiser, P. K., and Bawden, W. F., 1998. *Support of Underground Excavations in Hard Rock*. A. A. Balkema. 215pp.
- ISRM, 1981. Brown E. T. (ed). *Suggested Methods for Rock Characterisation, Testing and Monitoring*. Pergamon Press.
- Gutzmer, J., Beukes, N. J. and Yeh, H. W., 1997. Fault-controlled metasomatic alteration of Early Proterozoic sedimentary manganese ore at Mamatwan Mine, Kalahari manganese field, South Africa. *S. Afr. J. Geol.* **100** (1), 53-71.
- Grobbelaar, W. S., Burger, M. A., Pretorius, A. I., Marais, W. and van Niekerk, I. J. M., 1995. Stratigraphic and structural setting of the Griqualand West and the Olifantshoek Sequences at Black Rock, Beeshoek and Rooinekke Mines, Griqualand West, South Africa. *Mineral. Deposita.* **30**, 152-161.
- Jennings, M., 1986. The Middleplaats manganese ore deposit, Griqualand West. In: Anhaeusser, C. R. and Maske, S. (Eds). *Mineral Deposits of Southern Africa*. The Geological Society of South Africa. 979-983.
- Key, R. M. and Rundle, C. C., 1981. The regional significance of new isotopic ages from Precambrian windows through the "Kalahari Beds" in north-western Botswana. *Trans. Geol. Soc. S. Afr.*, **84**, 51-66.
- Key, R. M., Tidi, J., McGeorge, I., Aitken, G., Cadman, A. and Anscombe, J., 1998. The lower Karoo Supergroup geology of the southeastern part of the Gemsbok sub-basin of the Kalahari basin, Botswana. *S. Afr. J. Geol.* **101**, 225-236.
- King, L. C., 1962. *The Morphology of the Earth*. Oliver and Boyd, Edinburgh. 699pp.
- Kleyenstüber, A. S. E., 1984. The mineralogy of the manganese-bearing Hotazel Formation, of the Proterozoic Transvaal Sequence in Griqualand West, South Africa. *Trans. Geol. Soc. S. Afr.* **97**, 257-272.
- Meyer, R., Duvenhage, A. W. A., De Beer, J. H., and Huysen, R. M. J., 1985. A geophysical-geohydrological study along the Kuruman River in the Kuruman and Gordonia districts. *Trans. Geol. Soc. S. Afr.*, **88**, 501-515.
- Moore, A. E. and Dingle, R. V., 1998. Evidence for fluvial sediment transport of Kalahari sands in central Botswana. *S. Afr. J. Geol.* **101** (2), 143-153.
- Nel, C. J., Beukes, N. J. and De Villiers, J. P. R., 1986. The Mamatwan manganese mine of the Kalahari manganese field. In: Anhaeusser, C. R. and Maske, S. (Eds). *Mineral Deposits of Southern Africa*. The Geological Society of South Africa. 963-978.
- Norrish, K. and Hutton, J. T., 1969. Accurate X-ray spectrographic method for the analysis for the wide range of geological samples. *Geochemica et Cosmochimica Acta.* **33**, 431-453.
- Partridge, T. C. and Maud, R. R., 2000. *The Cenozoic of Southern Africa*. Oxford University Press. New York. 406pp.

- Partridge, T. C. and Maud, R. R., 1987. The geomorphic evolution of southern Africa since the Mesozoic. *S. Afr. J. Geol.* **90**, 179-208.
- South African Committee for Stratigraphy (SACS), 1980. *Stratigraphy of South Africa. Part 1* (Comp. L. E. Kent). Government Printer. 611pp.
- Standard methods of testing road construction materials, 1986. *Technical methods for highways (TMH1)*. Graphic Arts, CSIR. 232pp.
- Tankard, A. J., Jackson, M. P. A., Erikson, K. A., Hobday, D. K., Hunter, D. R. and Minter, W. E. L., 1982. *Crustal Evolution of South Africa – 3.8 Billion Years of Earth History*. Springer Verlag, Berlin, 523pp.
- Thomas, D. S. G., and Shaw, P. A., 1990. The deposition and development of the Kalahari Group sediments, central Southern Africa. *Journal of African Earth Sciences*. **10** (1/2), 187-197.
- Thomas, D. S. G., and Shaw, P. A., 1991. *The Kalahari Environment*. Cambridge University Press. 284 pp.
- Tyson, P. D. and Partridge, T. C., 2000. Evolution of Cenozoic climates. In: Partridge, T. C. and Maud, R. R., 2000. *The Cenozoic of Southern Africa*. Oxford University Press. 371-387.
- Van der Merwe, D. H., 1964. *The prediction of heave from the plasticity index and percentage clay fraction of soils*. SA Inst. Civ. Eng. **6** (6). 103-107.
- Verhagen, B. Th., 1985. Isotope hydrology of ground waters of the Kalahari, Gordonia. *Trans. Geol. S. Afr.*, **88**, 517-522.
- Visser, D. J. L., 1984. *Geological map of the republics of South Africa, Transkei, Bophuthatswana, Venda, and Ciskei and the kingdoms of Lesotho and Swaziland (1:1 000 000)*. Department of Minerals and Energy Affairs, South Africa. Gravity edition.
- Warkwick, D. W. and Speers, C., 1998. *Preliminary geotechnical investigation for portal and decline shaft excavation in "soft" horizons*. Steffen, Robertson & Kirsten (SRK) Consulting, Report No. **249711/2** (Unpublished)

APPENDIX A

DATA TABLES

NOTE:

*All appendices are contained on the attached compact disc.
Only example sheets have been printed.*

**TABLE A1 Summary of Face Map Records During the Advance of the
No.3 Decline Shaft**

Date	Map No.	Chainage (m)	Approx. vertical depth of floor from surface (m)	Lithology Intersected
31-Mar-00	1	151.4	32.0	Calcarenite
01-Apr-00	2	152.9	32.3	Calcarenite
03-Apr-00	3	153.7	32.4	Calcarenite
04-Apr-00	4	154.9	32.7	Calcarenite
06-Apr-00	5	156.9	33.1	Calcarenite
07-Apr-00	6	158.0	33.3	Calcarenite
11-Apr-00	7	160.1	33.7	Calcarenite
15-Apr-00	8	161.6	34.1	Calcarenite
25-Apr-00	9	165.5	35.3	Calcarenite
01-May-00	10	175.3	36.9	Calcarenite
05-May-00	11	181.8	38.2	Calcarenite
09-May-00	12	188.8	39.4	Calcarenite
18-May-00	13	201.8	42.0	Calcarenite & conglomerate
01-Jun-00	14	228.0	47.3	Calcarenite
22-Jun-00	15	267.7	55.2	Calcarenite & conglomerate
07-Jul-00	16	299.0	61.4	Calcarenite & conglomerate
10-Jul-00	17	303.4	62.3	Calcarenite & conglomerate
14-Jul-00	18	310.0	63.6	Calcarenite & conglomerate
15-Jul-00	19	311.5	63.9	Calcarenite & conglomerate
17-Jul-00	20	314.5	65.8	Calcarenite & conglomerate
20-Jul-00	21	319.3	66.8	Siltstone & conglomerate
23-Jul-00	22	321.8	66.0	Siltstone & conglomerate
25-Jul-00	23	323.8	66.4	Siltstone & conglomerate
27-Jul-00	24	327.8	67.2	Siltstone & conglomerate
29-Jul-00	25	330.9	67.8	Conglomerate & Red Clay
31-Jul-00	26	334.0	68.4	Conglomerate & Red Clay
03-Aug-00	27	341.8	69.9	Conglomerate & Red Clay
06-Aug-00	28	343.8	70.3	Conglomerate & Red Clay
08-Aug-00	29	344.8	70.6	Conglomerate & Red Clay
09-Aug-00	30	345.8	70.7	Conglomerate & Red Clay
11-Aug-00	31	346.8	71.4	Conglomerate & Red Clay
12-Aug-00	32	347.8	71.6	Conglomerate & Red Clay
14-Aug-00	33	348.8	71.8	Conglomerate & Red Clay
16-Aug-00	34	350.3	72.1	Conglomerate & Red Clay
17-Aug-00	35	351.3	72.3	Conglomerate & Red Clay
18-Aug-00	36	352.8	72.6	Conglomerate & Red Clay
19-Aug-00	37	353.8	72.8	Conglomerate & Red Clay
21-Aug-00	38	355.8	73.2	Red Clay
24-Aug-00	39	357.3	73.5	Red Clay
26-Aug-00	40	359.8	74.0	Red Clay
21-Sep-00	41	388.3	79.7	Red Clay
13-Jun-01	42	635.0	129.1	Shale

Table A2a Calculation of Gordonia Formation Phi Values from DPSH 1

Depth (m)	No. of blows (N)	Dry Density	Moisture Content	Bulk Density	Over Pressure	Cn.N	Cr	Corrected N	phi
0.3	12	1550	3	1597	5	2.02	0.61	15	32
0.6	19	1550	3	1597	9	1.79	0.62	21	33
0.9	20	1550	3	1597	14	1.66	0.64	21	33
1.2	19	1550	3	1597	19	1.56	0.65	19	33
1.5	14	1550	3	1597	23	1.49	0.66	14	31
1.8	12	1550	3	1597	28	1.43	0.67	11	30
2.1	13	1550	3	1597	33	1.37	0.68	12	31
2.4	10	1550	3	1597	38	1.33	0.70	9	30
2.7	10	1550	3	1597	42	1.29	0.71	9	30
3.0	13	1550	3	1597	47	1.25	0.72	12	31
3.3	14	1550	3	1597	52	1.22	0.73	13	31
3.6	14	1550	3	1597	56	1.19	0.74	12	31
3.9	14	1550	3	1597	61	1.17	0.76	12	31
4.2	18	1550	3	1597	66	1.14	0.77	16	32
4.5	17	1550	3	1597	70	1.12	0.78	15	32
4.8	13	1550	3	1597	75	1.10	0.79	11	30
5.1	18	1550	3	1597	80	1.08	0.80	16	32
5.4	20	1550	3	1597	84	1.06	0.82	17	32
5.7	18	1550	3	1597	89	1.04	0.83	16	32
6.0	22	1550	3	1597	94	1.02	0.84	19	33
6.3	24	1550	3	1597	99	1.01	0.85	21	33
6.6	27	1550	3	1597	103	0.99	0.86	23	34
6.9	29	1550	3	1597	108	0.98	0.88	25	34
7.2	40	1550	3	1597	113	0.96	0.89	34	37
7.5	31	1550	3	1597	117	0.95	0.90	26	35
7.8	31	1550	3	1597	122	0.94	0.91	26	35
8.1	29	1550	3	1597	127	0.92	0.92	25	34
8.4	37	1650	3	1700	140	0.89	0.94	31	36
8.7	38	1650	3	1700	145	0.88	0.95	32	36
9.0	33	1650	3	1700	150	0.87	0.96	27	35
9.3	33	1650	3	1700	155	0.86	0.97	27	35
9.6	39	1650	3	1700	160	0.84	0.98	32	36
9.9	31	1650	3	1700	165	0.83	1.00	26	35
10.2	34	1650	3	1700	170	0.82	1.00	28	35
10.5	38	1650	3	1700	175	0.81	1.00	31	36

Table A3a Rock strength results from Point Load Index testing and Laboratory UCS Testing for BH2

Top (m)	Sample depth to		Length (mm)	diam (mm)	load (N)	Is (MPa)	F	Is(50)	Is(50): UCS	UCS (inferred)	ISRM description	*UCS (actual)
	Bottom (m)	Midpoint (m)										
20.10	20.20	20.15	100	60	1150	0.3	1.0855	0.33	15	5	very weak	
20.83	20.94	20.89	110	60	4600	1.3	1.0855	1.41	15	21	weak	
21.70	21.81	21.76	110	60	4600	1.3	1.0855	1.41	15	21	weak	
22.81	22.90	22.86	90	60	2300	0.6	1.0855	0.65	15	10	weak	
23.28	23.40	23.34	120	60	6900	1.9	1.0855	2.06	20	41	medium strong	5.15
24.50	24.62	24.56	120	60	2300	0.6	1.0855	0.65	15	10	weak	5.15
25.43	25.57	25.50	140	60	3450	1.0	1.0855	1.09	15	16	weak	
26.43	26.52	26.48	90	60	2300	0.6	1.0855	0.65	15	10	weak	
27.64	27.77	27.71	130	60	6900	1.9	1.0855	2.06	20	41	medium strong	15.92
29.77	29.87	29.82	100	60	3450	1.0	1.0855	1.09	15	16	weak	15.92
30.64	30.74	30.69	100	60	2300	0.6	1.0855	0.65	15	10	weak	8.83
32.10	32.24	32.17	140	60	6900	1.9	1.0855	2.06	20	41	medium strong	8.83
32.89	33.00	32.95	110	60	36800	10.2	1.0855	11.07	25	277	extremely strong	27.00
34.12	34.26	34.19	140	60	36800	10.2	1.0855	11.07	25	277	extremely strong	34.93
35.70	35.83	35.77	130	60	32200	8.9	1.0855	9.66	25	242	very strong	
36.27	36.39	36.33	120	60	25300	7.0	1.0855	7.60	25	190	very strong	
37.40	37.54	37.47	140	60	34500	9.6	1.0855	10.42	25	261	extremely strong	
38.41	38.52	38.47	110	60	11500	3.2	1.0855	3.47	20	69	strong	
38.96	39.04	39.00	80	60	6900	1.9	1.0855	2.06	20	41	medium strong	
39.55	39.66	39.61	110	60	6900	1.9	1.0855	2.06	20	41	medium strong	
40.81	40.91	40.86	100	60	18400	5.1	1.0855	5.54	20	111	very strong	
41.35	41.44	41.40	90	60	13800	3.8	1.0855	4.12	20	82	strong	
42.44	42.58	42.51	140	60	11500	3.2	1.0855	3.47	20	69	strong	
43.10	43.22	43.16	120	60	4600	1.3	1.0855	1.41	15	21	weak	
44.21	44.36	44.29	150	60	4600	1.3	1.0855	1.41	15	21	weak	
45.82	45.94	45.88	120	60	4600	1.3	1.0855	1.41	15	21	weak	
46.69	46.79	46.74	100	60	3450	1.0	1.0855	1.09	15	16	weak	
48.22	48.35	48.29	130	60	2300	0.6	1.0855	0.65	15	10	weak	
49.26	50.16	49.71	900	60	4600	1.3	1.0855	1.41	15	21	weak	16.57
50.91	51.08	51.00	170	60	6900	1.9	1.0855	2.06	20	41	medium strong	16.57
51.43	51.55	51.49	120	60	6900	1.9	1.0855	2.06	20	41	medium strong	
53.04	53.12	53.08	80	60	4600	1.3	1.0855	1.41	15	21	weak	
54.41	54.54	54.48	130	60	6900	1.9	1.0855	2.06	20	41	medium strong	
55.30	55.41	55.36	110	60	4600	1.3	1.0855	1.41	15	21	weak	
56.04	56.21	56.13	170	60	6900	1.9	1.0855	2.06	20	41	medium strong	
56.98	57.11	57.05	130	60	9200	2.6	1.0855	2.82	20	56	strong	
57.98	58.13	58.06	150	60	6900	1.9	1.0855	2.06	20	41	medium strong	
59.00	59.08	59.04	80	60	13860	3.9	1.0855	4.23	20	85	strong	
59.95	60.05	60.00	100	60	4600	1.3	1.0855	1.41	15	21	weak	
61.13	61.23	61.18	100	60	4600	1.3	1.0855	1.41	15	21	weak	
61.64	61.76	61.70	120	60	23000	6.4	1.0855	6.95	25	174	very strong	
64.99	65.17	65.08	180	60	2300	0.6	1.0855	0.65	15	10	weak	

* UCS value of sample closest to PLI test.

Table A4a Calculation of Q value per core run of BH2

Depth (m)	RQD (%)	Jn	Jr	Ja	Jw	SRF	Q
20.10	17	9	3.0	3	1	1.3	1.453
21.60	24	9	3.0	3	1	1.3	2.051
23.10	35	9	3.0	3	1	1.3	2.991
23.70	67	9	3.0	3	1	1.3	5.726
25.20	47	9	3.0	3	1	1.3	4.017
26.00	70	9	2.0	1	1	1.3	11.966
27.75	66	9	2.0	1	1	1.3	11.282
28.39	93	9	2.0	2	1	1.3	7.949
29.89	69	9	3.0	2	1	1.3	8.846
30.74	64	9	3.0	3	1	1.3	5.470
32.24	100	9	3.0	3	1	1.3	8.547
33.00	100	9	3.0	3	1	1.3	8.547
34.50	29	9	2.0	2	1	1.3	2.479
36.02	95	9	2.0	2	1	1.3	8.120
37.54	86	9	3.0	2	1	1.3	11.026
39.04	90	9	3.0	2	1	1.3	11.538
39.94	91	9	1.5	2	1	1.3	5.833
41.44	35	9	1.5	1	1	1.3	4.487
42.94	63	9	1.5	1	1	1.3	8.077
44.44	57	9	1.5	1	1	1.3	7.308
*45.94	17	9	1.5	1	1	1.3	2.179
*47.44	26	9	3.0	1	1	1.3	6.667
*48.94	52	9	3.0	2	1	1.3	6.667
*50.24	16	9	3.0	1	1	1.3	4.103
*51.74	82	9	3.0	3	1	1.3	7.009
53.04	92	9	2.0	3	1	1.3	5.242
54.54	48	9	3.0	3	1	1.3	4.103
56.04	80	9	2.0	3	1	1.3	4.558
57.56	71	9	2.0	3	1	1.3	4.046
59.08	67	9	2.0	3	1	1.3	3.818
60.60	82	9	3.0	3	1	1.3	7.009
62.10	41	9	3.0	3	1	1.3	3.504
63.60	8	9	3.0	3	1	1.3	0.684
64.50	0	9	0.5	3	1	1.3	0.000

RQD = Rock Quality Designation Jn = Joint set number Jr = Joint roughness Ja = Joint alteration
 Jw = Joint water reduction factor SRF = Stress Reduction Factor

* Intersection depth of No.3 Decline Shaft

APPENDIX B

BOREHOLE LOGS

Table of all Boreholes, Nchwaning No.3 Decline Shaft Complex

No.	Borehole No.	X-Coord	Y-Coord
Current Investigation - Percussion Boreholes			
1	PD1	52389.000	13734.500
2	PD2	52383.700	13753.100
3	PD3	52375.200	13781.900
4	P1	52299.000	14006.000
5	PV1	51945.000	15505.200
Current Investigation - Percussion and Rotary cored boreholes			
6	BH2	52327.000	13910.000
7	BH3	52309.000	13972.000
8	BH4	52289.000	14040.000
9	BH5	52269.000	14106.000
10	BH6	51850.000	15680.000
11	BH7	52263.648	14125.923
12	BH8	52235.795	14221.540
13	BH9	52201.816	14336.535
Previous Investigation - Percussion and Rotary cored boreholes			
14	BH1	51799.975	15675.046
15	BH2	51580.944	15708.886
16	BH4	52288.136	14067.999
17	BH4	52163.945	14476.138
18	BH5	51941.981	15207.015
Exploration Boreholes - Percussion and Rotary cored boreholes			
19	N55	52333.204	14270.876
20	N61	52329.469	13933.471
21	N61E	52324.794	14100.047
22	N63A	51846.190	15621.496
23	N63B	51828.973	15250.642
24	N63C	51913.941	14934.487
25	N75	52108.072	14101.338
26	N75A	52091.450	14430.668
27	N75B	52075.866	14786.350
28	N75C	52077.876	15099.779
29	N91A	52074.594	14620.507
30	N91B	52325.245	14440.060

CURRENT INVESTIGATION

HOLE No: BH2
Sheet 2 of 5

JOB NUMBER: 5267

ROCK FABRIC
NF - massive
BF - bedded
FF - foliated
CF - cleaved
SF - schistose
GF - gneissose
LF - laminated

GRAIN SIZE
FG - fine grained
MG - medium grain
CG - coarse grain

JOINT SPACING
VCI - very close spacg
CI - close spacing
MI - medium spacing
WI - wide spacing
VWI - very wide spacing

JOINT ROUGHNESS
SJ - slickensided
SJ - smooth
RJ - rough

JOINT SHAPE
CUR - curvilinear
PLA - planar
UMD - undulating
STS - stepped
IRR - irregular

ROCK HARDNESS
EHK - extremely hard rock
VHK - very hard rock
HR - hard rock
MHR - medium hard rock
SR - soft rock
VSR - very soft rock



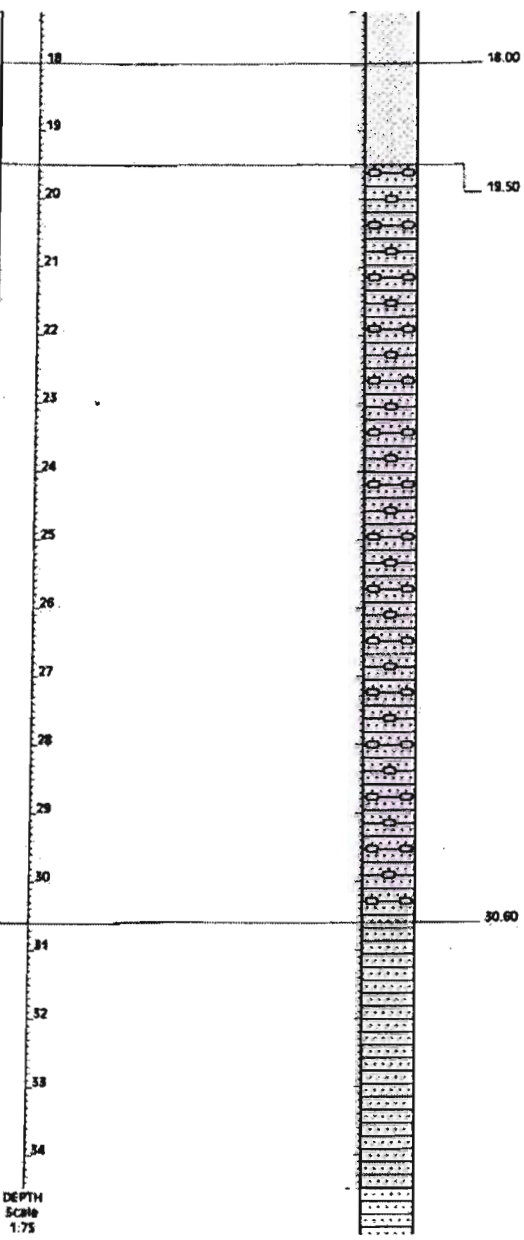
NCHWANING NO.3 DECLINE SHAFT
GEOTECHNICAL INVESTIGATION

HOLE No: BH2
Sheet 2 of 5

JOB NUMBER: 5267

NWD4

33	17	5	0,9	5
93	24	12	1,2	21
100	35	13	2,2	21
100	67	7	5,7	10
93	47	9	3,0	41
88	70	4	13,5	16
96	66	6	12,7	10
97	93	3	71,5	41
99	69	5	13,3	16
100		6	4,1	10
100		3	25,6	41
100		3	25,6	277
99		2	11,2	277



Moist, pale reddish orange, dense to very dense, massive, medium and fine SAND. AEOLIAN.

Note:
1. Unconformity at base of Gordonia Sand Formation.

Light brownish grey, mottled creamy white, stained brownish orange, highly weathered, fine to medium grained with scattered coarse grains, medium fractured, weak rock with thin medium strong layers. CALC-ARENITE.

Notes:
1. Some fractures are stained and filled with brownish orange, loose, fine sand.
2. Completely weathered, friable, very soft rock zones from 20,98-21,6m; 23,0-23,3m and 29,5-29,8m.
3. Medium strong rock zones from 28,3-29,0m and 23,3-23,7m.
4. Top of Kalahari Group, shows palaeo-weathering and secondary calcification.
5. Slickensided in completely weathered zone from 29,5-29,8m.

Very pale off-white, stained grey, mottled dark brown, slightly weathered, fine to medium-grained, widely fractured, very strong to extremely strong rock. CALC-ARENITE.

Notes:
1. Few red stained dissolution cavities, < 50mm.
2. Dark brown mottling from 33,3-35,0m (silcrete).

Drill Method	% Core Recovery	% RQD	Fractures per Metre	C-VALUE	ESTIMATED UCS (MPa)	DEPTH Scale 1:75
--------------	-----------------	-------	---------------------	---------	---------------------	------------------

HOLE No: BH2
Sheet 3 of 5

JOB NUMBER: 5267

ROCK FABRIC
MF - massive
DF - bedded
FF - foliated
CF - cleaved
SF - schistose
GF - gneissose
LF - laminated

GRAIN SIZE
FG - fine grained
MG - medium grain
CG - coarse grain

JOINT SPACING
VJ - very close spacg
CJ - close spacing
MJ - medium spacing
WJ - wide spacing
VWJ - very wide spacing

JOINT ROUGHNESS
SJ - slickensided
S - smooth
RJ - rough

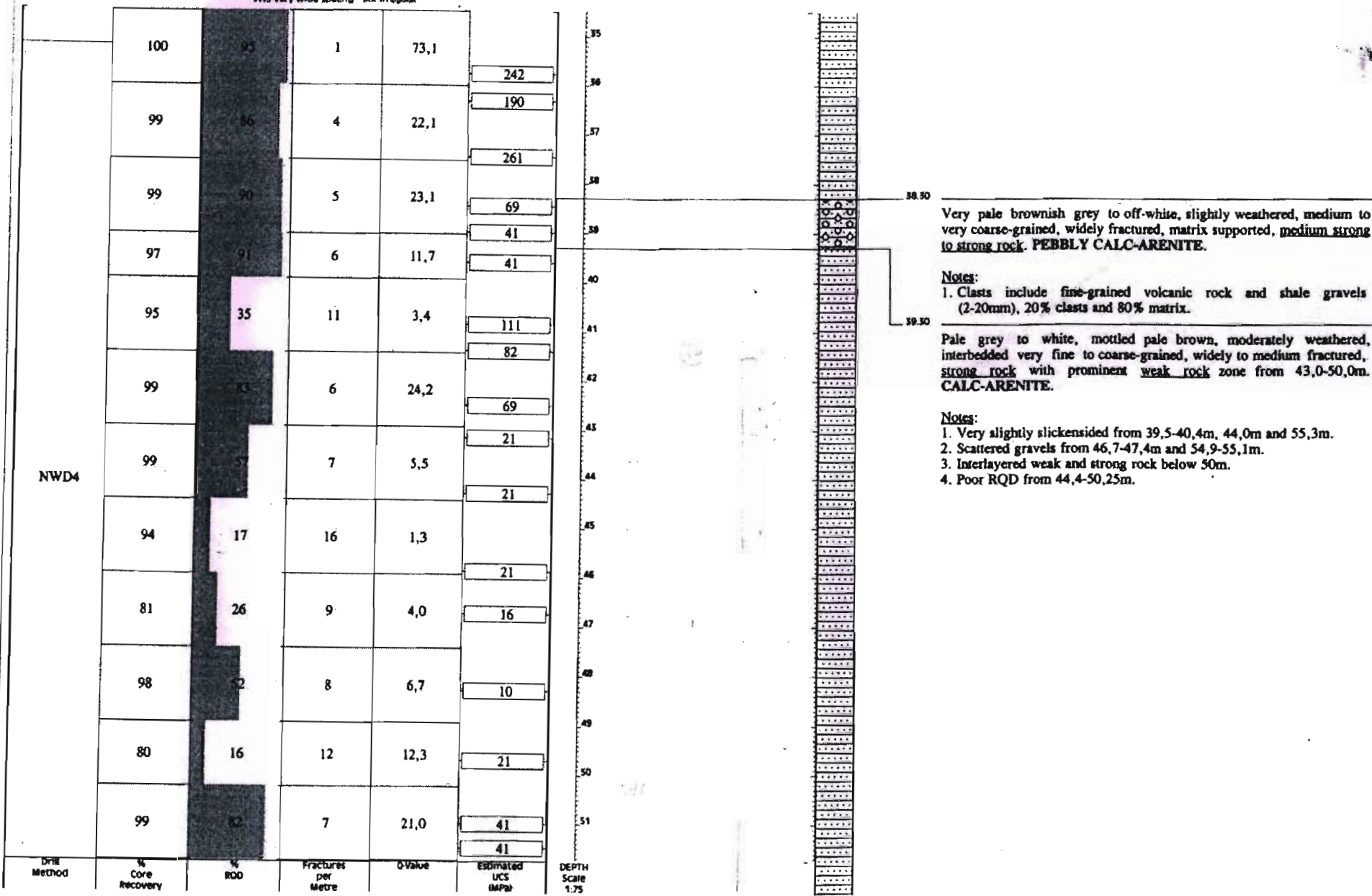
JOINT SHAPE
CUR - curvilinear
PLA - planar
UNP - undulating
STE - stepped
IRR - irregular

McKnight
Geotechnical Engineering Pty. Ltd.

NCHWANING NO.3 DECLINE SHAFT
GEOTECHNICAL INVESTIGATION

HOLE No: BH2
Sheet 3 of 5

JOB NUMBER: 5267



Very pale brownish grey to off-white, slightly weathered, medium to very coarse-grained, widely fractured, matrix supported, medium strong to strong rock. PEBBLY CALC-ARENITE.

Notes:
1. Clasts include fine-grained volcanic rock and shale gravels (2-20mm), 20% clasts and 80% matrix.

Pale grey to white, mottled pale brown, moderately weathered, interbedded very fine to coarse-grained, widely to medium fractured, strong rock with prominent weak rock zone from 43,0-50,0m. CALC-ARENITE.

Notes:
1. Very slightly slickensided from 39,5-40,4m, 44,0m and 55,3m.
2. Scattered gravels from 46,7-47,4m and 54,9-55,1m.
3. Interlayered weak and strong rock below 50m.
4. Poor RQD from 44,4-50,25m.

HOLE NO: BH2

Sheet 4 of 5

JOB NUMBER: 5267

ROCK FABRIC
MF - massive
BF - bedded
RF - foliated
CF - cleaved
SF - schistose
GF - gneissose
LF - laminated

GRAIN SIZE
FG - fine grained
MG - medium grain
CG - coarse grain

JOINT ROUGHNESS
SLJ - slickensided
SJ - smooth
RJ - rough

ROCK HARDNESS
EHR - extremely hard rock
VHR - very hard rock
HR - hard rock
MHR - medium hard rock
SR - soft rock
VSR - very soft rock

JOINT SPACING
VCJ - very close spacg
CJ - close spacing
MJ - medium spacing
WJ - wide spacing
VWJ - very wide spacng

JOINT SHAPE
CLJ - curvilinear
PLA - planar
UND - undulating
STE - stepped
IRR - irregular

McKnight

NCHWANING NO.3 DECLINE SHAFT
GEOTECHNICAL INVESTIGATION

HOLE NO: BH2

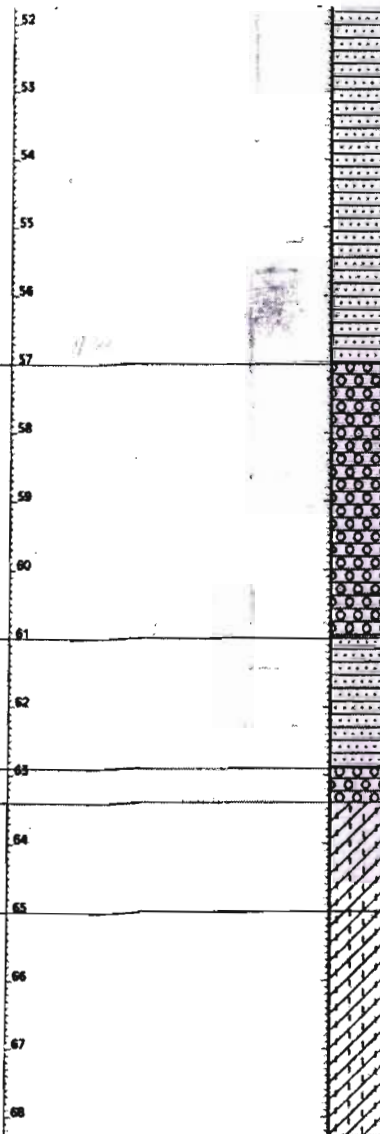
Sheet 4 of 5

JOB NUMBER: 5267

NWD4

97	92	5	70,8
93	48	9	9,2
95	80	5	41,0
92	71	6	13,7
97	67	6	12,9
100	52	6	21,0
81	41	9	2,6
92	8	> 10	1,2
89	-	-	0,0
95	-	-	0,0
94	-	-	0,0
75	-	-	0,0

21
41
21
41
56
41
85
21
21
174
10



57.00
Pale grey to white, mottled pale brown, moderately weathered, interbedded, coarse-grained, widely to medium fractured, medium strong to strong rock CONGLOMERATE and bands of friable weak rock CALC-ARENITE.

Notes:
1. Individual matrix supported gravel and cobble bands from 57,0-57,2m, 57,7-58,1m, 60,2-60,4m and 60,8-61,0m.
2. Clasts are 10-70mm diameter, rounded, fine-grained volcanic rock, shale and quartzite.

61.00
Pale grey to white, mottled pale brown, highly to completely weathered, coarse grained, closely fractured, friable, weak rock. CALC-ARENITE, probably tending to residual sand.

Notes:
1. Crossbedding within unit.

62.90
Pale yellow brown, highly weathered, coarse-grained, closely fractured, clast supported, very soft to soft rock. CONGLOMERATE tending to very weak rock.

65.00
Slightly moist to moist, off white to very pale reddish brown, very stiff, highly slickensided, relict jointed, silty CLAY. RESIDUAL TUFF.

Slightly moist to moist, brownish red, stiff to very stiff, highly slickensided, relict jointed, silty CLAY. RESIDUAL TUFF.

68.50
End of hole.

Drill Method	% Core Recovery	% ROD	Fractures per Metre	D-Value	Estimated UCS (MPa)	DEPTH Scale 1:75
--------------	-----------------	-------	---------------------	---------	---------------------	------------------

HOLE No: BH2

Sheet 5 of 5

JOB NUMBER: 5267

ROCK FABRIC
 MF-massive
 BF-bedded
 FF-foliated
 CF-cleaved
 SF-schistose
 CF-gristose
 LF-laminated

GRAIN SIZE
 FG-fine grained
 MG-medium grain
 CG-coarse grain

JOINT SPACING
 VCJ-very close spacg
 CJ-close spacing
 MJ-medium spacing
 WJ-wide spacing
 VWJ-very wide spacng

JOINT ROUGHNESS
 SJ-slickensided
 SJ-smooth
 RJ-rough

JOINT SHAPE
 CUR-curvilinear
 PLA-planar
 LIR-irregular
 STE-stepped
 IRR-irregular

ROCK HARDNESS
 EHR-extremely hard rock
 VHR-very hard rock
 HR-hard rock
 MHR-medium hard rock
 SR-soft rock
 VSR-very soft rock



NCHWANING NO.3 DECLINE SHAFT
 GEOTECHNICAL INVESTIGATION

HOLE No: BH2

Sheet 5 of 5

JOB NUMBER: 5267

NOTES

- 1) Washbored and cased to 19.5m.
- 2) Water loss at 45.94m depth.
- 3) Hole stopped due to collapse in red clay.

Drill Method	% Core Recovery	% ROD	Fractures per Metre	Q-value	Estimated UCS (MPa)	DEPTH Scale 1:75

CONTRACTOR: Stratadata
 MACHINE: SECO B12
 DRILLED BY: Elias
 LOGGED BY: R A Puchner

TYPE SET BY: CLM
 SETUP FILE: BH.SET

CLIENT: Read, Swatman & Voigt
 INCLINATION: Vertical
 DATE DRILLED: 04-10 April 2000
 DATE LOGGED: April 2000

DATE: 08/06/00 15:17
 TEXT: c:\Vogs\BH2.TXT

ELEVATION: 1047.5m
 X-COORD: 52 327
 Y-COORD: 13 910

HOLE No: BH2
 Black Rock

MINE DRILLED

HOLE NO. N 55

MINE : NCHWANING

ELEVATION: -782,766

CO-ORDINATES: + 14270,876Y +52333,204X

GEOLOGICAL DESCRIPTION OF CORE:

GRAPHICAL LOG

0	-	19	Sand
19	-	40	Sandy limestone
40	-	42	Gravel and limestone
42	-	46	Limestone
46	-	50	Gravel and limestone
50	-	51	Gravel
51	-	57	Sand and limestone
57	-	63	Gravel and sand
63	-	64	White clay
64	-	84	Red clay
84	-	87	B.I.S. gravel
87	-	92	Gravel
92	-	117	Gravel and limestone
117	-	140	Weathered Tillite
140	-	155	Tillite
155	-	156	Tillite (black shale)
156	-	183	Dark blue shale
183	-	191	Grey to red shale
191	-	213	Black to grey shale
213	-	217	Grey shale
217	-	243	Black shale
243	-	248	Grey shale
248	-	254	Grey to brown shale
254	-	315	White quartzite
315	-	324,65	Black carbonaceous shale dip 2-5°
324,65	-	341,5	Grey shale with reverse faults dip 3°
341,5	-	366,3	Red shale with white stringers dip 1-3°
366,3	-	405	Pink-grey shale dip 1-10°
405	-	417	Red shale with white bands
417	-	420,4	Sugary quartzite
420,4	-	424	Grey shale
424	-	440,2	Red shale with white stringers
440,2	-	455	Grey well banded B.I.S. with silica bands dip 2°
455	-	468	Red ferruginous poorly banded B.I.S. grading to medium banded red B.I.S. with 1cm wide calcite bands // to bedding dip 2°
468	-	473	Manganese with calcite bands and nodules
473	-	477,2	Red ferruginous medium banded B.I.S. with calcite stringers dip 2°
477,2	-	489,3	Grey well banded B.I.S. dip 2°
489,3	-	492,4	Red jaspery well banded B.I.S. with vertical calcite veins 0,5 - 1cm thick
492,4	-	493,9	Grey well banded B.I.S. grading to red ferr. B.I.S. dip 2°
493,9	-	495,7	Manganese with red calcite nodules and stringers dip 2°
495,7	-	497,7	Red jaspery B.I.S. with calcite stringers dip 2°
497,7	-	500,75	Grey well banded B.I.S. grading to red ferruginous poorly banded B.I.S. with calcite stringers dip 2°
500,75	-	508,36	Compact manganese with odd calcite stringers dip 1-2°
508,36	-	515,4	Red ferr. poorly banded B.I.S. grading to grey

PREVIOUS INVESTIGATION

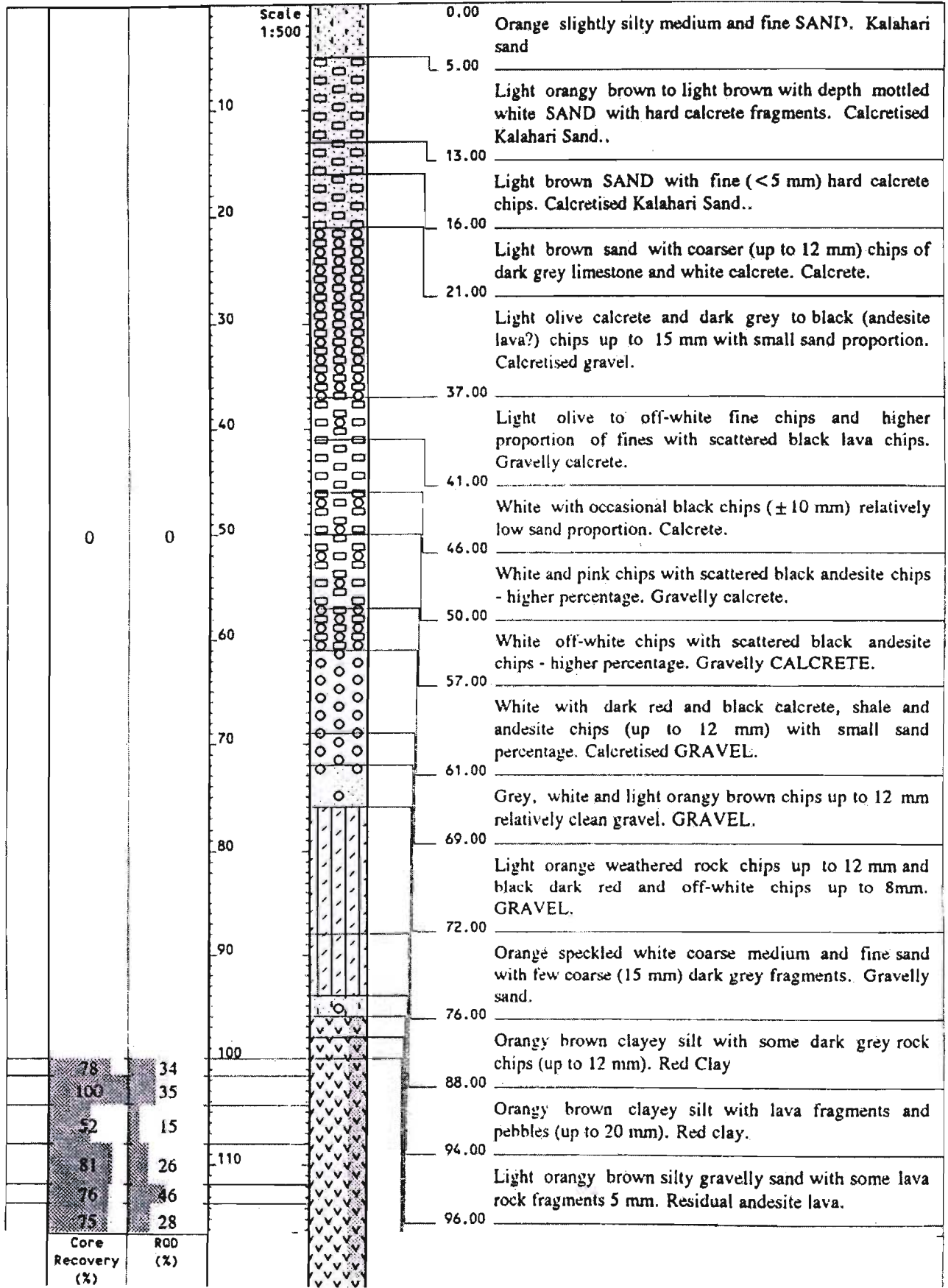


**ASSOCIATED MANGANESE
BLACK ROCK**

**HOLE No: BH 1
Sheet 1 of 4**

STEFFEN ROBERTSON & KIRSTEN

JOB NUMBER: 249711



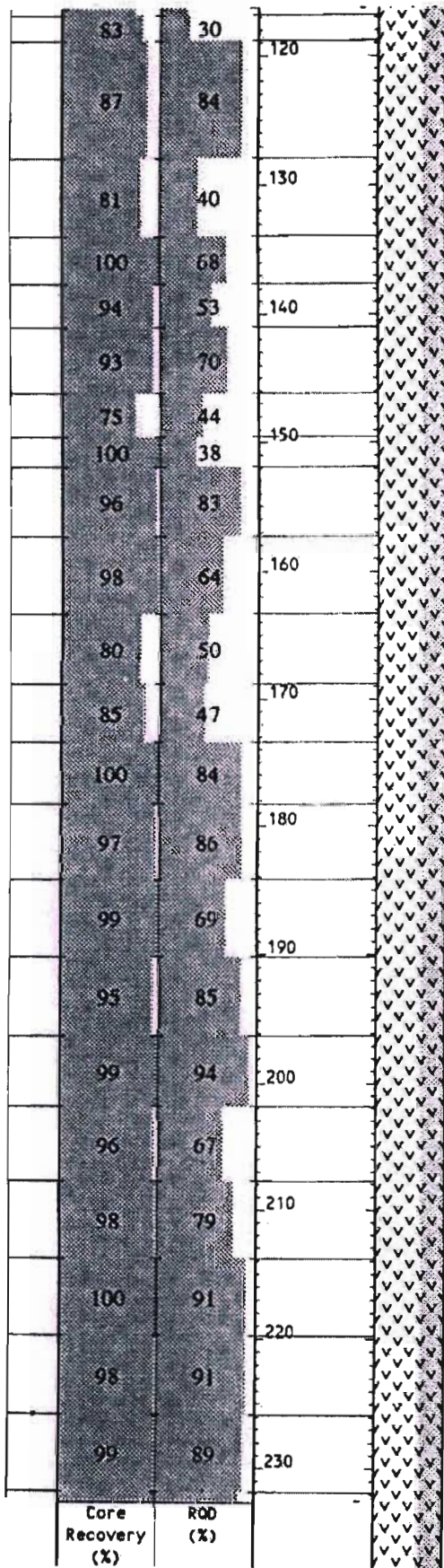


**ASSOCIATED MANGANESE
BLACK ROCK**

HOLE No: BH 1
Sheet 2 of 4

STEFFEN ROBERTSON & KIRSTEN

JOB NUMBER: 249711



Dark grey slightly weathered lava rock fragments up to lava with small percentage of light orange sand. Weathered ANDESITE.

98.00

Dark grey unweathered andesite fragments, <5 mm. Unweathered ANDESITE.

100.00

Fresh massive green medium grained very hard rock. ANDESITE Lava.

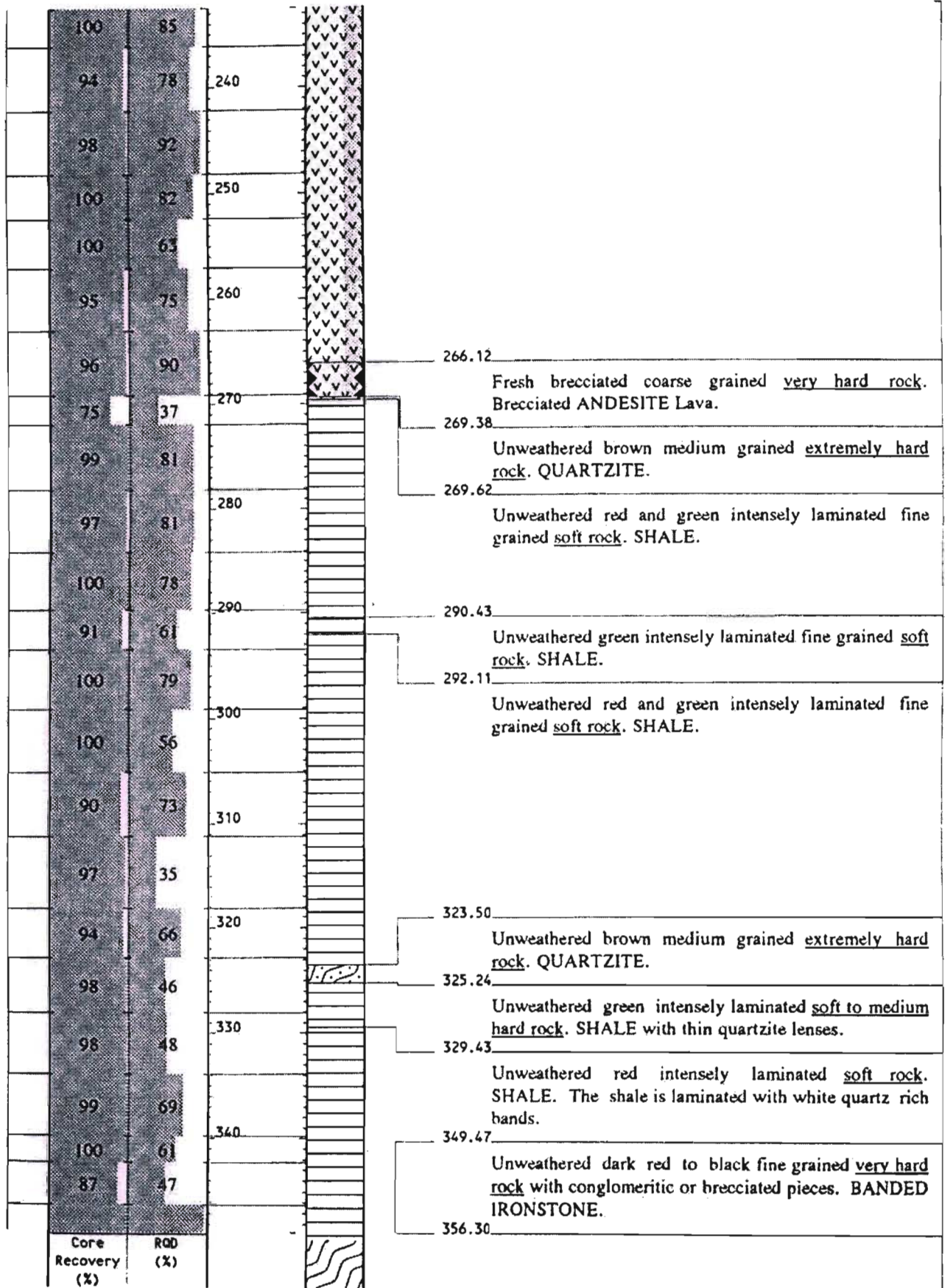


ASSOCIATED MANGANESE BLACK ROCK

HOLE No: BH 1
Sheet 3 of 4

STEFFEN ROBERTSON & KIRSTEN

JOB NUMBER: 249711



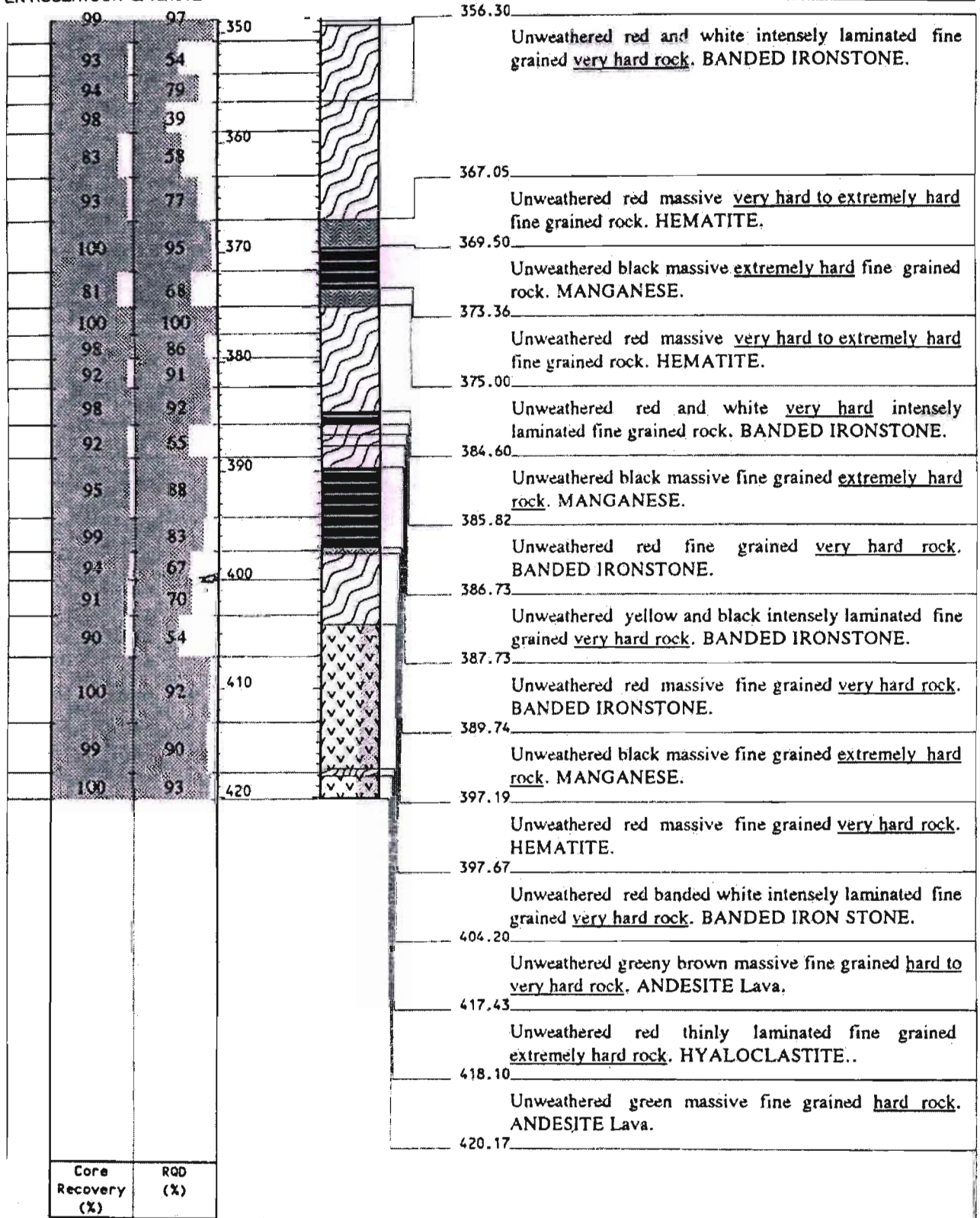


**ASSOCIATED MANGANESE
BLACK ROCK**

HOLE No: BH 1
Sheet 4 of 4

JOB NUMBER: 249711

STEFFEN ROBERTSON & KIRSTEN



CONTRACTOR : BOOYSEN BORE
MACHINE :
DRILLED BY :
PROFILED BY : G Bell
TYPE SET BY : G Bell
SETUP FILE : STANDARD.SET

INCLINATION : Vertical
DIAM : 41 mm
DATE : 3/11/98

ELEVATION :
X-COORD :
Y-COORD :

DATE : 14/01/99 13:12
TEXT : g:\proj\249711\PROFSALL.TXT

HOLE No: BH 1

APPENDIX C

LABORATORY TEST RESULTS

STANDARD TEST METHODS TMH1 (1986)

TECHNICAL METHODS FOR HIGHWAYS

TMH1

**STANDARD METHODS
OF TESTING ROAD
CONSTRUCTION MATERIALS**

**Second edition
1986**

First edition 1979

Second edition published in 1986 by the
National Institute for Transport and
Road Research
of the
Council for Scientific and Industrial Research
P O Box 395
Pretoria
0001 South Africa

ISBN 0 7988 3653 9

*Printed in the
Republic of South Africa
by Graphic Arts, CSIR*

TMH1, pp 1 – 232, Pretoria, South Africa, 1985

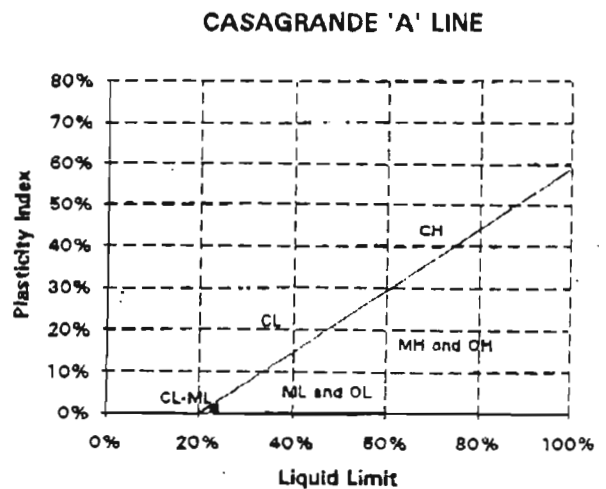
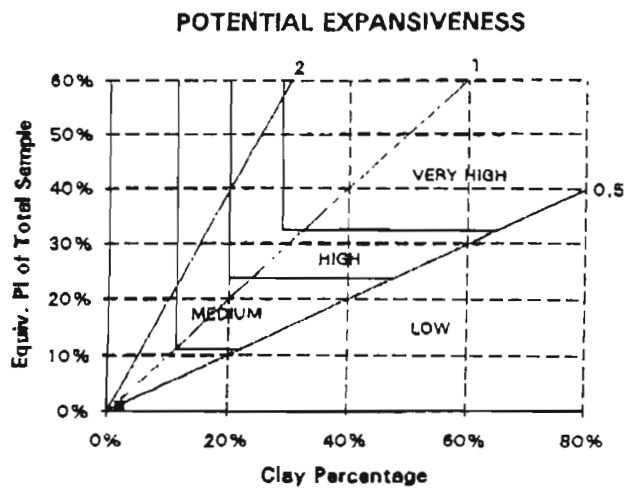
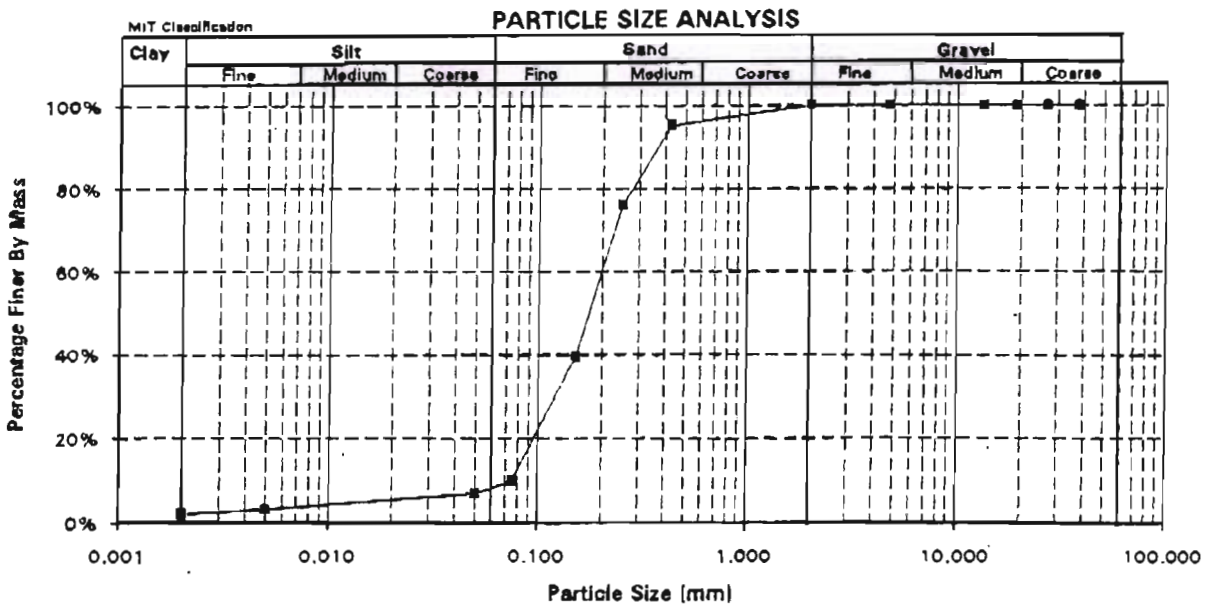
CONTENTS

	Page
<i>Preface</i>	iii
<i>Foreword</i>	iv
A Tests on soils and gravels	
Method A1(a) The wet preparation and sieve analysis of gravel, sand and soil samples	1
Method A1(b) The dry preparation and sieve analysis of gravel, sand and soil samples	9
Method A2 The determination of the liquid limit of soils by means of the flow curve method	11
Method A3 The determination of the plastic limit and plasticity index of soils	17
Method A5 The determination of the percentage of material passing a 0,075 mm sieve in a soil sample	19
Method A6 The determination of the grain size distribution in soils by means of a hydrometer	21
Method A7 The determination of the maximum dry density and optimum moisture content of gravel, soil and sand	27
Method A8 The determination of the California Bearing Ratio of untreated soils and gravels	35
Method A9 The determination of the California Bearing Ratio of lime-stabilized soils and gravels	47
Method A10(a) The determination of the in-place dry density of soil or gravel by the sand replacement method	49
Method A10(b) The determination of the in-place density and moisture content of soils and gravels by nuclear methods	55
Method A11T Tentative method for the determination of the maximum dry density and optimum moisture content of graded crushed stone and cohesionless sand by means of vibration compaction	63
Method A12T Tentative method for the determination of the relative density of soils	69
Method A14 The determination of the unconfined compressive strength of stabilized soils, gravels and sands	73
Appendix to Method A14 Procedure for the making of specimens for the determination of the unconfined compressive strength of stabilized soils, gravels and sands	75
Method A15(a) The determination of the cement or lime content of stabilized materials by means of the Ethylene Diamine Tetra Acetate (EDTA) test	81
Method A15(b) The determination of the cement or lime content of cement-stabilized or lime-stabilized materials by means of a flame photometer	85
Method A15(c) The determination of the lime content of lime-stabilized material using ammonium chloride	87
Method A15(d) The determination of the cement or lime content of stabilized materials by means of the back titration (acid base) method	89
Method A16T Tentative method for the determination of the indirect tensile strength of stabilized materials	93
Method A19 The wet-dry durability test for cement-treated materials	97
Appendix to Method A19 Procedure for the making of specimens of soil-cement for the wet-dry durability test	98
Method A20 The electrometric determination of the pH value of a soil suspension	103
Method A21T Tentative method for the determination of the conductivity of a saturated soil paste and water	105
Method A22T Tentative method for the quantitative determination of acid-soluble sulphates in soils and aggregates by means of a nephelometer	113

GORDONIA FORMATION SANDS

FOUNDATION INDICATOR

Client Project Site	McKnight & Associates 5267 Nchwane No3 Decline Shaft	Date Job #	13/08/99 22041								
Test Pos Sample	PD2/1 Kalahari Sand	Depth	1.5-2.0m								
SIEVE ANALYSIS		ATTERBERG LIMITS		PRA Classification	Unified Classification	Pl of whole sample	% Gravel	% Sand	% Silt	% Clay	
Sieve(mm)	% Passing	Sieve(mm)	% Passing								Test 1
37.500	100%	0.250	76%	Liquid Limit	23.6%	23.5%					A-3
25.000	100%	0.150	40%	Average	23.5%						SP/SM
19.000	100%	0.075	10%	Plastic Limit	22.6%	22.5%					0.9%
13.200	100%	0.050	7%	Average	22.6%						0.0%
4.750	100%	0.005	3%	Plasticity Index (PI)	0.9%						91.7%
2.000	100%	0.002	2%	Linear Shrinkage	0.0%						6.1%
0.425	95%			Grading Modulus	0.95						2.2%



CLIENT M^c Knight & Associates

DATE 11.8.99

PROJECT Nchwaning No 3 Decline Shaft

JOB No

SITE

TEST No A



SHEAR BOX TEST

TYPE OF TEST : Quick

SERIAL No : 1767

SAMPLE DISCRIPTION :

Initial DD: 156 kg/m² MC: 2%

SAMPLE DEPTH : 1.5-2.0
2.5-4.0
5.5-6.0

RING CONSTANT : ① 1.2060
② 1.1547
③ 1.1517

MACHINE No : 1475

REMARKS : Rate of strain: 0.5 mm/min

Normal Load kN		0.250		2.500		5.000			
Converted Load kN/m ²		69		694		1289			
Time	Horizontal Displacement	Proving Ring Dial Reading	Vertical Dial Reading	Proving Ring Dial Reading	Vertical Dial Reading	Proving Ring Dial Reading	Vertical Dial Reading	Proving Ring Dial Reading	Vertical Dial Reading
MIN									
1		27	920	116	679	195	561		
2		21	922	191	669	208	556½		
3		26	918½	242	660	290	552		
4		29	917½	281	657	462	547		
5		41	917½	210	647½	527	542½		
6		42½	918	232	642½	581	539½		
7		42	919½	246	640½	622	528		
8		42	921	256	638½	657	527		
9		42½	922½	267	638	685	526½		
10		42	924	267	627½	704	526		
11				268	627½	717	526		
12				268	627½	725	527		
13				267	628	725	528		
14				265½	640	724	529½		
15						721	541		
16									
17									
18									
19									
20									
21									
22									
23									
24									
25									
26									
27									
28									
maximums		42		268		725			
Converted. Max.		52		425		875			
Moisture Content After						2.96%			

SOILTECH

CLIENT M^c Knight & Associates

DATE 11-8-99

PROJECT Nchwaning No 3 Decline Shaft

JOB No

SITE

TEST No A

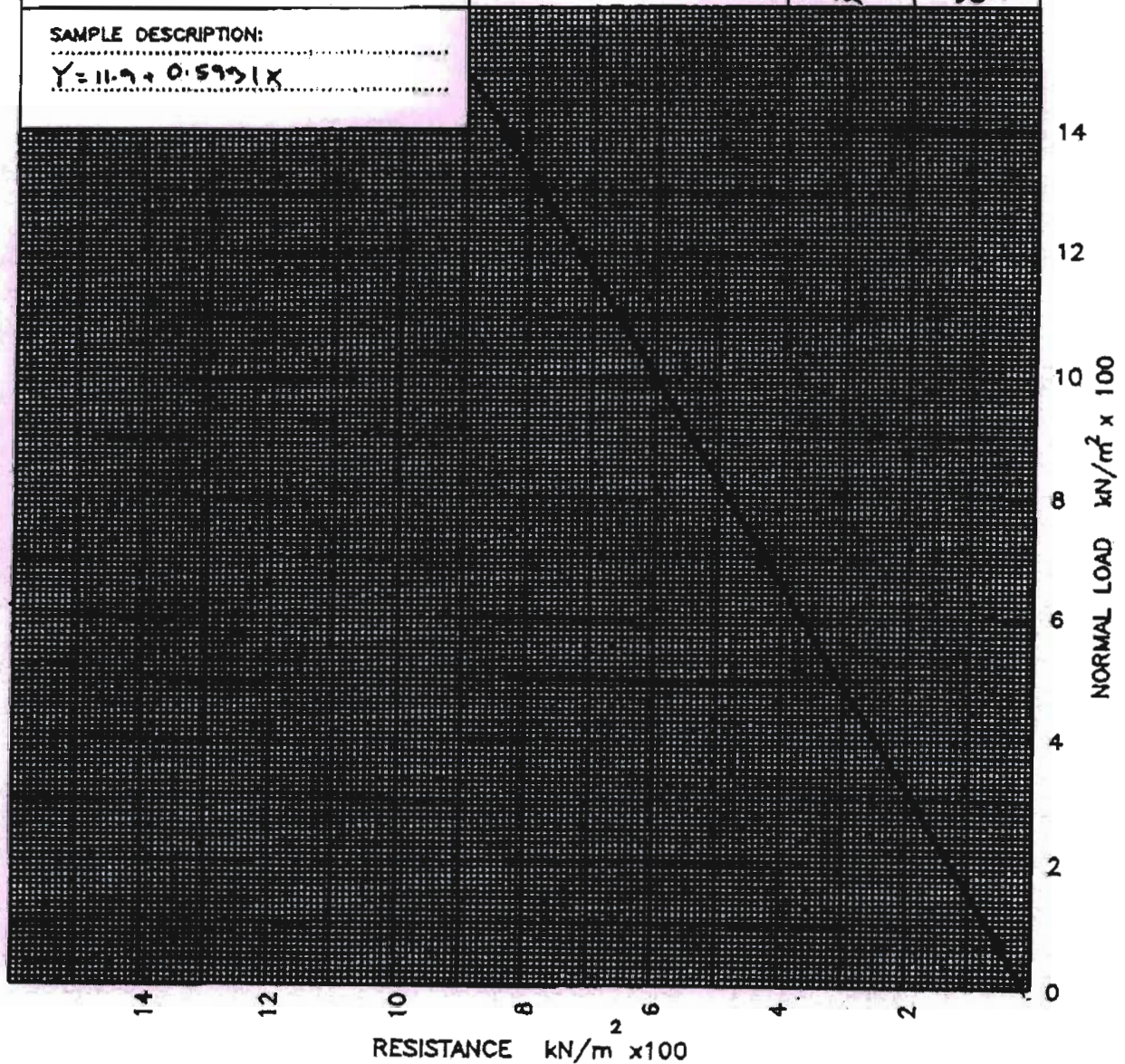


SHEAR BOX TEST

	C kN/m ²	φ DEGREE
TOTAL STRESS VALUE		
EFFECTIVE STRESS VALUE	12	30.7°

SAMPLE DESCRIPTION:

$Y = 11.9 + 0.593X$



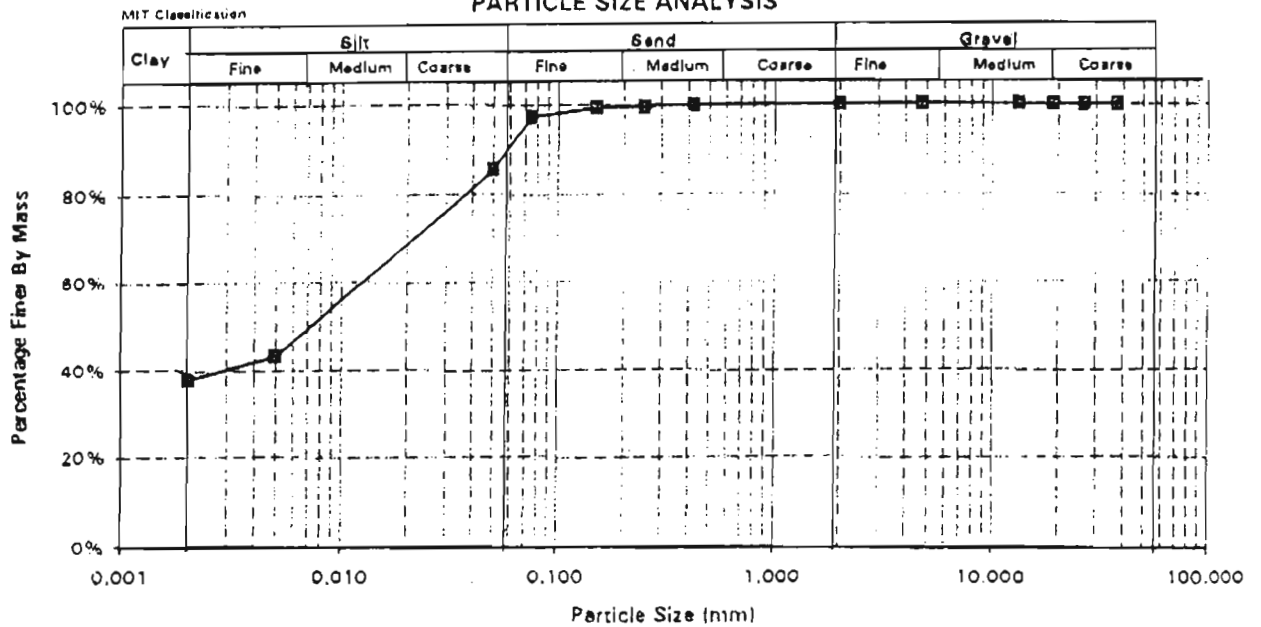
SOILTECH

RED CLAY

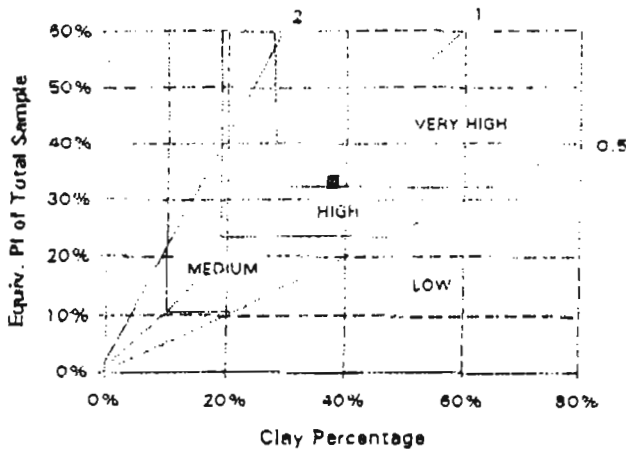
FOUNDATION INDICATOR

Client	McKnight Geotechnical Consulting	Date	20/04/2000				
Project	Nchwanging No. 3 Decline Shaft	Job #	22456				
Site	Nchwanging Mine						
Test Pos	BH 3	Depth	65.25-85.5m				
Sample	Sample No. 1 (Clay)						
SIEVE ANALYSIS				ATTERBERG LIMITS			
Sieve(mm)	% Passing	Sieve(mm)	% Passing		Test 1	Test 2	
37.500	100%	0.250	99%	Liquid Limit	85.0%	84.8%	PRA Classification
26.500	100%	0.150	99%	Average	84.8%		Unified Classification
19.000	100%	0.075	97%	Plastic Limit	52.2%	51.5%	PI of whole sample
13.200	100%	0.050	88%	Average	51.8%		% Gravel
4.750	100%	0.005	43%	Plasticity Index (PI)	33.0%		% Sand
2.000	100%	0.002	38%	Linear Shrinkage	14.0%		% Silt
0.425	100%			Grading Modulus	0.03		% Clay

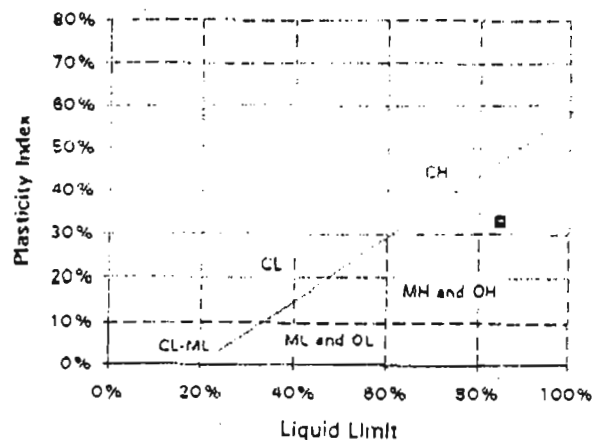
PARTICLE SIZE ANALYSIS



POTENTIAL EXPANSIVENESS



CASAGRANDE 'A' LINE





SOILTECH


QUALITY IS OUR FOUNDATION

DENSITY DETERMINATION

Client McKnight Geotechnical Consulting
 Project # 3 Nchwaneng Decline Mine
 Site Black Rock Mine

Date 14/08/2000
 Job No 22667

TEST NUMBER		MC 1	MC 2
DEPTH	m	Grab	Grab
Wet soil + wax (air)	gm	497.2	437.4
Wet soil	gm	474.6	415.4
Wax	gm	22.6	22.0
Volume of wax	cc	25.1	24.4
Wet soil + wax (water)	gm	143.9	208.6
Volume of wet soil + wax	cc	353.3	228.8
Volume of wet soil	cc	328.2	204.4
Wet soil + pan	gm	585.9	573.2
Dry soil + pan	gm	500.1	483.2
Mass of pan	gm	139.4	141.0
Mass of water	gm	85.8	90.0
Mass of dry soil	gm	360.7	342.2
Moisture Content	%	23.8	26.3
Wet Density of Soil	kg/m ³	1446.1	2032.7
Dry Density of Soil	kg/m ³	1168.2	1609.4
Mod AASHTO of Soil	kg/m ³		
% Mod AASHTO	%		
Remarks			

CLIENT M^c Knight Geotechnical Consulting	DATE 21.8.2000	
PROJECT No 3 Nchwaneung Decline Shaft	JOB No	
SITE Black Rock Mine	TEST No A2	

KONSOLIDASIE TOETS – CONSOLIDATION TEST


Diepte van Monster: **Grab** Volg No.: **1888** Toets Nr. **1**
 Depth of Sample: Serial No.: Test No.
 Opmerkings: **Soaked at 11 kpa**
 Remarks:

Aangewende Druk Applied Pressure	Finale Meterlesing Final Dial Reading	Dikte Verandering Change in Thickness	Monster Hoogte Sample Thickness	Ruimte Hoogte Height of Voids	Ruimte VERhouding Void Ratio $e = \frac{H - H_s}{H_s}$
kN / m ²	mm	ΔH mm	H mm	H-Hs mm	
0	0		20.000	7.871	0.649
11	-1.914		21.914		0.807
25	-1.848		21.848		0.801
50	-1.742		21.742		0.793
125	-1.516		21.516		0.774
250	-1.264		21.264		0.753
500	-0.916		20.916		0.724
1000	-0.454		20.454		0.686
2000	0.152		19.848		0.626
1000	-0.016		20.016		0.650
500	-0.208		20.208		0.666
250	-0.422		20.422		0.684
125	-0.662		20.662		0.704
50	-0.996		20.996		0.721
25	-1.286		21.286		0.755
11	-1.646		21.646		0.785
0					
11					
25					
50					
125					
250					
500					
1000					
2000					

KONSOLIDASIE PARAMETERS – CONSOLIDATION PARAMETERS

	Terrain Monster Field Sample	Toets Monster Test Sample	
VOLUME <small>volume solids</small>			$e_0 = \frac{e_1 - e}{\log_{10} \sigma_1 - \log_{10} \sigma_2}$
VOLUME <small>Ruimte Voids</small>			$A_v = \frac{e_1 - e}{\sigma_1 - \sigma_2}$
Ruimte Verhouding Void Ratio			
0.42 e			
Gemiddelde Digtheid Average Density			$M_v = \frac{\Delta e}{1 + e_1} \times \frac{1}{\Delta \sigma}$
e_0	e_{st}, P_0		

SOILTECH

CLIENT <i>McKnight Geotechnical Consulting</i>	DATE <i>21.8.2000</i>	
PROJECT <i>No 3 Nchwaneng Decline Shaft</i>	JOB No	
SITE <i>Black Rock Mine</i>	TEST No <i>A2</i>	

KONSOLIDASIE TOETS – CONSOLIDATION TEST

Diepte van Monster:
Depth of Sample: *Grab m*

Monster: Onversteurd:
Sample: Undisturbed

Monster Beskrywing:
Sample Description

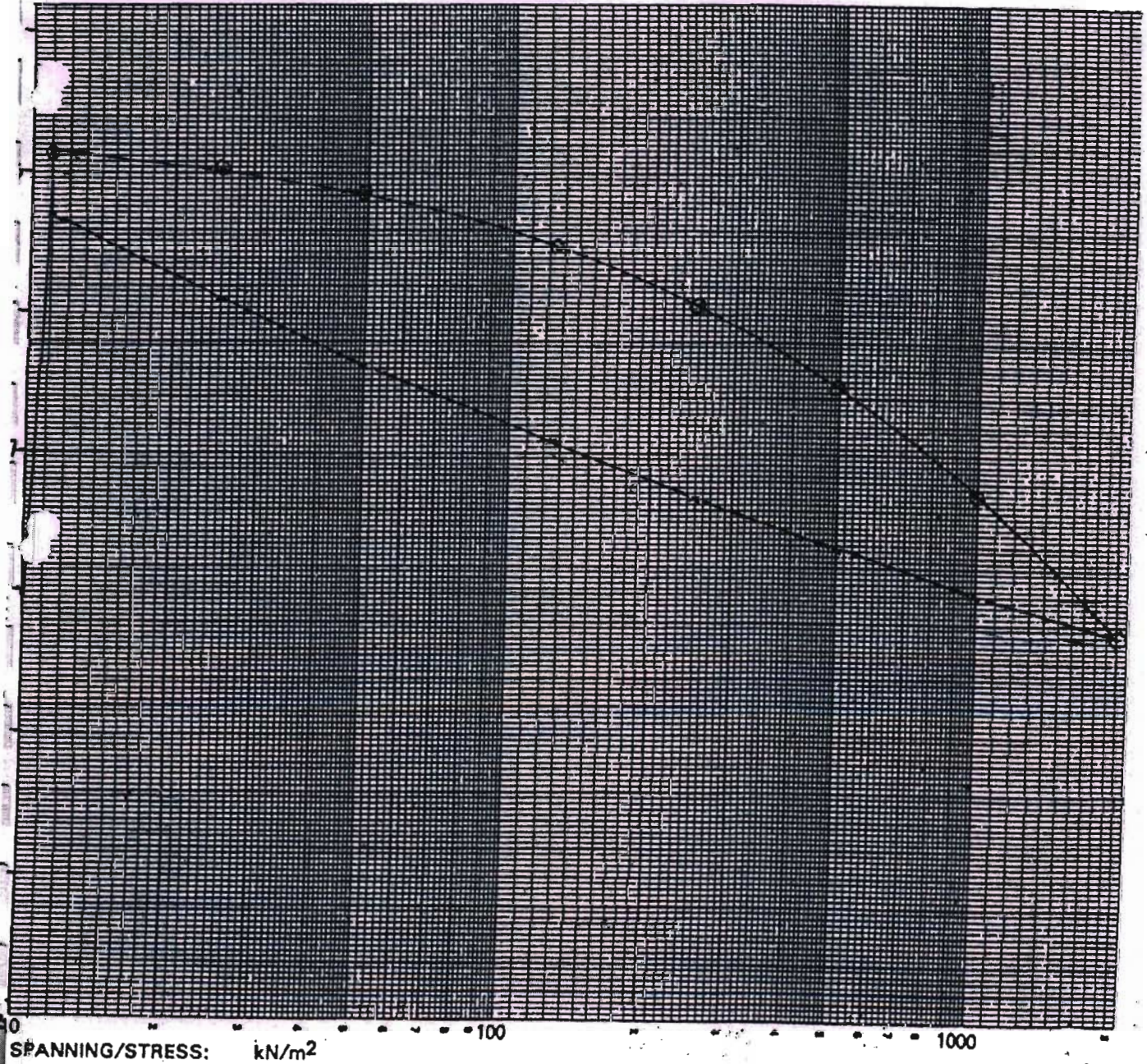
Opmerkings:
Comments: *Soaked at 11 kpa*

Soortlike Gewig:
Specific Gravity: *2.72*

Aanvanklike Droë Digtheid:
Initial Dry Density: *1650* kg/m³

Aanvanklike Voggehalte:
Initial Moisture Content: *23.79* %

Finale Voggehalte:
Final Moisture Content: *28.75* %



SPANNING/STRESS: kN/m² 0 100 1000

CLIENT McKnight Geotechnical Consulting

DATE 21.8.2000

PROJECT No 3 Nohwaneng Decline Shaft

JOB No

SITE Black Rock Mine

TEST No A2



KONSOLIDASIE TOETS - CONSOLIDATION TEST

Diepte van Monster: Grab
Depth of Sample:

Opmerking: Soaked at 11 kpa
Remarks:

Toets Nummer: 1
Test Number:

Volgnummer: 1888
Serial Number:

TYD - VERSAKKINGS LESINGS
TIME - SETTLEMENT READINGS

Lading Load Korreksie Correction	kN/m ²	25		50		125		250		500		1000		2000	
		Meter Lesing	Dial Reading	Meter Lesing	Dial Reading	Meter Lesing	Dial Reading	Meter Lesing	Dial Reading	Meter Lesing	Dial Reading	Meter Lesing	Dial Reading	Meter Lesing	Dial Reading
Tyd Time	(min-t)	1	2	3	4	5	6	7	8	9	10	11	12	13	14
0.0	.00	-957	-917	-860	-811	-747	-688	-610	-526	-429	-329	-229	-129	-27	52
0.2	.02	-944	-900	-846	-791	-726	-667	-587	-497	-397	-297	-197	-97	17	52
0.3	.03	-942	-897	-843	-788	-723	-664	-584	-494	-394	-294	-194	-94	17	52
0.4	.04	-940	-895	-841	-786	-721	-662	-582	-492	-392	-292	-192	-92	17	52
0.5	.05	-929	-884	-830	-775	-710	-651	-571	-481	-381	-281	-181	-81	17	52
0.6	.06	-928	-883	-829	-774	-709	-650	-570	-480	-380	-280	-180	-80	17	52
0.8	.08	-924	-879	-825	-770	-705	-646	-566	-476	-376	-276	-176	-76	17	52
1.0	1.0	-921	-876	-822	-767	-702	-643	-563	-473	-373	-273	-173	-73	17	52
1.5	1.5	-921	-876	-822	-767	-702	-643	-563	-473	-373	-273	-173	-73	17	52
2.0	2.0	-929	-884	-830	-775	-710	-651	-571	-481	-381	-281	-181	-81	17	52
2.5	2.5	-928	-883	-829	-774	-709	-650	-570	-480	-380	-280	-180	-80	17	52
3.0	3.0	-927	-882	-828	-773	-708	-649	-569	-479	-379	-279	-179	-79	17	52
3.5	3.5	-926	-881	-827	-772	-707	-648	-568	-478	-378	-278	-178	-78	17	52
4.0	4.0	-925	-880	-826	-771	-706	-647	-567	-477	-377	-277	-177	-77	17	52
5.0	5.0	-924	-879	-825	-770	-705	-646	-566	-476	-376	-276	-176	-76	17	52
6.0	6.0	-923	-878	-824	-769	-704	-645	-565	-475	-375	-275	-175	-75	17	52
7.0	7.0	-922	-877	-823	-768	-703	-644	-564	-474	-374	-274	-174	-74	17	52
8.0	8.0	-921	-876	-822	-767	-702	-643	-563	-473	-373	-273	-173	-73	17	52
9.0	9.0	-920	-875	-821	-766	-701	-642	-562	-472	-372	-272	-172	-72	17	52
10.0	10.0	-920	-875	-821	-766	-701	-642	-562	-472	-372	-272	-172	-72	17	52
15.0	15.0	-920	-875	-821	-766	-701	-642	-562	-472	-372	-272	-172	-72	17	52
20.0	20.0	-919	-874	-820	-765	-700	-641	-561	-471	-371	-271	-171	-71	17	52
30.0	30.0	-917	-872	-818	-763	-698	-639	-559	-469	-369	-269	-169	-69	17	52
Final Comp	mm	-1848	-860	-871	-742	-758	-610	-622	-429	-458	-189	-227	128	76	152

1	2	3	4	5	6	7	8	9	10	11	12	13	14
1	2	3	4	5	6	7	8	9	10	11	12	13	14
Onlaai/Rebound	Onlaai/Rebound	Onlaai/Rebound	Onlaai/Rebound	Onlaai/Rebound	Onlaai/Rebound	Onlaai/Rebound	Onlaai/Rebound	Onlaai/Rebound	Onlaai/Rebound	Onlaai/Rebound	Onlaai/Rebound	Onlaai/Rebound	Onlaai/Rebound
1888	25kPa	50kPa	125kPa	250kPa	500kPa	1000kPa	2000kPa						
-799	-615	-467	-498	-797	-271	-174	-211	-62	-104	28	-8		

Richard Puchner

XRF

02/09/2002

Sample Number	%SiO2	%TiO2	%Al2O3	%Fe2O3	%MnO	%MgO	%CaO	%Na2O	%K2O	%P2O5	%LOI	%TOTAL
RP	32.89	0.50	6.80	3.79	0.34	12.49	12.82	0.00	0.15	0.08	30.43	100.26

Sample Number	ppm Rb	ppm Sr	ppm Y	ppm Zr	ppm Nb	ppm Co	ppm Ni	ppm Cu	ppm Zn	ppm V	ppm Cr	ppm Ba
RP	19	181	18	82	10	14	17	28	26	149	47	450
RP	19	181	19	82	10	14	15	24	25	145	45	443

Sample Number	%K
RP	0.12

Philips Analytical X-Ray B.V.

PC-APD, Diffraction software

Sample identification: rp
 Data measured at: 19-Aug-2002 9:28:00

Diffraction type: PW1710 BASED
 Tube anode: Cu
 Generator tension [kV]: 40
 Generator current [mA]: 20
 Wavelength Alpha1 [Å]: 1.54056
 Wavelength Alpha2 [Å]: 1.54439
 Intensity ratio (alpha2/alpha1): 0.500
 Divergence slit: 1°
 Receiving slit: 0.1
 Monochromator used: YES

Start angle [°2θ]: 3.000
 End angle [°2θ]: 70.000
 Step size [°2θ]: 0.020
 Maximum intensity: 529.0000
 Time per step [s]: 0.800
 Type of scan: CONTINUOUS

Peak positions defined by: Top of smoothed peak
 Minimum peak tip width: 0.01
 Maximum peak tip width: 1.00
 Peak base width: 2.00
 Minimum significance: 0.75
 Number of peaks: 30

Angle [°2θ]	d-value α1 [Å]	d-value α2 [Å]	Peak width [°2θ]	Peak int [counts]	Back. int [counts]	Rel. int [%]	Signif.
5.565	15.8675S	15.9069	0.960	14	36	2.6	1.06
8.435	10.4739P	10.4999	0.320	88	18	16.7	4.42
13.900	6.3658P	6.3816	0.400	11	6	2.1	1.59
16.285	5.4385P	5.4520	0.240	9	7	1.7	0.83
19.845	4.4702P	4.4813	0.200	45	8	8.5	1.23
20.835	4.2599P+Q	4.2705	0.160	44	8	8.2	1.78
21.410	4.1468P	4.1571	0.320	20	8	3.8	0.96
21.965	4.0433D	4.0533	0.160	14	8	2.7	0.84
24.070	3.6942D+P+H3	3.7034	0.120	31	10	5.9	1.69
26.645	3.3428Q+P	3.3511	0.120	193	11	36.5	5.10
27.780	3.2087P	3.2167	0.640	18	12	3.3	1.55
30.935	2.8883D	2.8955	0.120	529	11	100.0	4.61
33.525	2.6708D+H2	2.6775	0.160	37	10	7.0	1.33
35.290	2.5412D+P+H2	2.5475	0.160	59	10	11.2	2.19
36.535	2.4574Q	2.4635	0.120	17	10	3.2	1.26
37.355	2.4053D	2.4113	0.240	34	10	6.4	3.04
41.125	2.1931D+H	2.1986	0.100	108	12	20.4	1.47
42.445	2.1279Q	2.1332	0.240	10	10	1.9	0.76
43.785	2.0658D	2.0710	0.200	12	9	2.2	1.20
44.925	2.0160D	2.0210	0.060	62	8	11.8	0.89
49.265	1.8481D+H	1.8527	0.120	18	6	3.3	1.33
50.525	1.8049Q+D1	1.8094	0.160	55	6	10.4	1.58

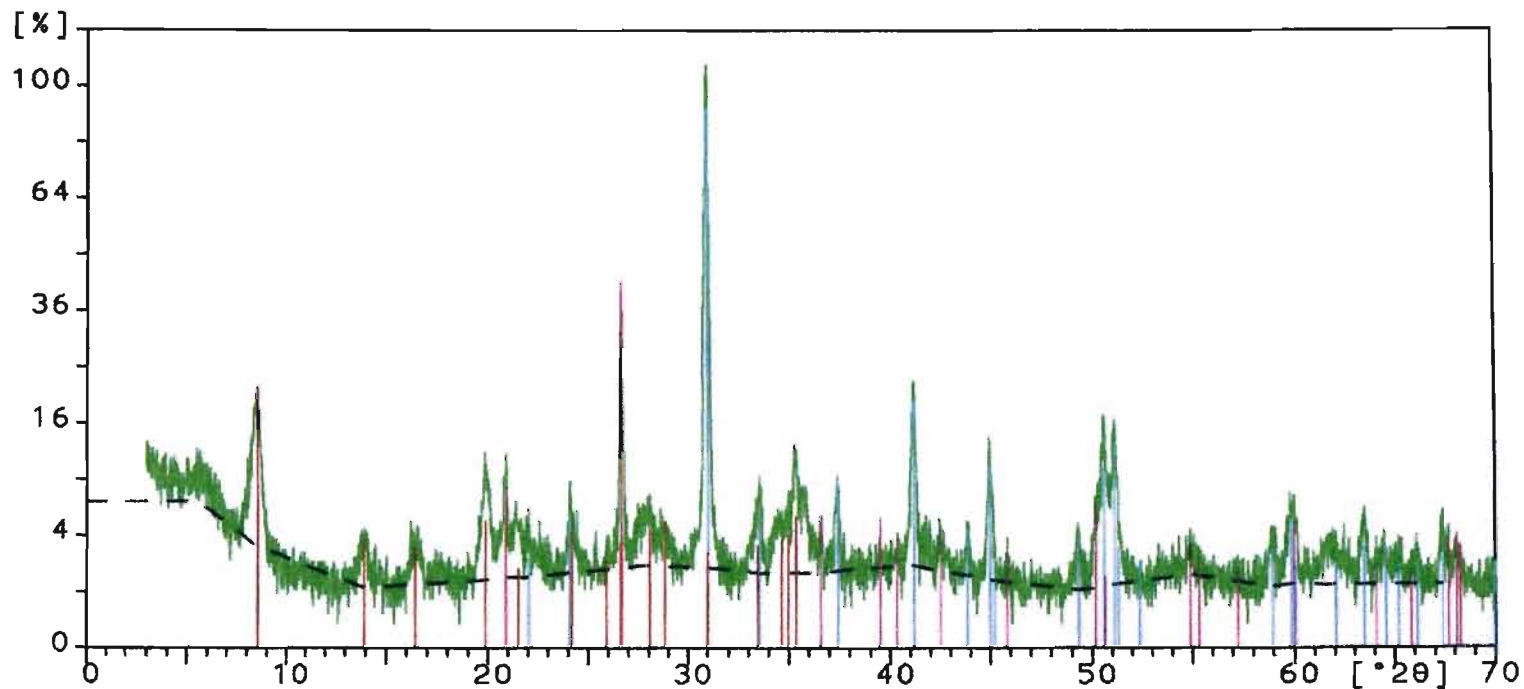
=====

PC-APD, Diffraction software

Angle [°2 θ]	d-value α 1 [Å]	d-value α 2 [Å]	Peak width [°2 θ]	Peak int [counts]	Back. int [counts]	Rel. int [%]	Signif.
51.080	1.7866D	1.7910	0.140	74	7	14.0	1.54
54.960	1.6693H	1.6734	0.640	6	9	1.1	1.08
58.905	1.5666D	1.5705	0.400	12	6	2.2	1.77
59.880	1.5434D	1.5472	0.400	27	7	5.1	2.84
61.700	1.5021H	1.5059	0.480	11	7	2.1	1.53
63.440	1.4651D-H-M	1.4687	0.100	23	7	4.4	0.79
66.020	1.4139D	1.4174	0.320	8	7	1.5	0.85
67.365	1.3889D	1.3924	0.120	21	7	4.0	0.92

Sample ident.: rp

24-Mar-2003 13:05



RP

36-0426	Dolomite	$\text{CaMg}(\text{CO}_3)_2$
31-0783	Palygorskite	$\text{Mg}_5(\text{Si}, \text{Al})_8\text{O}_{20}(\text{OH})_2 \cdot 8\text{H}_2\text{O}$
46-1045	Quartz, syn	SiO_2